Master's Thesis

Master's degree in Energy Engineering

Design and simulation of converters operating in a renewable energy based smart grid.

REPORT

Author: Ignacio García-Tetuá Del Cueto
Director: Eduardo Prieto Araujo
Convocatòria: July 2023

ETSEIB

Escola Tècnica Superior
d'Enginyeria Industrial de Barcelona

UPC

Resum

En el treball de fi de màster "Disseny i simulació d'un convertidor que funciona en una xarxa intel·ligent basada en energies renovables" s'aborda el disseny i la simulació d'un convertidor per a la seva integració en una xarxa intel·ligent basada en energies renovables. L'objectiu principal d'aquest projecte és investigar i desenvolupar dos sistemes proposats: en primer lloc, la integració d'una planta fotovoltaica en la xarxa elèctrica; i, en segon lloc, la integració d'una planta fotovoltaica juntament amb un sistema d'emmagatzematge d'energia i una càrrega de corrent altern connectat mitjançant un inversor.

L'estudi se centra en la recerca i la recopilació d'informació sobre les xarxes intel·ligents basades en energies renovables, explorant els conceptes i tecnologies clau necessaris per a la integració reeixida de fonts d'energia renovable en les xarxes elèctriques. A més, es durà a terme una anàlisi exhaustiva sobre l'emmagatzematge d'energia, investigant les diferents tecnologies i sistemes d'emmagatzematge disponibles. Així mateix, s'investiga el disseny i el control de convertidors utilitzats en la formació de xarxes, analitzant els principis de funcionament i els algorismes de control necessaris per a regular la tensió i la freqüència de la xarxa.

Es duu a terme una anàlisi detallada del sistema proposat, estudiant la seva configuració, els components involucrats i la seva interconnexió amb la xarxa elèctrica existent. A partir d'aquesta anàlisi, es realitza el disseny i desenvolupament dels convertidors necessaris per al sistema de generació i emmagatzematge d'energia. Es dimensionen adequadament els convertidors i es dissenyen els algorismes de control necessaris per a garantir el funcionament òptim del sistema.

Per a avaluar i analitzar el rendiment del sistema proposat, s'utilitza el paquet de programari MATLAB/Simulink per al modelatge i la simulació. Això permet realitzar proves en diferents condicions i ajustar els paràmetres de disseny i control dels convertidors per a aconseguir un acompliment òptim del sistema. Els resultats obtinguts en les simulacions són validats mitjançant comparacions amb dades reals o resultats experimentals, assegurant l'eficàcia i fiabilitat del disseny proposat.

Aquest treball es documenta en un informe complet i analític, que inclou una explicació detallada dels fonaments teòrics, la descripció dels passos de disseny i simulació, la presentació dels resultats obtinguts i una anàlisi crítica d'aquests.

ETSEIB

Resumen

En el trabajo de fin de máster "Diseño y simulación de un convertidor que funciona en una red inteligente basada en energías renovables" se aborda el diseño y la simulación de un convertidor para su integración en una red inteligente basada en energías renovables. El objetivo principal de este proyecto es investigar y desarrollar dos sistemas propuestos: en primer lugar, la integración de una planta fotovoltaica en la red eléctrica; y, en segundo lugar, la integración de una planta fotovoltaica junto con un sistema de almacenamiento de energía y una carga de corriente alterna conectada mediante un inversor.

El estudio se centra en la investigación y la recopilación de información sobre las redes inteligentes basadas en energías renovables, explorando los conceptos y tecnologías clave necesarios para la integración exitosa de fuentes de energía renovable en las redes eléctricas. Además, se llevará a cabo un análisis exhaustivo sobre el almacenamiento de energía, investigando las diferentes tecnologías y sistemas de almacenamiento disponibles. Asimismo, se investiga el diseño y el control de convertidores utilizados en la formación de redes, analizando los principios de funcionamiento y los algoritmos de control necesarios para regular la tensión y la frecuencia de la red.

Se lleva a cabo un análisis detallado del sistema propuesto, estudiando su configuración, los componentes involucrados y su interconexión con la red eléctrica existente. A partir de este análisis, se realiza el diseño y desarrollo de los convertidores necesarios para el sistema de generación y almacenamiento de energía. Se dimensionan adecuadamente los convertidores y se diseñan los algoritmos de control necesarios para garantizar el funcionamiento óptimo del sistema.

Para evaluar y analizar el rendimiento del sistema propuesto, se utiliza el paquete de software MATLAB/Simulink para el modelado y la simulación. Esto permite realizar pruebas en diferentes condiciones y ajustar los parámetros de diseño y control de los convertidores para lograr un desempeño óptimo del sistema. Los resultados obtenidos en las simulaciones son validados mediante comparaciones con datos reales o resultados experimentales, asegurando la eficacia y fiabilidad del diseño propuesto.

Este trabajo se documenta en un informe completo y analítico, que incluye una explicación detallada de los fundamentos teóricos, la descripción de los pasos de diseño y simulación, la presentación de los resultados obtenidos y un análisis crítico de los mismos.

ETSEIB

Abstract

The Master's thesis "Design and simulation of a converter operating in a smart grid based on renewable energies" deals with the design and simulation of a converter for its integration in a smart grid based on renewable energies. The main objective of this project is to investigate and develop two proposed systems: firstly, the integration of a photovoltaic plant into the power grid; and secondly, the integration of a photovoltaic plant together with an energy storage system and an AC load connected by an inverter.

The study focuses on research and information gathering on smart grids based on renewable energy, exploring the key concepts and technologies required for the successful integration of renewable energy sources into power grids. In addition, a comprehensive analysis of energy storage will be carried out, investigating the different storage technologies and systems available. The design and control of converters used in grid formation is also investigated, analyzing the operating principles and control algorithms required to regulate the voltage and frequency of the grid.

A detailed analysis of the proposed system is carried out, studying its configuration, the components involved and its interconnection with the existing electrical network. Based on this analysis, the design and development of the converters required for the energy generation and storage system is carried out. The converters are adequately sized and the necessary control algorithms are designed to guarantee the optimal operation of the system.

To evaluate and analyze the performance of the proposed system, the MATLAB/Simulink software package is used for modeling and simulation. This allows testing under different conditions and adjusting the design and control parameters of the converters to achieve optimal system performance. The results obtained in the simulations are validated by comparisons with real data or experimental results, ensuring the effectiveness and reliability of the proposed design.

This work is documented in a comprehensive and analytical report, which includes a detailed explanation of the theoretical background, description of the design and simulation steps, presentation of the results obtained and a critical analysis of the results.

Contents

ETSEIB

ETSEIB

List of Figures

ETSEIB

Listo f Tables

ETSEIB

1. Introduction

Currently, the integration of renewable energies into electrical grids is of vital importance in achieving a more sustainable and efficient energy system. Increasing awareness of environmental impacts and the need to reduce greenhouse gas emissions have driven the transition to cleaner and renewable energy sources. Distributed generation and smart grids play a key role in this transition, enabling the optimal integration of renewable energies into the existing electrical infrastructure.

The objective of this project is to investigate and develop solutions for the integration of renewable energy sources into a smart grid. Specifically, the design and simulation of a converter for integration into a renewable energy-based smart grid will be addressed. Key concepts and technologies necessary for successful integration, such as distributed generation, energy storage, and grid control, will be explored.

The project will be based on a comprehensive study of scientific and technical literature related to smart grids and renewable energies. Different components and their interconnection with the existing electrical grid will be analyzed. Furthermore, the necessary converters for the generation and storage system will be researched and designed.

The MATLAB/Simulink software will be used for modeling and simulation of the proposed system. This will allow evaluating the system's performance in different scenarios and adjusting design and control parameters of the converters to achieve optimal operation.

At the conclusion of the project, the obtained findings will be presented, summarizing the results and discussing practical implications and potential areas for future research in the field of smart grids and renewable energies.

1.1. Motivation

During my last year of my bachelor's degree, I had the opportunity to work in a combined cycle power plant in Soto de Ribera for the company EDP. This experience allowed me to enter the energy sector and learn about the operation of an electricity generation plant. It was then that I realized the importance of looking for more sustainable and environmentally friendly alternatives in the energy field.

This experience awakened in me a deep interest in the field of renewable energies, smart grids and distributed generation. I believe that renewable energies are the future and represent a promising solution to face the current challenges related to energy generation and climate change mitigation.

ETSEIB

Therefore, I decided to come to study in Barcelona, at the UPC, looking for the opportunity to expand my knowledge and skills in these fields. I wanted to take advantage of the resources and expertise offered by this institution to be able to contribute significantly to the transition towards a more sustainable and efficient energy system, where smart grids play a fundamental role in the integration of renewable energy sources.

I am excited about the opportunity to research and develop solutions that enable the successful integration of renewable energies into smart grids. I believe this field has great potential to transform the way we obtain and use energy, optimizing its distribution and consumption.

To carry out this project, I acquired knowledge in a wide range of topics, from basic electrical engineering and power systems, to power electronics, dynamic systems, energy storage, and photovoltaics and wind energy. In addition, it was necessary to master the MATLAB/Simulink software package to develop and test all components of the final smart grid model.

My goal is to bring new ideas and innovative solutions that will drive the adoption of renewable energy and smart grids. I strongly believe in the power of technology and research to create a cleaner, more efficient and sustainable energy future.

1.2. Objectives

The main points of the Master's Thesis are focused on performing the following tasks related to the project:

- Research and documentation of Smart Grids based on renewable energies: you will have to research and collect information on Smart Grids using renewable energy sources. This will involve understanding the key concepts and technologies involved in the integration of renewable energy into power grids.
- Research and documentation of design and control of grid-forming converters: You will need to research and study the design and control of converters that play a crucial role in grid formation. This will include understanding the operating principles of converters and the control algorithms used to regulate the voltage and frequency of the grid.
- System analysis and understanding of the proposed system: You will need to analyze and understand in detail the system proposed in the project. This will involve studying the system configuration, the components involved and their interconnection with the power grid.
- Design and control of the generation system converters: You will have to design and develop the converters used in the system. This will include sizing the converters appropriately and designing the necessary control algorithms to ensure

optimal operation of the generation and storage system.

- Modeling and simulation with relevant software package (MATLAB and SIMULINK): You will use software tools such as MATLAB and SIMULINK to perform modeling and simulation of the proposed system. This will allow you to evaluate the performance of the system, analyze its behavior under different conditions and adjust the design and control parameters of the converters.

- Design validation: Once you have performed the design and simulation, you must validate its performance through testing and analysis. This involves comparing the results obtained in the simulation with real or experimentally validated data to ensure the effectiveness and reliability of the proposed design.

- Documentation and analysis: Finally, you should document the entire research, design, simulation and validation process in a comprehensive and analytical report. This will include explaining the theoretical background, describing the design and simulation steps, presenting the results obtained, and performing a critical analysis of the results.

ETSEIB

2. State of art

This chapter will focus on the current state of technology and trends in the energy field. In this section, several key topics are discussed that are fundamental to understanding the current energy landscape and future directions of development.

2.1. Energy markets

The energy market plays a crucial role in the production, distribution, and commercialization of energy. In this chapter, we will examine different aspects related to the energy market, including the generation, distribution, and commercialization of electrical energy. We will also analyze different market models, regulations, stakeholders, and trends in the transition towards cleaner and more sustainable energy sources. In addition to melting glaciers and rising sea levels, global warming is causing other climate changes such as desertification and an increase in extreme events like hurricanes, floods, and fires.

In December 2015, after the Paris Climate Change Conference, an international agreement was signed, setting the goal of keeping global warming below 2 degrees Celsius above pre-industrial levels by the end of this century.

To achieve this goal, the main tool is energy transition, which means shifting from a fossil fuel-based energy system to a low-carbon or carbon-free system based on renewable sources and decentralized systems. A significant contribution to decarbonization comes from the electrification of consumption, replacing electricity produced from fossil sources with electricity generated from renewables. Energy transition is not only limited to the gradual closure of coal power plants and the development of clean energies but represents a paradigm shift of the entire system.

In an increasingly interconnected and energy-dependent world, understanding the dynamics and functioning of the energy market is crucial. Access to reliable, secure, and affordable energy has become a basic necessity for the economic and social development of nations. Moreover, the energy market has a direct impact on the environment, as how we generate and use energy can significantly contribute to climate change and environmental degradation [1].

This benefits not only the climate but also the economy and society. The digitalization of grids enables smart networks and opens the way for new services for consumers. From an environmental perspective, renewable energies and electric mobility reduce pollution, while coal power plants can shift to a circular economy perspective.

ETSEIB

Renewable energies have improved their records in Spain in 2021, a year in which these technologies continued their growth until the end of the year, representing 56.6% of the national production capacity. Additionally, renewables reached a generation share close to 47% and produced 10% more than in 2020, values that demonstrate that we are in the midst of an energy paradigm shift.

In total, the national electrical system added over 4,000 new renewable MW in 2021, reaching 63,896 MW of green capacity. Renewable technologies recorded their highest share in the generation mix since records began. Specifically, these technologies produced 121,305 GWh, a 9.7% increase compared to 2020. It is a historic record of renewable production. After wind power, which is the technology with the highest installed capacity in the country with 28,175 MW (25%), combined cycles come next, with 26,250 MW (23.3% of the total); hydropower, with 17,094 MW (15.1%); and photovoltaic solar (13.3%). According to the report, coal has reduced its installed capacity by almost 2,000 MW and records the largest decline of the year, reducing its capacity by 34.3% compared to 2020 [1].
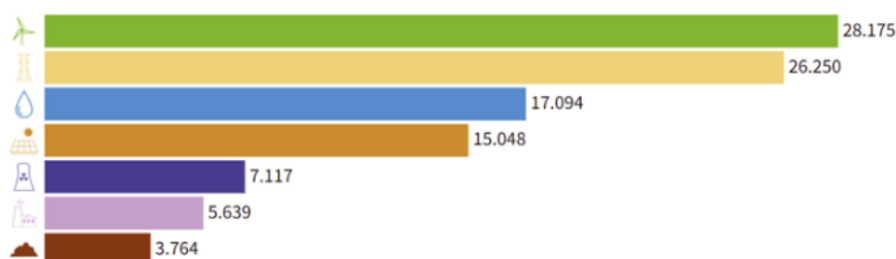
Figure 1 Evolution of installed capacity in Spain 2016-2021 [1].

The energy market is undergoing significant changes due to the increasing adoption of renewable energy sources, the need to reduce carbon emissions and the transition to more decentralized energy systems. These changes are driving the implementation of technologies and practices that enable greater integration of distributed energy sources.

2.1.1.   Dependency on the Spanish electricity system

In the case of Spain, the country has experienced significant growth in renewable energy generation capacity in recent years. According to data from Red Eléctrica de España, in 2020, renewable energies accounted for approximately 43% of the installed capacity for electricity generation in the country. This increase in renewable generation has been driven by investments in technologies such as wind energy and photovoltaic solar energy.

However, due to different and complex circumstances, the Spanish electricity system is still subject to the logic and volatility of the European and world energy market [2]. According to data from the electricity grid itself in 2021, Spain had a demand of 256,387 GWh and a generation of 259,905 GWh, with 46.7% of renewable origin. Therefore, the problem does

not come from the purchase of final energy, since in that sense a surplus is available.

However, 17.1% of this generation is still the product of combined cycle power plants, which operate with natural gas as the primary energy source, amounting to about 45,000 GWh. Most of these come from imports, either as Liquefied Natural Gas (LNG), mostly from the United States and Nigeria (54.5%), or through pipelines (45.5%), mainly from Algeria. Other important players in these imports include France, Russia, Qatar, and Trinidad. This configuration, coupled with the system for establishing the price of electricity in Spain, creates a direct and dependent effect on the changes and crises that the global energy market may suffer, as evidenced by the recent increase in the price of electricity over the last few months. Additionally, this generation source accounts for 48.4% of CO_2 emissions from electricity generation, emitting a total of 17.4 $MtCO_2$ in 2021 [3].

On the other hand, Spain continues to trade large amounts of final electrical energy with its neighboring countries, with the majority being of renewable origin. These international networks connect Spain with France, Portugal, Andorra, and Morocco, enabling the exchange of electricity according to the specific needs of demand and generation. In 2021, total exports reached up to 16,524 GWh, resulting in a net importing balance of 884 GWh [4].

Essentially, the purpose of these exchanges is to buy electricity at a cheaper price than what is sold. In fact, according to recent data, the Spanish electricity system is expected to receive 110 million euros as a result of annual electricity exchange auctions with neighboring countries France and Portugal by 2022. This income represents a 233% increase compared to the auctions held last year for 2021 and would be used to reduce the regulated costs of the system. However, it should be noted that this phenomenon is seasonal and can occasionally contribute to an increase in the price of energy due to circumstances beyond the control of the Spanish grid, such as the closure of nuclear power plants in France [5].

In any case, the European Union promotes this type of system as it also facilitates the optimization of electricity generation by avoiding waste when peaks arise that demand cannot be absorbed. The European Union has set a requirement of 10% of international connections by 2020 and 15% by 2030. Consequently, projects are being carried out, such as the one in the Basque country, which plans to install submarine cabling to double the interconnection with France, currently at less than 4%. However, this could pose a challenge for the promotion and advancement of the photovoltaic and wind turbine system, as producing surpluses that cannot be absorbed would require the machines to be stopped.

2.2. Smart grids

This section focuses on smart grids, also known as Smart Grids, which are electric power supply systems that integrate advanced communication, control and automation technologies. These grids represent an evolution of traditional electrical systems by integrating advanced technologies to optimize energy generation, distribution and consumption.

One of the main benefits of Smart Grids is the improvement of energy efficiency. These grids enable real-time monitoring of energy demand and supply, which facilitates more accurate and efficient resource management. In addition, Smart Grids encourage the integration of renewable energy sources by facilitating the connection and control of distributed generation. This contributes to reducing greenhouse gas emissions and promoting the transition to a cleaner energy matrix.

Another key aspect of Smart Grids is active demand management. These grids enable two-way communication between users and electricity system operators, which facilitates the implementation of demand response measures. Users can receive real-time information on energy prices and availability, allowing them to adjust their consumption according to supply and demand. This helps to balance the load on the power grid and reduce peak demand, which in turn improves system efficiency and reliability.

The existing global electricity system was built around the turn of the last century, with large central generators supplying electricity through a high-voltage grid that interconnects consumers with producers over long distances through a series of step-down transformers. The main characteristics of these grids are:

- Centralized generation
- One-way communication
- Unidirectional power flow between producers and consumers
- Manual testing, control and resetting
- Electromechanical hierarchical structure

As the population grows and civilized areas increase, it also has an impact on the demand for electricity, which increases exponentially and in recent years has had an increase of around 5% per year. This, added to the fact that an important part of the transmission and distribution network equipment has a useful life longer than the one foreseen at the time of its design, makes necessary both its replacement and its modernization, changing equal elements, but also using new elements in order to minimize energy losses [6].

ETSEIB

The International Energy Agency (IEA) presented eight different characteristics that describe an overall smart grid [8]:

1. Wide area monitoring and control: Aimed at monitoring, controlling and optimizing the electrical system over a wide geographic area, avoiding interruptions and outages of the electrical supply and facilitating the integration of renewable energy sources.

2. ICT integration: Aimed at achieving real-time two-way communication for more efficient energy management.

3. Integration of renewable energy resources and distributed generation: Expansion of the generation capacity of the electricity system through additional photovoltaic arrays, wind farms and other distributed renewable energy sources. This involves the installation of renewable energy generators in geographically dispersed locations, such as solar roofs on buildings, wind turbines in rural areas, and small-scale hydroelectric power systems.

4. Energy efficiency: Use of smart technologies and systems to optimize energy consumption, identify usage patterns, and promote efficiency in electricity demand.

5. Energy storage: Incorporation of storage systems to manage intermittent generation from renewable sources and improve the stability and flexibility of the system.

6. Demand management: Implementation of tools and technologies to control and adjust energy demand in real time, encouraging the active participation of consumers.

7. Power quality: Continuous monitoring and control of power quality parameters, such as voltage, frequency and harmonic distortion, to ensure a reliable and high quality supply.

8. Security and reliability: Implementation of cyber security and risk management mechanisms to protect the electric infrastructure from potential threats and ensure a reliable and secure supply.

These features combine to create an electricity system that is more efficient, sustainable, resilient and adaptable to changes in energy demand and generation. Smart grids enable more effective energy management, facilitating the integration of renewable energy sources, promoting active consumer participation, and improving the efficiency and reliability of the overall power system.

Smart grids also provide benefits at the individual level, allowing consumers to control and monitor their energy consumption in real time, access more flexible tariffs, and participate in demand response programs. In addition, the implementation of smart grid technologies contributes to the reduction of greenhouse gas emissions and the development of a more sustainable and environmentally friendly energy system.

The implementation of smart grids poses several challenges. In many countries, the lack of resources and adequate infrastructure makes it difficult to adapt to the needs of distributed

generation plants, which would entail significant investment. Interoperability is another major challenge, as it involves establishing the interconnections, interfaces, requirements and technical standards for the successful deployment of smart grid technology. In addition, renewable resources, such as wind and solar energy, present the difficulty of depending on weather conditions, which requires efficient energy storage and poses challenges in terms of operation and protection of the smart grid under dynamic conditions [9] [10].

Power generation in microgrids can be either direct current or alternating current, depending on the energy sources used. If the generation is in alternating current, the power generated is rectified to direct current and integrated into the grid by means of a voltage source inverter controlled by the pulse width modulation technique. This allows microgrids to manage local generations and loads, improving power quality, efficiency and safety of critical loads [7].

A microgrid can be single-phase or three-phase, connected to medium or low voltage, and can operate in two different operating modes: grid-connected or islanded. In the grid-connected mode, the microgrid receives power from both the utility and the generation sources connected to the system. During this mode, most of the actual power required by the load is met by the distribution connected to the system, while the remainder and variations in the actual power demand are obtained from the utility grid. In islanded mode, load and generation are disconnected to maintain energy balance, and critical loads undergo load shedding [8].

2.3. Energy Storage Systems

Energy storage systems, which play a key role in the integration of intermittent renewable energy sources and demand management, are addressed. Different storage technologies are explored, such as batteries, supercapacitors, thermal storage, among others. Energy storage systems are a key technology to improve the flexibility and efficiency of energy systems. The different types of energy storage systems, such as batteries, thermal storage, pumped storage and hydrogen storage, are investigated. The applications of these systems in renewable energy integration, demand side management and grid stabilization are discussed.

The energy storage capacity in the power grid is about 125 GW, most of which comes from pumped hydro power plants. This represents about 3% of the world's energy storage capacity [11]. Increasing energy storage capacity in the power grid would allow most plants to operate much closer to their peak load, which would reduce energy losses due to electricity transmission.

The growing renewable energy market and diversification of energy sources are directly dependent on improved and increased energy storage devices. Energy storage devices would allow generation sources to operate efficiently while dealing with variations in

ETSEIB

demand, rather than having to increase or decrease their capacity [12].

Applications that can benefit from grid energy storage have a wide range of requirements. In some isolated areas, seasonal energy storage is required, necessitating storage of MWh for several months at a time [12]. On the other hand, stabilization of transmission and distribution networks can store energy only for several minutes before releasing it and can have energy capacities on the watt-hour scale [13].

To work on all these time and energy scales, many forms of energy storage have been developed, and an efficient and secure management system is required. Different energy storage technologies differ in several aspects. On the one hand, there are dedicated large-scale devices such as pumping and compressed air installations. On the other hand, flywheels, capacitors, and superconducting magnetic storage systems are limited due to their dependence on location, capacity and sensitivity in response [14].

2.3.1. Batteries (BESS)

Electrochemical storage devices offer great flexibility in terms of capacity, location and quick response to meet network demands. Compared to other types of storage, they have a wider range of functions. Although battery energy storage systems (BESSs) represent a small part of the overall role in the grid, significant results have been achieved in their use due to their efficiency, versatility, and high energy density [14].

BESSs are increasingly suitable for grid applications due to their progressively decreasing price, increasing performance and lifetime [15]. They can also respond almost instantaneously to grid demands and operate for longer periods of time. Due to its historical maturity in technology, lead-acid chemistry is the most widely used in large-scale BESS systems [16].

However, the advancement and study in new types of battery chemistry has enabled a wide and varied range of battery options for new and different storage applications. Their robustness and functionality have also increased within the power grid.

Over the past five years, numerous BESS-related experiments and projects have been conducted for many new chemistries, including sodium-sulfur, lithium (Li) ions, such as lithium titanate and lithium iron phosphate, nickel-cadmium, nickel-cadmium, nickel-cadmium, lithium iron phosphate and lithium iron phosphate, nickel-cadmium, sodium-nickel chloride, sodium ion, lithium magnesium and lithium sulfur ions, metal-air, and various flow battery chemistries that pump the electrolyte to charge or discharge and store energy in the electrolyte [17]. For the comparison to be made later, most of the chemistries will be grouped together and lithium, sodium-sulfur, and metal-air ions will be detailed. Regardless of chemistry, each BESS must be properly controlled to ensure safe and efficient operation, meeting the requirements of different grid applications.

The use of battery kinetic storage is closely linked to the increasing availability of renewable energy. The relationship between energy generation and demand is difficult to regulate, so it is important to store energy in excess of demand in order to return it to the grid when needed. Therefore, the AC to DC conversion process and its accumulation in BESS plays an important role in kinetic storage. A schematic of a BESS storage system with AC/DC conversion systems, control panels and corresponding ventilation is shown in Figure 2.
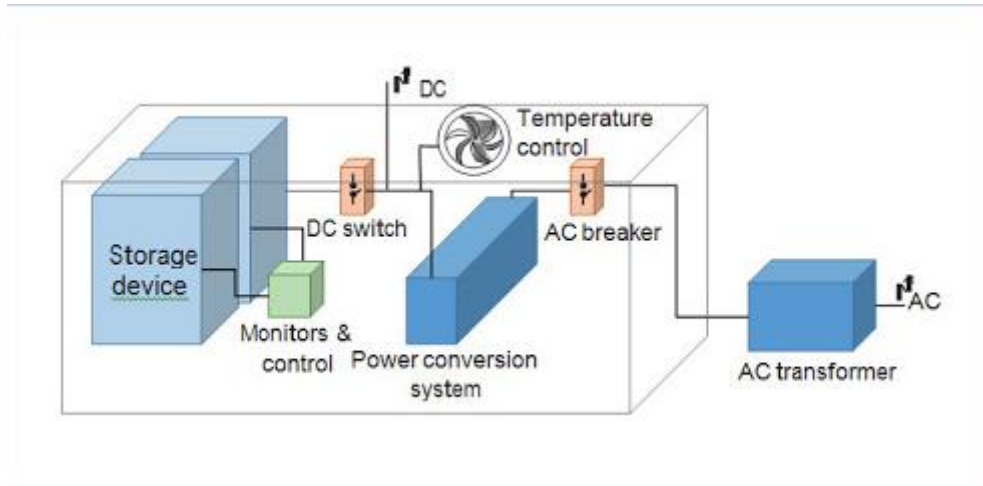
Figure 2 BESS storage scheme [24].

Through the use of energy storage systems, energy can be stored and used when needed. These systems are especially useful for providing intermittent power inputs and maintaining constant system frequency. They can also provide active power inputs at times of high demand. The energy inputs from the batteries can be over short or long periods, depending on the application for which they are used.

2.3.2. Pumped Hydro Storage (PHS)

Reversible hydropower plants, also known as pumped storage plants, use reversible hydraulic pumps to store energy in the form of water and adapt to the energy needs of the system. This type of plant dates back to the early 1890s and allows energy storage in two water tanks located at different elevations, as shown in Figure 3. During off-peak hours, electricity is used to pump water from the lower tank to the upper tank (shown in red). When there is an increase in energy demand, the stored water is discharged from the upper tank to the lower tank through a high-pressure turbine, generating electrical energy that is transmitted to the grid.
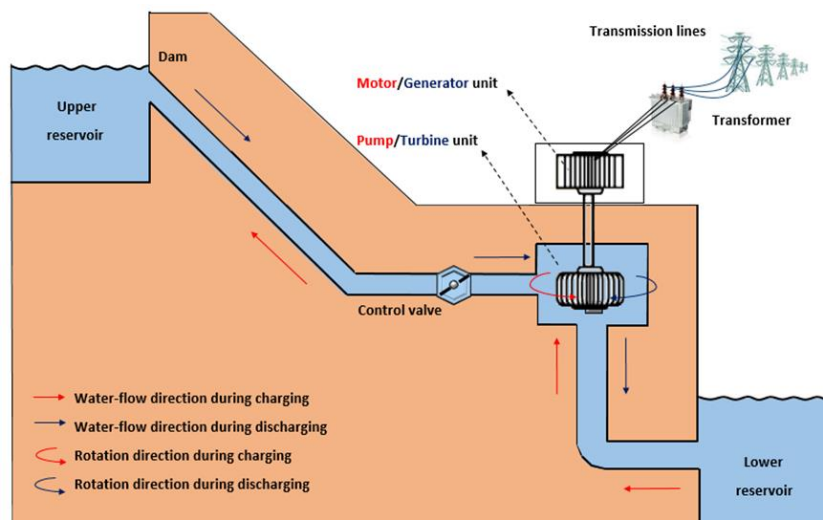
Figure 3 Schematic diagram of PHS plant operation [25].

Pumped storage is considered the most promising technological option for increasing the penetration of renewable energy into the power system [20, 21]. The power rating of pumped storage equipment depends on the water pressure and its flow through the turbine, as well as the power rating of the pump/turbine and the generator/motor set. Pumped storage power plants can have a power rating of between 1 and 3000 MW, a cycle efficiency of about 70% to 85%, and a lifetime of more than 40 years [18, 19, 22]. As for the payback period, it is reported to be as low as 2.5-5.5 years [23]. Currently, much research is being conducted on stand-alone renewable systems using pumped storage, including micro pumped storage systems.

2.3.3. Compressed air energy storage system (CAES)

Figure 4 shows the operation of a CAES system. During the compression stage, air is compressed to a pressure of 60 to 70 bar using low-cost electricity that powers a string of compressors. The compressed air is stored at the temperature of the surrounding formation and at a certain pressure, which is defined by the selected subway cavern. To improve the efficiency of the compression stage and minimize thermal stress on the walls of the storage tank, intercoolers are used between the compressors and an aftercooler before injection into the cavern, which is covered by a salt dome.

Furthermore, in the absence of fuel combustion and with an air temperature equal to that of the tank wall, the power plant would require a much higher air flow rate to generate the same amount of power as the turbine. This would reduce both the generation time and the power generated, as well as the power plant performance indices [15].
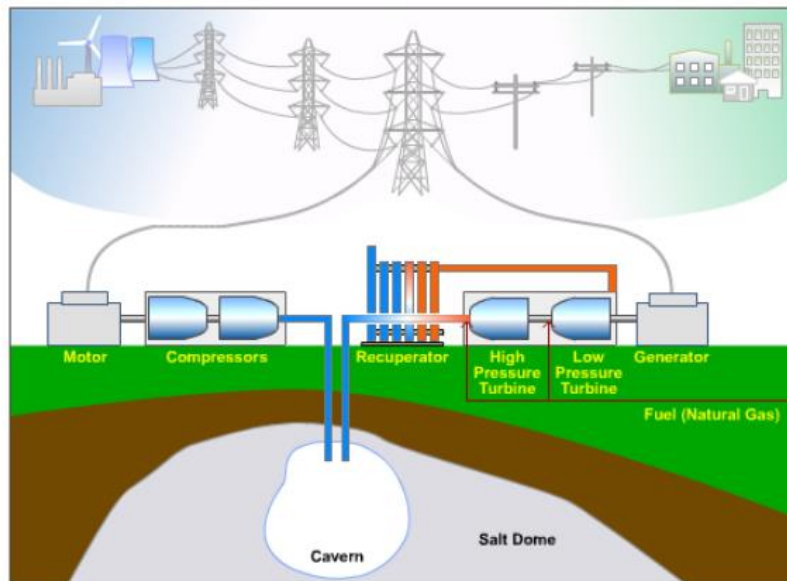
Figure 4 CAES plant schematic [15].

The main characteristics of CAES systems include:

- Capacity to store large amounts of energy.
- High response speed.
- Low storage cost.
- Higher energy density than pumping plants with the same capacity, although useful chambers are usually smaller in volume than water reserves in pumping plants.
- Need for sealed storage chambers.
- Technology still under development.

In contrast to conventional gas turbine engines, where compression and expansion occur simultaneously and much of the power from the expansion stage is used to run the compressor, in CAES systems these processes occur independently and at different times. This means that all of the turbine power can be used to generate electricity during expansion, while the compressor charging system will be sized to match the electrical power sources (such as nuclear power plants or intermittent power sources) and maximize the efficiency of the CAES system. As for the turbines, because they are independent of the compressor train, they have a high ramp rate, allowing the system to respond quickly to changes in the electrical system and provide support for baseload plants with a slow response. Because the plant is controlled by varying the air flow rate and operating temperatures are maintained below the metallurgy capabilities and TITs of standard gas turbine machines, CAES is very reliable [26, 27].
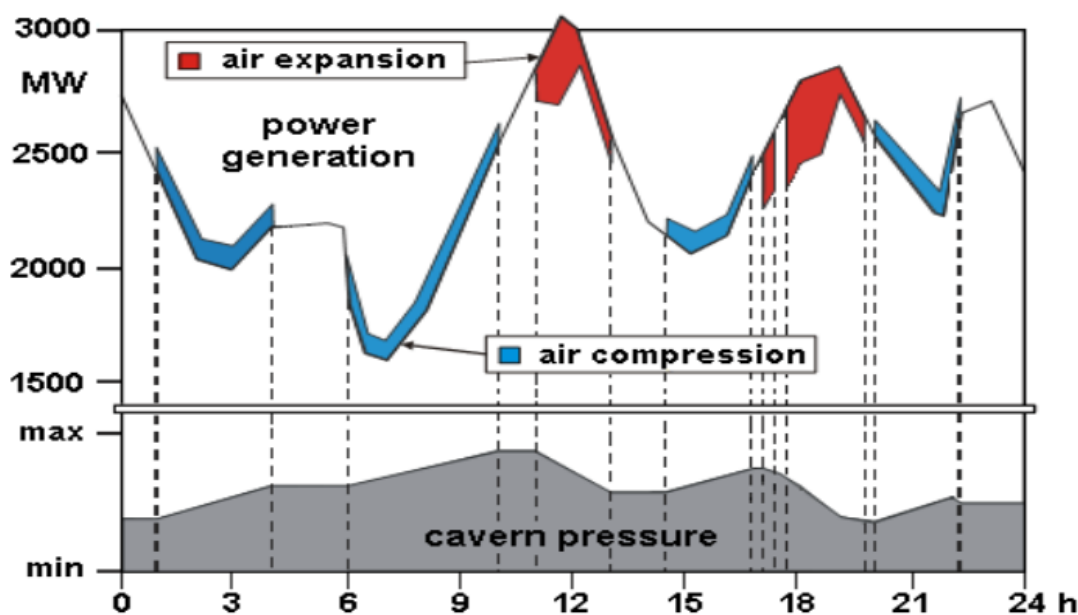
Figure 5 Operation of a CAES plant throughout the day [28].

CAES technology also offers the possibility of keeping coal and nuclear power generation units operating at full capacity during off-peak periods, resulting in economic benefits by reducing the operating costs of such units, as well as improvements in their reliability and efficiency [27].

A special type of CAES plants are the so-called adiabatic CAES plants (A-CAES). In this case, the heat generated during air compression is stored in adiabatic chambers and released during the expansion stage. This increases the temperature of the air entering the turbine, which not only increases the power generated but also prevents the risk of freezing on the turbine blades, without the need to use additional fuels as in conventional CAES plants. This technology significantly improves plant efficiency, reaching values close to 70% (similar to those of pumped-storage plants). It should be noted that there are both large-scale CAES systems and Micro-CAES systems.

2.3.4. Magnetic superconductors (SMES)

Magnetic superconductors, also known as Superconducting Magnetic Energy Storage (SMES), are a type of Distributed Energy Storage (DES) device in which electrical energy flowing through a superconducting coil is stored in a magnetic field. The fundamental difference from a conventional coil is that the superconducting coil must be cryogenically cooled to a temperature below its critical temperature to exhibit its superconducting properties. The basic diagram of the operation of an SMES device is shown below [29].
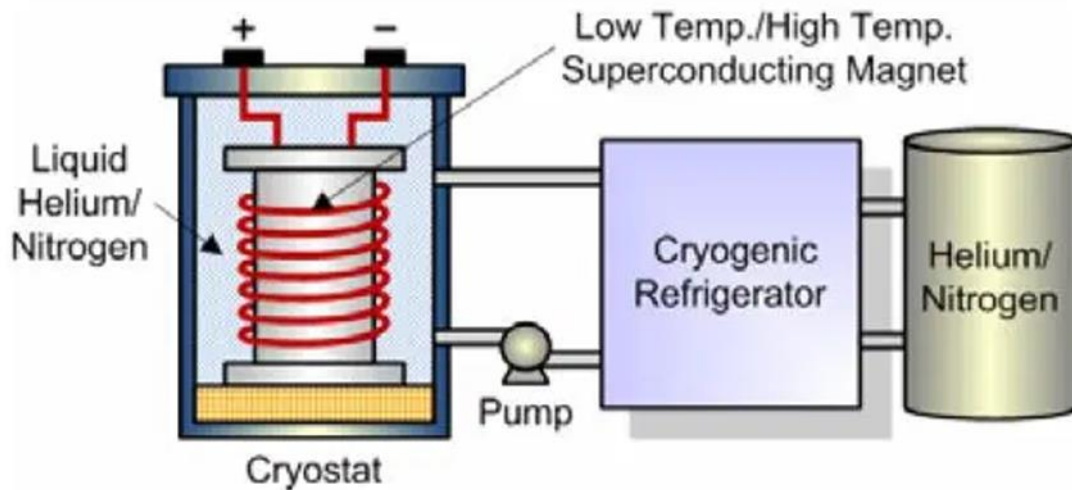
Figure 6 Basic structure of an SMES device [29].

The SMES (Superconductivity Magnetic Energy Storage Device) is characterized by its high efficiency (up to 95%), compared to other energy storage systems, due to the absence of resistive losses. In addition, these devices have a fast response time, since they operate solely by means of electromagnetic transformations of electricity, without the need to use other types of energy. The SMES concept is based on the ability to store energy in pure form in the magnetic field generated by the direct current in the winding [30].

The conversion from alternating current (AC) to direct current (DC) and vice versa is the only conversion process performed in the SMES. Therefore, there are no thermodynamic losses associated with the conversion from one type of energy to another. The solenoid and toroidal windings are the source of the magnetic field. In the solenoid winding, a strong magnetic field is generated in a wide area around the winding, while in a toroid, the magnetic field is produced in a smaller space, although the amount of energy obtained from the same amount of superconducting wire is smaller.

Equation 1

$$E = \frac{1}{2} * V * \mu * H^2 = \frac{1}{2} * V * \frac{B^2}{\mu}$$

where:

- B - magnetic field induction.
- V- volume of the magnetic field.
- H - magnetic field strength.
- μ - magnetic permeability.

2.3.5.   Pilas de combustible

Fuel cell-based energy storage systems enable separate energy conversion and storage, allowing each function to be individually optimized for performance, cost or other installation factors. This ability to optimize each component of an energy storage system can provide significant benefits for many applications. Hydrogen is used as an energy storage medium based on various fuel cell or electrolyzer energy storage concepts and applications that adopt these concepts. Fuel cells are becoming the preferred method of distributed power generation due to their high fuel conversion efficiency, environmental friendliness, reliability and low noise level.

When used as an energy storage device, the fuel cell is combined with a fuel generation device (usually an electrolyzer) to create an RFC regenerative fuel cell system. This system can convert electrical energy into storable fuel and then use this fuel in a fuel cell reaction to provide electricity when needed. Figure 7 shows the most common type of proposed RFC, which uses hydrogen as the storage medium for energy produced by the electrolysis of water. This hydrogen-oxygen RFC cycle and the potential application of this technology in traditional energy storage applications. The key to the efficiency of the RFC system is the ability to separate the energy storage function from the energy conversion function, allowing each to be optimized. [31]
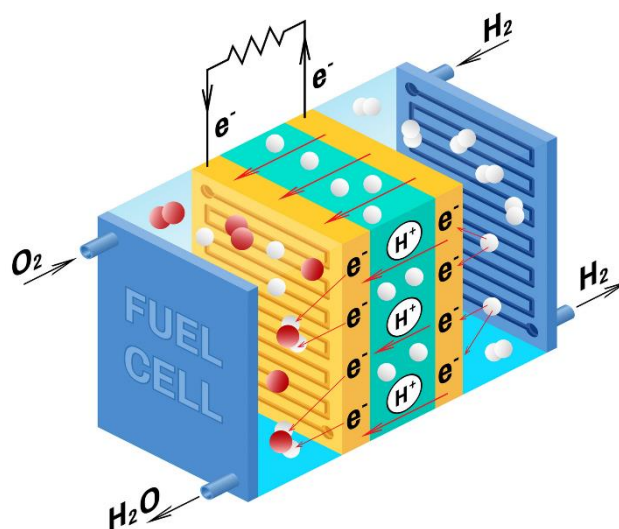
Figure 7 Schematic fuel cell storage [32].

For example, if moderate power of about 5 kW is sought for backup energy storage in an IT facility, a small fuel cell can be installed inside the facility near the load. Hundreds of kilowatt-hours of energy in the form of hydrogen can be safely stored outside the building. When power is needed, the hydrogen supplied by the fuel cell will allow full-load operation for many days. In addition, a positive indication of the remaining charge level, measured by the amount of hydrogen remaining and displayed by the pressure stored in the tank, will be available at all times [31].

The result is a system that can provide full long-term backup power by using hydrogen as the energy storage medium, which is safely stored outside the building. In contrast, storing the same amount of energy using traditional lead-acid batteries would require an environmentally controlled room. The stored hydrogen is not affected by temperature, storage duration or number of storage cycles, and can be fully discharged without reducing its lifetime. When the water tank needs to be refilled, it can be done by electrolysis of the water with energy from the primary energy source. Although the potential of RFCs has been studied for many years, no practical applications have been found due in part to the high cost of fuel cells and the lack of a cost-effective way to generate and store hydrogen [31].

2.3.6.   Comparación de tecnologías

In order to compare the different energy storage technologies, we have chosen to evaluate the four aspects considered most important in this field. The article [16] entitled "Progress in electrical energy storage system: A critical review" (April 15, 2008), written by H. Chen, T. N. Cong, W. Yang and others, was used as a reference point for this section. This article deals in a concise and summarized manner with the most relevant aspects in the comparison of these technologies. Although this paper contains many aspects that could be compared between the different technologies, their inclusion in their entirety would result in an excessive extension of the present work.

ETSEIB

2.3.6.1. Technical maturity

Figure 8 presents a summary of the technical maturity of the different Energy Storage Systems (ESS). These technologies can be classified into three categories according to their degree of maturity.
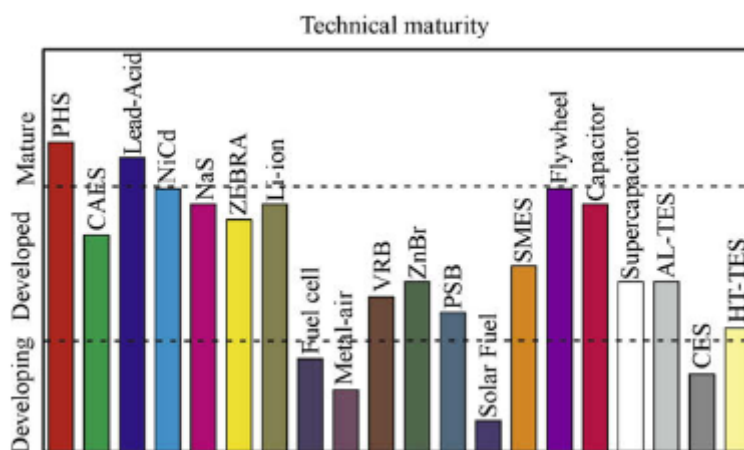
Figure 8 Comparison of technical maturity of the different EES [16].

Mature technologies, which are those that have been refined over time. Pumped hydro storage (PHS) and lead-acid batteries are considered mature technologies and have been in use for more than 100 years.

Developed technologies, which are technically advanced and commercially available, although their implementation in real applications, especially on a large scale for utilities, is not yet widespread. Their competitiveness and reliability still need to be proven by the electricity industry and the market. This category includes systems such as compressed air energy storage (CAES), nickel-cadmium (NiCd), sodium-sulfur (NaS), lithium-ion (Li-ion) and flow batteries, as well as systems such as superconducting magnetic energy storage (SMES), flywheels and supercapacitors.

Technologies under development, which are those that are not yet mature in commercial terms but are technically feasible and have been the subject of research by several institutions. These technologies have great potential for industrial implementation in the near future, driven primarily by energy cost considerations and environmental concerns. Examples of these developing technologies include fuel cells and metal-air batteries.

2.3.6.2. Power and discharge time

Table 1 compares the power capacities of different energy storage technologies (EES). This second section is divided into three distinct categories.

- *Energy management*: PHS and CAES technologies are used in large-scale energy management applications, such as spinning power reserves and load leveling and tracking. Fuel cells and large-scale batteries are useful for medium-scale energy management applications, with capacities between 10 and 100 MW. In comparison, the aforementioned PHS and CAES can operate in systems above 100 MW, even in hourly or daily production periods.
- *Power Quality*: Typical power applications in this category are less than 1 MW. They include flywheels, batteries, SMES systems and supercapacitors due to their fast response, which can be as fast as milliseconds. These technologies are highly reliable when it comes to ensuring power quality in situations such as instantaneous brownouts, short-term uninterruptible power supply (UPS) systems and flicker reduction.
- *Bridging power*: The most common operating power in this type of application is between 100 kW and 10 MW. Technologies that fall into this category are batteries and fuel cells, as they not only offer a relatively fast response (approximately 1 second), but also have a relatively long discharge time (hours). These technologies best fit the concept of "bridging power". Bridging power applications are defined as real, continuous systems of regulated and conditioned reactive power to provide support during the transition from one energy source to another. [16]

2.3.6.3. Storage life

In Table 1 mentioned previously, the self-discharge values (i.e., energy dissipation) per day of different energy storage systems (EES) are also presented. The different systems and their respective self-discharge rates are described below:

1. NaS link: a high self-discharge rate is observed due to their high operating temperature and the need to be kept warm to utilize the stored energy. The proper storage period for this type of system should be several tens of minutes.
2. Lead-acid systems, NiCd and lithium-ion bonds: These systems have moderate self-discharge rates and are suitable for storage periods not exceeding several tens of days. However, it is recommended to use them only for short storage cycles of up to several hours.
3. PHS, CAES and fuel cells: These systems exhibit a very low self-discharge rate, which makes them suitable for extended storage periods. As for SCES systems, they exhibit a daily discharge between 20% and 40% of their capacity and have a storage period varying from seconds to hours. Finally, flywheels lose 100% of their

stored energy if the storage period exceeds one day, so a suitable storage period of several tens of minutes is recommended.

Systems	Power rating and discharge time		Storage duration		Capital cost		
	Power rating	Discharge time	Self discharge per day	Suitable storage duration	$/kW	$/kWh	¢/kWh-Per cycle
PHS	100–5000 MW	1–24 h+	Very small	Hours–months	600–2000	5–100	0.1–1.4
CAES	5–300 MW	1–24 h+	Small	Hours–months	400–800	2–50	2–4
Lead-acid	0–20 MW	Seconds–hours	0.1–0.3%	Minutes–days	300–600	200–400	20–100
NiCd	0–40 MW	Seconds–hours	0.2–0.6%	Minutes–days	500–1500	800–1500	20–100
NaS	50 kW–8 MW	Seconds–hours	~20%	Seconds–hours	1000–3000	300–500	8–20
ZEBRA	0–300 kW	Seconds–hours	~15%	Seconds–hours	150–300	100–200	5–10
Li-ion	0–100 kW	Minutes–hours	0.1–0.3%	Minutes–days	1200–4000	600–2500	15–100
Fuel cells	0–50 MW	Seconds–24 h+	Almost zero	Hours–months	10,000+		6000–20,000
Metal-Air	0–10 kW	Seconds–24 h+	Very small	Hours–months	100–250	10–60	
VRB	30 kW–3 MW	Seconds–10 h	Small	Hours–months	600–1500	150–1000	5–80
ZnBr	50 kW–2 MW	Seconds–10 h	Small	Hours–months	700–2500	150–1000	5–80
PSB	1–15 MW	Seconds–10 h	Small	Hours–months	700–2500	150–1000	5–80
Solar fuel	0–10 MW	1–24 h+	Almost zero	Hours–months	–	–	–
SMES	100 kW–10 MW	Milliseconds–8 s	10–15%	Minutes–hours	200–300	1000–10,000	
Flywheel	0–250 kW	Milliseconds–15 min	100%	Seconds–minutes	250–350	1000–5000	3–25
Capacitor	0–50 kW	Milliseconds–60 min	40%	Seconds–hours	200–400	500–1000	
Super-capacitor	0–300 kW	Milliseconds–60 min	20–40%	Seconds–hours	100–300	300–2000	2–20
AL-TES	0–5 MW	1–8 h	0.5%	Minutes–days		20–50	
CES	100 kW–300 MW	1–8 h	0.5–1.0%	Minutes–days	200–300	3–30	2–4
HT-TES	0–60 MW	1–24 h+	0.05–1.0%	Minutes–months		30–60	

Table 1 Comparison of technical characteristics of EES systems [16].

2.3.6.4. Capital cost

Table 2 provides relevant information on costs per kWh, per kW, and kWh per cycle, which is useful for evaluating the cost of storage in frequent charging and discharging applications, such as load leveling. The cost per cycle is defined as the cost per unit of energy divided by the useful life of the cycle, and the costs per unit of energy are adjusted for storage efficiency to obtain the cost per useful output energy.

It is important to note that this comparison does not consider operating, maintenance, disposal, replacement and other ownership costs, as some of this data is not available for emerging technologies. For example, lead-acid batteries may appear to be an economical option due to their low capital cost, but their lifetime is relatively short for certain applications, which may not make them the most cost-effective option for energy management, such as load leveling.

In terms of capital cost, sodium-sulfur (NaS) and lithium-ion batteries have slightly higher costs compared to high-head water pumping systems (PHS), although this difference is gradually narrowing. Metal-air batteries have high energy density and reduced costs, but their life cycle is limited, and they are still under development. Compressed air energy storage systems (CAES) are competitive from an economic perspective due to their low overall cost.

ETSEIB

As for supercapacitor, flywheel and superconducting magnetic energy storage (SMES), they are suitable for high-power, short-duration applications, as they are economical in terms of power output, but expensive in terms of energy storage capacity. Fuel cells will require more time to become economically competitive due to their high cost per cycle.

It is important to note that this comparison is based on a preliminary study conducted in 2009, so the capital costs of energy storage systems may have changed significantly since then. Factors such as system size, plant location, construction time and costs, as well as technological advances, may influence these variations.

Systems	Energy and power density				Life time and cycle life		Influence on environment	
	Wh/kg	W/kg	Wh/L	W/L	Life time (years)	Cycle life (cycles)	Influence	Description
PHS	0.5–1.5		0.5–1.5		40–60		Negative	Destruction of trees and green land for building the reservoirs
CAES	30–60		3–6	0.5–2.0	20–40		Negative	Emissions from combustion of natural gas
Lead-acid	30–50	75–300	50–80	10–400	5–15	500–1000	Negative	Toxic remains
NiCd	50–75	150–300	60–150		10–20	2000–2500		
NaS	150–240	150–230	150–250		10–15	2500		
ZEBRA	100–120	150–200	150–180	220–300	10–14	2500+		
Li-ion	75–200	150–315	200–500		5–15	1000–10,000+		
Fuel cell	800–10,000	500+	500–3000	500+	5–15	1000+	Negative	Remains and/or combustion of fossil fuel
Metal-Air	150–3000		500–10,000			100–300	Small	Little amount of remains
VRB	10–30		16–33		5–10	12,000+	Negative	Toxic remains
ZnBr	30–50		30–60		5–10	2000+		
PSB	–	–	–	–	10–15			
Solar fuel	800–100,000		500–10,000		–	–	Benign	Usage and storage of solar energy
SMES	0.5–5	500–2000	0.2–2.5	1000–4000	20+	100,000+	Negative	Strong magnetic fields
Flywheel	10–30	400–1500	20–80	1000–2000	~15	20,000+	Almost none	
Capacitor	0.05–5	~100,000	2–10	100,000+	~5	50,000+	Small	Little amount of remains
Super-			capacitor	2.5–15	500–5000			100,000+
						10–30		
20+		100,000+	Small	Little amount of remains				
AL-TES	80–120		80–120		10–20		Small	
CES	150–250	10–30	120–200		20–40		Positive	Removing contaminates during air liquefaction (Charge)
HT-TES	80–200		120–500		5–15		Small	

Table 2 Comparison of technical characteristics of EES systems [16].

2.4. Photovoltaic solar energy

Solar photovoltaic energy is a form of renewable energy produced from the direct conversion of sunlight into electricity using solar cells. This technology has become one of the main sources of renewable energy worldwide due to its great potential and numerous advantages, such as its low environmental impact, low long-term cost, and its ability to generate electricity in remote areas.

Solar photovoltaic energy is produced through the use of solar cells, which convert sunlight into electricity. Solar cells are made up of layers of semiconductor materials, such as silicon,

ETSEIB

which have the property of releasing electrons when exposed to sunlight.

The process of converting sunlight into electricity is based on the photoelectric effect, which was discovered by Albert Einstein in 1905. This effect occurs when a photon of light strikes an electron in a layer of semiconductor material, thereby releasing an electron. These released electrons travel along an electrical circuit, thus generating an electric current.

The efficiency of solar cells is measured in terms of the amount of solar energy that is converted into electricity. The efficiency of solar cells varies depending on factors such as the quality of the materials used, cell design and climatic conditions. Current commercial solar cells have a typical efficiency of 15% to 20% [33].

2.4.1. Solar Resource

The solar resource is the amount of solar energy that reaches the earth's surface in a specific area during a given period of time. The amount of solar energy reaching the earth's surface varies with geographic location, time of day, time of year, and climatic conditions.

The solar energy reaching the earth's surface can be measured using instruments such as pyranometers and solar radiometers. These instruments measure global solar radiation, which is the amount of solar energy reaching the earth's surface from all directions.

The amount of solar energy available at a specific location can be calculated using solar radiation models or using measured data from weather stations. Solar radiation models use factors such as geographic location, altitude, solar panel orientation and climatic conditions to estimate the amount of solar energy available at a specific location [33].

2.4.2. Types of technology

There are several types of PV technologies available today. These include [33]:

1. Monocrystalline silicon solar cells - These solar cells are made from a single piece of crystalline silicon and are the most efficient at converting sunlight into electricity. They are also the most expensive.
2. Polycrystalline silicon solar cells: These solar cells are made of silicon fragments fused together and have slightly lower efficiency than monocrystalline silicon cells but are less expensive.
3. Thin film solar cells: These solar cells are produced by depositing a thin layer of semiconductor material on a substrate. They are less efficient than silicon solar cells but are less expensive and can be produced in large quantities.
4. Organic solar cells: These solar cells are produced using organic materials, such as polymers, instead of inorganic materials such as silicon. Although they currently have a much lower efficiency than silicon solar cells, their low cost and flexibility make them attractive for specific applications, such as consumer electronics.

2.4.3.   Applications

Solar photovoltaics are used in a wide variety of applications, from generating electricity in large solar power plants to powering small electronic devices. Some of the most common applications of solar PV include [33]:

1. Electrical power generation in large solar power plants: solar power plants are large installations that use thousands of solar panels to generate electrical power on a large scale.
2. Residential solar power systems: These systems use solar panels to generate electricity for residential use. The systems can be grid-connected or stand-alone.
3. Solar energy systems for remote applications: These systems use solar panels to generate electricity in remote areas where there is no access to the electrical grid.
4. Solar power systems for consumer electronics: These systems use solar cells to power portable electronic devices such as cell phones, watches, and calculators.

ETSEIB

3. Methodology

3.1. Voltage Source Converter

Power electronics is a fundamental technology that enables the transformation of conventional electrical systems into smart grids. These systems are capable of controlling power flows and voltages in a matter of milliseconds. In particular, alternating current to direct current (AC-DC) converters with bidirectional power capability are key elements in the implementation of microgrids [34]

The system under analysis is shown in Figure 9. It is a three-phase three-wire electrical network. In this system, a two-level voltage source converter (VSC) is used to exchange power between the alternating current (AC) side and the direct current (DC) side. The VSC consists of three branches, each equipped with two IGBTs (Insulated Gate Bipolar Transistors). The midpoint of these branches is connected to the mains through inductances that allow a smooth connection between the converter and the mains. By means of a suitable modulation of the IGBT switches, the desired three-phase voltages are generated on the AC side, which allows controlling the flow of active and reactive power.
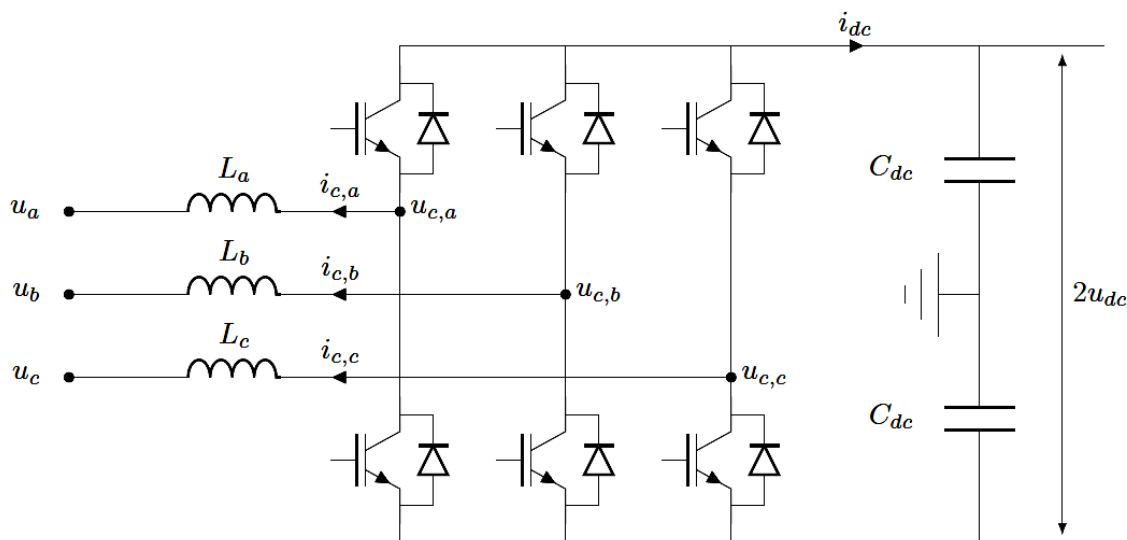

Figure 9 VSC Schematic [34].

In the context of photovoltaic and battery storage systems, bidirectional AC-DC converters are necessary to inject power into the grid. These converters play an essential role in the interconnection between solar generation systems and the conventional power grid.

The VSC (Voltage Source Converter) is a crucial component in power systems, enabling the conversion of alternating current (AC) to direct current (DC) and vice versa. Although the operation of the VSC converter is based on the discrete switch states of IGBTs (insulated gate bipolar transistors), for control design purposes it is convenient to use a more simplified equivalent model.

A voltage source converter can be represented as the connection of two distinct sources: DC and AC. The generation and/or storage elements are connected to the DC side and can be represented as a voltage or current source connected in parallel with a capacitor, denoted as C (Figure 10). On the other side of the converter, the power grid is connected and represented as a three-phase voltage source.
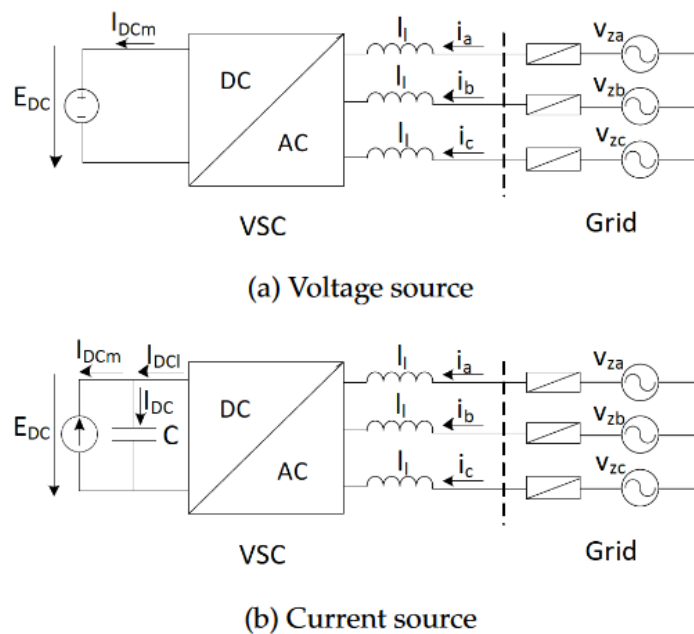

(a) Voltage source

(b) Current source

Figure 10 DC Sources [34].

In the context of (Figure 10), considering the inductance, denoted as Ll, a current source is assumed. Therefore, the converter can be connected to the power grid.

It is worth noting that this simplified representation facilitates control design and analysis, while still capturing the fundamental behavior of the VSC converter. In practice, the converter's design and implementation may involve additional components and considerations to ensure reliable and efficient operation. Further exploration of specific control strategies and detailed models is recommended for a comprehensive understanding of VSC converters and their integration into power systems.

The simplified model of the VSC converter can be obtained by decoupling the DC and AC parts of the converter (Figure 11). On the DC side, the model includes a current source and

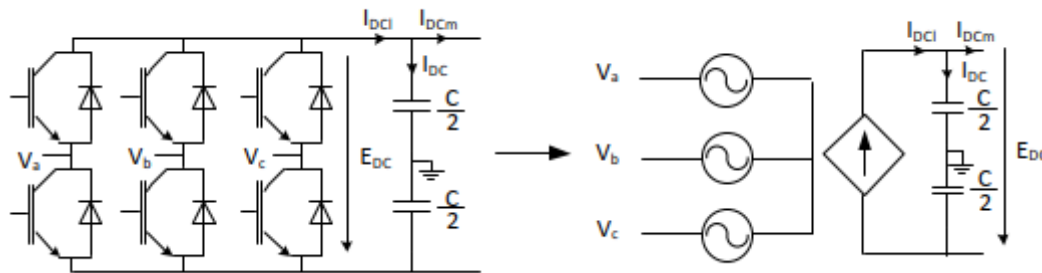a capacitor, while on the AC side AC voltage sources are used.

Figure 11 Simplified model [34].

On the DC side, the current source represents the active power exchange between the AC side and the DC side and ensures the power balance in the system. The dc source current can be calculated considering that the converter losses are negligible:

Equation 2

$$IDCl = \frac{P_{ac}}{E_{DC}}$$

Where I_{DCl} is the source DC current, Pac is the active power exchanged between the VSC converter and the grid on the AC side, and E_{DC} is the DC bus voltage.

The capacitor voltage on the DC side is obtained from the differential equation:

Equation 3

$$IDC = C\frac{dEDC}{dt} \rightarrow I_{DCl} - I_{DCm} = C\frac{dEDC}{dt}$$

Integrating this expression, the DC voltage can be expressed as a function of current:

Equation 4

$$E_{DC} = E_{DC0} + \frac{1}{C}\int_{0}^{t} I_{DC} = E_{DC0} + \frac{1}{C}\int_{0}^{t} (I_{DCl} - I_{DCm})$$

Where E_{DC0} is the initial DC bus voltage, C is the capacitor capacitance, I_{DCl} is the source DC current, and I_{DCm} is the average converter DC current.

By using the simplified model, a more convenient representation for the control design of the VSC converter is achieved. This provides a better understanding of the converter behavior and facilitates the implementation of appropriate control strategies to ensure

optimal system operation.

3.2. Clarke Transformation

The Clarke transform is a mathematical technique used in power system theory to analyze three-phase systems. The Clarke transform converts a three-phase signal into a two-dimensional orthogonal coordinate system. These coordinates are called Clarke's α and β components. The Clarke transform is useful in applications such as measuring three-phase currents and voltages, eliminating unbalance, and detecting faults in electric motors.

The Clarke transform is mathematically defined as:

Equation 5

$$[x_{\alpha\beta0}] = [T_{\alpha\beta0}][x_{abc}]$$

This expression can also be written as:

Equation 6

$$\begin{bmatrix} x_\alpha \\ x_\beta \\ x_0 \end{bmatrix} = \begin{bmatrix} \dfrac{2}{3} & -\dfrac{1}{3} & -\dfrac{1}{3} \\ 0 & \dfrac{\sqrt{3}}{3} & \dfrac{-\sqrt{3}}{3} \\ \dfrac{1}{3} & \dfrac{1}{3} & \dfrac{1}{3} \end{bmatrix} \begin{bmatrix} x_a \\ x_b \\ x_c \end{bmatrix}$$

where Iα and Iβ are the Clarke components, I0 is the zero component, Ia, Ib and Ic are the phase currents.

The zero component (I0) represents the average value of the three-phase signal. The Clarke components (Iα and Iβ) represent the magnitude and phase of the positive components of the three-phase signal [37]..

The inverse Clarke transform is used to obtain the phase currents from the Clarke components. This transform is mathematically defined as:

Equation 7

$$[x_{abc}] = [T_{\alpha\beta0}]^{-1}[x_{\alpha\beta0}]$$

ETSEIB

Design and simulation of converter operating in a
renewable energy based smart grid
Pág. 39

This expression can also be written as:

Equation 8

$$\begin{bmatrix} x_a \\ x_b \\ x_c \end{bmatrix} = \begin{bmatrix} 1 & 0 & 1 \\ -\dfrac{1}{2} & \dfrac{\sqrt{3}}{2} & 1 \\ -\dfrac{1}{2} & \dfrac{-\sqrt{3}}{2} & 1 \end{bmatrix} \begin{bmatrix} x_\alpha \\ x_\beta \\ x_0 \end{bmatrix}$$

where x_α and x_β are the Clarke components, x_0 is the zero component, x_a, x_b and x_c are the phase currents.

The αβ plane representation is a graphical representation commonly used in control systems and three-phase electrical system analysis. It is derived from the Clarke transform, which converts three-phase signals into two orthogonal components: α and β [37]..
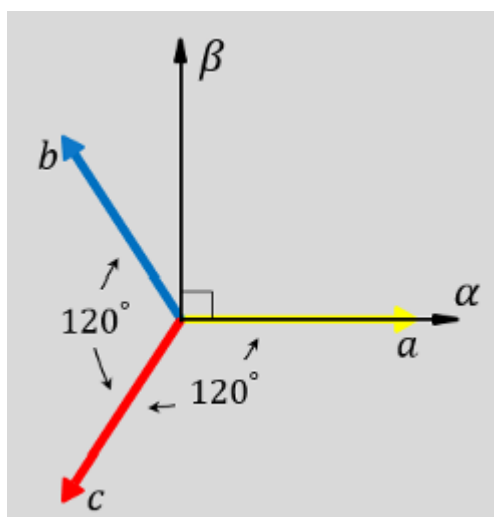

Figure 12 αβ plane representation Clarke transformation [35].

In this transformation, the instantaneous signals x_a, x_b and x_c, represent the voltage or current values in the abc frame, are converted to the transformed quantities x_α, x_β and x_0 in the $\alpha\beta 0$ frame.

In the $\alpha\beta$-plane representation (Figure 12), the α-axis represents the direct component, while the β-axis represents the quadrature component. These components are obtained from the original three-phase signals using the Clarke transform. The $\alpha\beta$ plane provides a convenient way to visualize and analyze the behavior of three-phase systems, especially in control applications.

By representing the three-phase signals in the $\alpha\beta$ plane, various analysis techniques can be applied, such as vector control, Park transform and space vector modulation. These techniques allow decoupling of control variables and simplify the implementation of control algorithms in three-phase systems.

The $\alpha\beta$-plane representation is widely used in fields such as power electronics, electric drives and renewable energy systems. It enables clear visualization of system dynamics, simplifies control design and facilitates analysis of system performance and stability [37]..

3.2.1. Instantaneous Power Theory in the αβ0 Frame

In a three-phase three-wire system, the voltage source converter (VSC) consists of three branches and a two-stage insulated gate bipolar transistor (IGBT). The generation or storage source can be connected to the direct current (DC) side of the converter and can be modeled as a DC voltage source or as a current source with a shunt capacitor. On the other hand, the alternating current (AC) side can be modeled using the Thevenin equivalent model of the mains source, or in a more simplified way, as an AC voltage source with inductances that allow it to be considered as an AC source.

In a balanced three-phase system, the instantaneous voltages and currents are expressed as a function of time by the following equations:

Equation 9

$$x_a(t) = \sqrt{2}X \cos(\omega t + \phi)$$

Equation 10

$$x_b(t) = \sqrt{2}X \cos\left(\omega t + \phi - \frac{2\pi}{3}\right)$$

Equation 11

$$x_c(t) = \sqrt{2}X \cos\left(\omega t + \phi + \frac{2\pi}{3}\right)$$

By transforming these sinusoidal signals from system abc to phasors in system $\alpha\beta0$, the three signals are expressed as follows:

Equation 12

$$x\alpha = \sqrt{2}X \cos(\omega t + \phi)$$

Equation 13

$$x\beta = -\sqrt{2}X \cos(\omega t + \phi)$$

Design and simulation of converter operating in a
renewable energy based smart grid
Pág. 41

Equation 14

$$x0 = 0$$

Neglecting the zero components, which are always 0 in a balanced three-phase system, the phasor representation of the rest of the two signals in the system $\alpha\beta$ is expressed as:

Equation 15

$$\sqrt{2}\underline{V^{\alpha\beta}} = v_\alpha - jv_\beta$$

Equation 16

$$\sqrt{2}\,\underline{I^{\alpha\beta}} = i_\alpha - ji_\beta$$

The power in a three-phase system can be expressed as:

Equation 17

$$\underline{S} = P + jQ = P + jQ = 3\underline{V^{\alpha\beta}}\,\underline{I^{\alpha\beta*}} = 3\,\left(\frac{v_\alpha - jv_\beta}{\sqrt{2}}\right)\left(\frac{i_\alpha + ji_\beta}{\sqrt{2}}\right)$$

By decoupling the active and reactive power, they can be expressed as:

Equation 18

$$P = \frac{3}{2}\,(v_\alpha i_\alpha + v_\beta i_\beta)$$

Equation 19

$$Q = \frac{3}{2}\,(v_\alpha i_\beta + v_\beta i_\alpha)$$

Therefore, the expression of active and reactive power as functions of voltages and currents in the αβ0 frame have been obtained [37].

3.3. Park Transformation

To design the control part of the system, it is necessary to have constant electrical quantities instead of oscillating ones, as in the αβ0 reference frame, which shares the same nature as the abc frame. To achieve this, a third reference frame is introduced, where the quantities remain constant through the use of the Park transformation and the synchronous reference frame. The Park transformation can be represented as [37].:

Equation 20

$$[x_{\alpha\beta 0}] = [T_{\alpha\beta 0}][x_{abc}]$$

The transformation matrix is:

Equation 21

$$T(\theta) = \frac{2}{3}\begin{bmatrix} \cos(\theta) & \cos\left(\theta - \frac{2\pi}{3}\right) & \cos\left(\theta + \frac{2\pi}{3}\right) \\ \sin(\theta) & \sin\left(\theta - \frac{2\pi}{3}\right) & \sin\left(\theta + \frac{2\pi}{3}\right) \\ \frac{1}{2} & \frac{1}{2} & \frac{1}{2} \end{bmatrix}$$

The inverse of this matrix is:

Equation 22

$$T^{-1}(\theta) = \frac{2}{3}\begin{bmatrix} \cos(\theta) & \sin(\theta) & 1 \\ \cos\left(\theta - \frac{2\pi}{3}\right) & \sin\left(\theta - \frac{2\pi}{3}\right) & 1 \\ \cos\left(\theta + \frac{2\pi}{3}\right) & \sin\left(\theta + \frac{2\pi}{3}\right) & 1 \end{bmatrix}$$

The Park transformation can be better visualized through its geometrical representation (Figure 13).
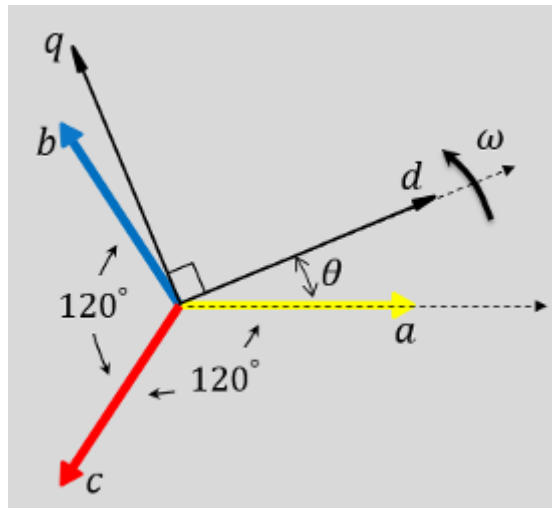

Figure 13 qd plane representation Park transformation [36].

3.3.1. Instantaneous Power Theory in the Synchronous Reference Frame

As mentioned previously, in order to achieve constant steady-state quantities, the angle θ
used in the Park transformation corresponds to the electrical voltage angle. By substituting
θ with the electrical angle θ = ωt + φ0, and transforming the abc voltages and currents into
the qd0 frame, we can define the following voltage and current phasors, similar to the Clarke
transformation [37].:

Equation 23

$$\underline{V}^{qd} = \frac{v_q\sqrt{-jv_d}}{2}$$

Equation 24

$$\underline{I}^{qd} = \frac{i_q\sqrt{-ji_d}}{2}$$

In this case, the power of a three-phase system can be expressed as:

Equation 25

$$\underline{S} = P + jQ = P + jQ = 3\underline{V}^{qd}\,\underline{I}^{qd*} = 3\,(\frac{v_q - jv_d}{\sqrt{2}})\,(\frac{i_q + ji_d}{\sqrt{2}})$$

Reordering this expression, the active and reactive power can be expressed as functions
of voltages and currents in the qd0 frame [37].:

Equation 26

$$P = \frac{3}{2}\,(v_q i_q + v_d i_d)$$

Equation 27

$$Q = \frac{3}{2}\,(v_d i_d + v_d i_d)$$

The voltages in the qd0 frame can be represented accordingly.

3.4. Current loop control

The current loop is a fundamental component in controlling a voltage source converter as it enables the regulation of the current flowing from the converter to the grid. Two different control approaches exist for managing the q and d components of the current [37]:

- Multivariable control: This approach utilizes a single two-dimensional controller to control both components simultaneously.
- Decoupling control: This approach focuses on independently controlling the q and d components in the synchronous reference frame.

In this project, the second approach will be employed, requiring voltage decoupling. The decoupling equations are as follows:

Equation 28

$$\begin{bmatrix} v_{lq} \\ v_{ld} \end{bmatrix} = \begin{bmatrix} -\hat{v}_{lq} + v_{zq} - l_l\omega_e i_{ld} \\ -\hat{v}_{ld} + l_l l_l \omega_e i_{lq} \end{bmatrix}$$

Where $\hat{v}_{lq}$ and $\hat{v}_{ld}$ are the outputs of the current controllers, and v_{lq} and v_{ld} are the voltages to be applied by the converter. Substituting these values into the voltage equations:

By applying the Laplace transformation, the transfer functions between the controller voltages and converter currents can be derived:

Equation 29

$$\frac{i_q(s)}{\hat{v}_{lq}(s)} = \frac{1}{l_{ls} + r_l}$$

Equation 30

$$\frac{i_d(s)}{\hat{v}_{ld}(s)} = \frac{1}{l_{ls} + r_l}$$

The proportional and integrator constants can be calculated as follows:

Equation 31

$$K_p = \frac{l_l}{\tau}$$

Design and simulation of converter operating in a
renewable energy based smart grid
Pág. 45

Equation 32

$$K_i = \frac{r_l}{\tau}$$

Where τ represents the closed-loop time constant of the electrical system, which must be chosen considering the physical limitations of the converter. The overall current controller can be implemented accordingly [37].
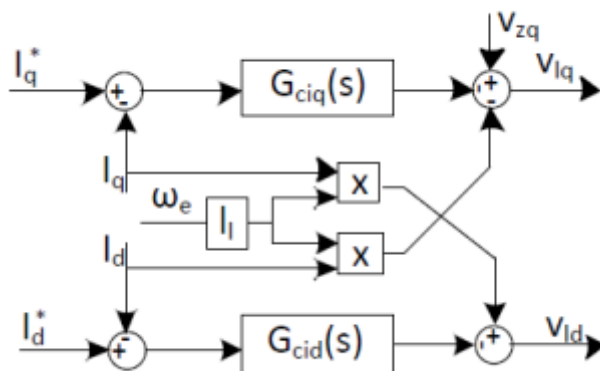

Figure 14 Current controller schematic [37].

3.5. Phase locked loop (PLL)

A phase-locked loop (PLL) is utilized for determining the angle and angular velocity of an electrical network. In a three-phase PLL, the d-axis voltage component is fed back through a PI controller. The controller output provides the electrical grid's angular velocity (ω_e), and integrating this signal yields the grid angle (θ_e). Figure 15 illustrates a typical PLL configuration [37].
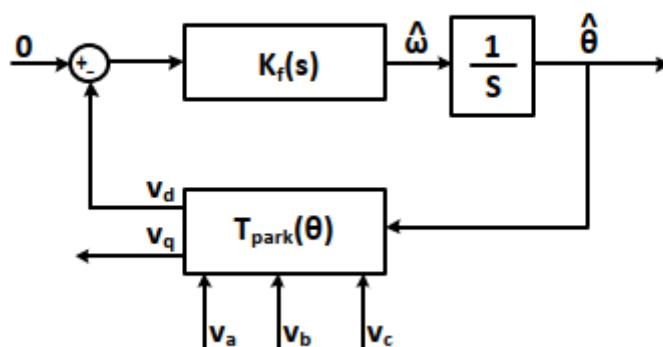

Figure 15 Phase locked loop scheme [37].

ETSEIB

To analyze the PLL controller design, it is possible to linearize the system by assuming a small angle error. The resulting second-order system is expressed as follows:

Equation 33

$$\frac{\hat{\theta}(s)}{\theta(s)} = \frac{2\xi\omega_n s + \omega_n^2}{s^2 + 2\xi\omega_{n+\omega_n^2}}$$

In this equation, $\hat{\theta}(s)$ represents the estimated grid angle, and $\theta(s)$ represents the real grid angle.

The PLL controller is defined as:

Equation 34

$$K_f(s) = K_p\left(\frac{\dfrac{1}{\tau_{PLL}} + s}{s}\right)$$

where τ_{PLL} is the PLL time constant.

The controller parameters, Kp and τPLL, can be computed using Equation X:

Equation 35

$$\omega_n = \sqrt{\frac{K_p E_m}{\tau_{PLL}}}$$

Equation 36

$$\xi = \sqrt{\frac{\tau_{PLL} K_p E_m}{2}}$$

where, E_m denotes the admitted peak voltage value, ξ represents the damping ratio, and ω_n indicates the electrical angular velocity [37].

ETSEIB

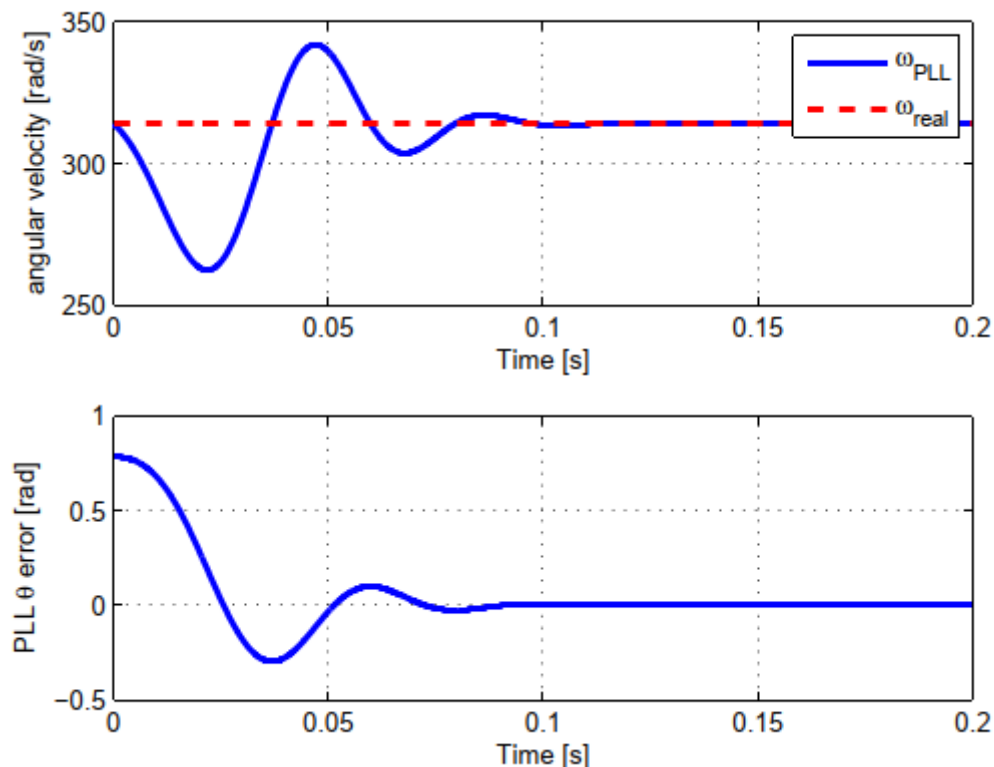Figure 16 provides an example of the initial transient of a PLL.

Figure 16 PLL Initial transient [37].

3.6. DC Voltage control

The control system described here necessitates a DC voltage regulator to manage the voltage of the DC bus, thereby ensuring power balance between the AC and DC sides of the converter. The outlined control scheme is depicted as follows:
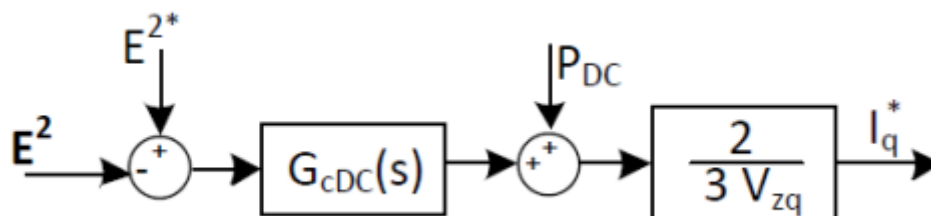

Figure 17 DC Voltage control schematic [37].

The control scheme proposed is illustrated in Figure 13, indicating that the variable under control is E2, and a feed-forward scheme is employed to enhance the system's response. This approach is commonly used as E2 is directly proportional to the energy stored in the

capacitor, and the controller's output is the active power injected into the capacitor, denoted as PC. Consequently, the power reference for the power converter will be $P^* = P_C^* + P_{DC}$, where P_{DC} represents the measured power before the capacitor [37].

The P controller will be modeled using the following equation:

Equation 37

$$Kp_{DC} = \frac{C}{2 * \tau_E}$$

where τ_E is the desired DC voltage response time constant [37].

3.7. Power Block

3.7.1. PV Array

The current equation for a photovoltaic panel can be modeled using the equation for the current of a photovoltaic cell, which takes into account several factors. A common way to represent this equation is as follows:

Equation 38

$$I = I_{pv} - I_0 \left[\exp \frac{(V + R_S I)}{V_t a} - 1 \right] - \frac{V + R_S I}{R_p}$$

where,

- I is the output current of the photovoltaic panel.
- I_{pv} is the current photogenerated by the incident solar radiation.
- I_0 is the reverse saturation current or dark current of the panel.
- V is the voltage across the panel.
- R_S is the series resistance of the panel.
- V_t is the thermal voltage or equivalent voltage of the photovoltaic cell.
- n is the ideality factor.
- R_p is the parallel resistance of the panel.

This equation takes into account the PV current generation, the dark or reverse saturation current, the losses due to the series resistance and the parallel resistance of the panel.

It is important to note that this equation is a simplified representation and there are other factors that can affect the output current of a PV panel, such as temperature, solar irradiance and specific panel characteristics. In practical applications, it is common to use

more detailed models and consider other factors to obtain a more accurate prediction of PV panel current.

Solar photovoltaics is a form of electricity generation from solar radiation using solar cells. Solar cells, also known as solar panels, convert solar energy into electricity through the photovoltaic effect.

The current generated by a photovoltaic panel depends on several factors, including the intensity of the incident solar radiation, the temperature, the characteristics of the semiconductor material, and the electrical components of the panel.

The current equation I mentioned above is a simplified way of modeling the current of a PV panel. Let me explain some of the terms and concepts involved:

Photogenerated current (I_{pv}): This is the current generated by the solar radiation incident on the surface of the PV panel. This current depends on the intensity of the solar radiation and the efficiency of the panel. This current can be calculated using the datasheet parameters and the irradiance and temperature (standard values have been calculated with an arbitrary temperature of "25ºC" and irradiance of "1000 W/m2"). A common way to represent this equation is as follows:

Equation 39

$$I_{pv} = \left[I_{pv,n} + K_I(T - T_n)\right]\frac{G}{G_n}$$

where,

- $I_{pv,n}$ is the reference photogenerated current, which is obtained under reference temperature and irradiance conditions.
- K_I is the temperature coefficient of the photogenerated current, which indicates how the panel current varies with changes in temperature.
- T is the current temperature of the photovoltaic panel.
- T_n is the reference temperature.
- G is the current incident solar irradiance on the panel.
- G_n is the reference irradiance.

This equation takes into account the influence of temperature and irradiance on the photogenerated current, using the temperature coefficients and reference values to adjust the current. This allows a more accurate estimation of the current generated by the panel under different temperature and irradiance conditions.

It is important to note that the values of $I_{pv,n}$, K_I, T_n and G_n should be obtained from the PV panel specifications or from experimental tests performed on the panel to ensure the

accuracy of the results.

Inverse saturation current (I_0): This is a dark current flowing through the PV cell even in the absence of solar radiation. It represents the current flowing through the p-n junction of the cell when it is reverse polarized. This current can also be calculated with datasheet parameters and temperature. In the Simulink implementation of this equation, Vt was substituted to use T as a variable. A common way to represent this equation is as follows:

Equation 40

$$I_0 = \frac{I_{sc,n} + K_I(T - T_n)}{\exp\left[\dfrac{\left(V_{oc,n} + K_V(T - T_n)\right)}{(V_t a)}\right] - 1}$$

Where,

- $I_{sc,n}$ is the reference short-circuit current, which is obtained under reference temperature conditions.
- K_I is the temperature coefficient of the short-circuit current, which indicates how the short-circuit current varies with changes in temperature.
- T is the current temperature of the PV panel.
- T_n is the reference temperature.
- V_{oc},n is the reference open circuit voltage, which is obtained under reference temperature conditions.
- K_V is the temperature coefficient of the open-circuit voltage, which indicates how the open-circuit voltage varies with changes in temperature.
- V_t is the thermal stress of the panel, which is calculated as $V\_t = (k * T) / q$, where k is Boltzmann's constant and q is the elementary charge.

This equation takes into account the influence of temperature on the reverse saturation current, short circuit current and open circuit voltage, using temperature coefficients and reference values to adjust these parameters. This allows a more accurate estimation of the reverse saturation current at different temperature conditions.

As in the previous equation, it is important to obtain the values of $I_{sc,n}, K_I, T_n, V_{oc}, n, K_V$ and other constants from the PV panel specifications or from experimental tests to ensure the accuracy of the results.

Thermal voltage (V_t): Also known as equivalent cell voltage, this is a constant that depends on the semiconductor material used in the PV panel and the temperature. It is related to the voltage variation as a function of temperature.

ETSEIB

Series resistance (R_S): This is the resistance that represents the voltage losses due to the internal resistance of the panel and the connection cables. This resistance limits the panel current.

Ideality factor (n): It is a parameter that takes into account the imperfections and non-idealities of the photovoltaic cell. Typical values of n vary between 1 and 2.

Parallel resistance (R_p): This is the resistance that represents the current losses due to the leakage current and load losses of the panel. This resistance limits the current flowing through the panel when there is no solar radiation.

It is important to note that this simplified equation does not consider all aspects and factors that can influence the output current of a PV panel. In practical applications, more complex and detailed models are used to account for other variables such as temperature, solar irradiance, specific panel characteristics and environmental conditions.

Modeling and analysis of photovoltaic panels is a broad and complex field of study, involving aspects of semiconductor physics, electrical engineering, and materials science. More advanced techniques, such as single- or dual-diode modeling, are employed to more accurately account for the different effects and behaviors of PV panels. These more complex models can provide more accurate and detailed results for solar PV system design and analysis applications.

3.7.2. PV Boost Converter

Boost converters, also known as step-up converters, are commonly found in many modern electronic devices. They allow for the amplification of a direct current (DC) voltage to a higher magnitude. The characteristic circuit of the converter can be observed in Figure 18. Essentially, they are composed of a DC source, which in our case will be the photovoltaic plant, a switching device, and a low-pass filter that supplies power to a specific load. In our case, the switching device will be a MOSFET/IGBT transistor.
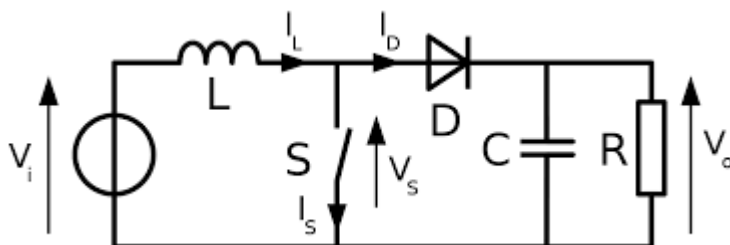

Figure 18 Boost Converter Circuit [38].

In our particular case, the load to be powered will be our DC bus connected to the VSC (Voltage Source Converter). Once the required voltage has been reached through the

Boost converter, it will be fed through a DC bus to a three-phase inverter that will power the pump.

3.7.3.   Battery Bidirectional Charger

A bi-directional battery charger (DC-DC Converter) is a device that allows both charging and discharging power from a battery. Unlike conventional unidirectional chargers, which only allow charging of one battery, bidirectional chargers provide the flexibility to feed power back to the grid or use it to power other devices.

This type of charger is especially useful in energy storage systems, where the ability to charge and discharge the battery as needed by the user is required. For example, in solar power applications, a bi-directional charger allows maximum use of the energy generated by the solar panels, storing the excess in the battery during the day and supplying it back to the grid or devices at night or at times of high demand. In Figure 19, the schematic of the charger with two IGBT/MOSFET devices can be seen.
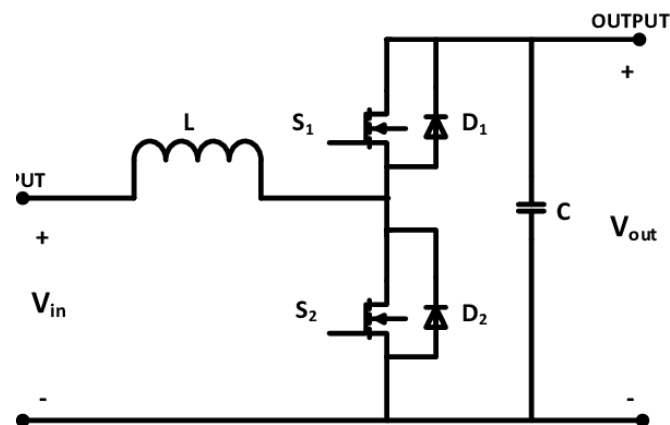
Figure 19 Bidirectional DC-DC Charger Circuit [39]

The bi-directional battery charger uses advanced control techniques to regulate the flow of energy in both the charging and discharging stages. This ensures efficient and safe charging of the battery, avoiding overcharging or excessive discharging that could damage the battery. In addition, the ability to discharge the battery in a controlled manner allows its use in backup power applications or to supply power to critical devices during power outages.

3.7.4.   Load Three Phase Inverter

A three-phase inverter is a device used to convert direct current into three-phase alternating current. In the context of our load (pump), a three-phase inverter is used to power and control the pump motor. The use of a three-phase inverter offers several advantages for pump operation. First, it allows precise control of the speed and torque of the pump motor, which makes it easier to adapt to different operating conditions and flow demand. This

ETSEIB

means that the pump can be adjusted to provide the right amount of liquid based on the needs of the system.

In addition, three-phase inverters offer higher energy efficiency compared to other control methods. By adjusting the frequency and output voltage, pump operation can be optimized to minimize energy losses and reduce long-term operating costs.

In summary, using a three-phase inverter to power a pump provides precise control, increased energy efficiency and motor protection. This ensures optimal pump operation and contributes to an efficient and reliable pumping system. Thus, as can be seen in Figure 20, we have three branches formed by two pairs of MOSFETs/IGBTs that will be responsible for feeding the three loads which, in our case, will be the stator winding.
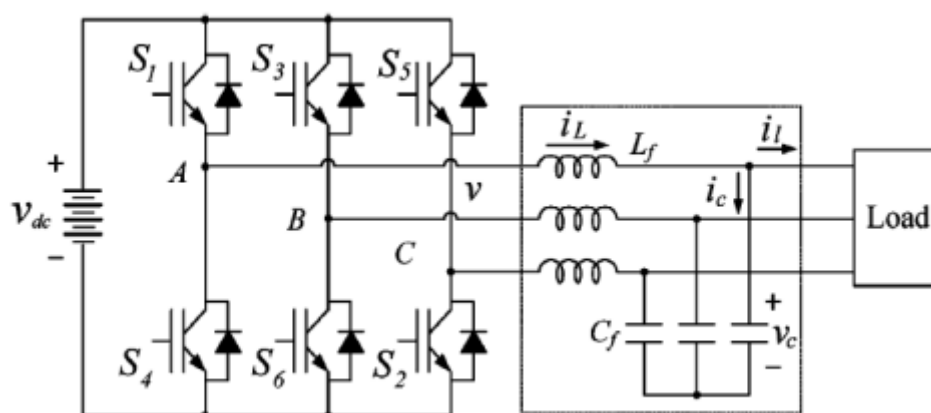
Figure 20 Three-phase inverter circuit [40].

In the specific case of three-phase wave cleaning in a three-phase inverter system to power a pump, the LC filter scheme can be implemented with the inductor (L) in series and the capacitor (C) in parallel. In our project, we have calculated them through an experimental process.

When the inductor is placed in series with the load (in this case, the pump), it acts as an impedance that limits the high-frequency current flow. This helps to reduce the harmonics generated by the inverter and smooth the current waveform. The inductor also provides greater system stability by helping to control current and voltage variations.

4. Case Study 1: PV Plant

The first case study focuses on grid connection of a photovoltaic plant using a Voltage Source Converter (VSC). Different control methods will be evaluated and compared for their effectiveness in this context.

4.1. Grid model

In this section, the model of the electrical grid to which the PV plant will be connected is discussed. The objective is to understand and adequately represent the characteristics and parameters of the grid to achieve an effective integration of the photovoltaic plant. Next, the schematic of the three-phase voltage source that will simulate the power grid will be detailed.

4.1.1. Three-phase voltage source

In Figure 21, the structure of the three-phase voltage source used in the model is shown. This structure is composed of three sinusoidal voltage sources out of phase with each other by 120 degrees.
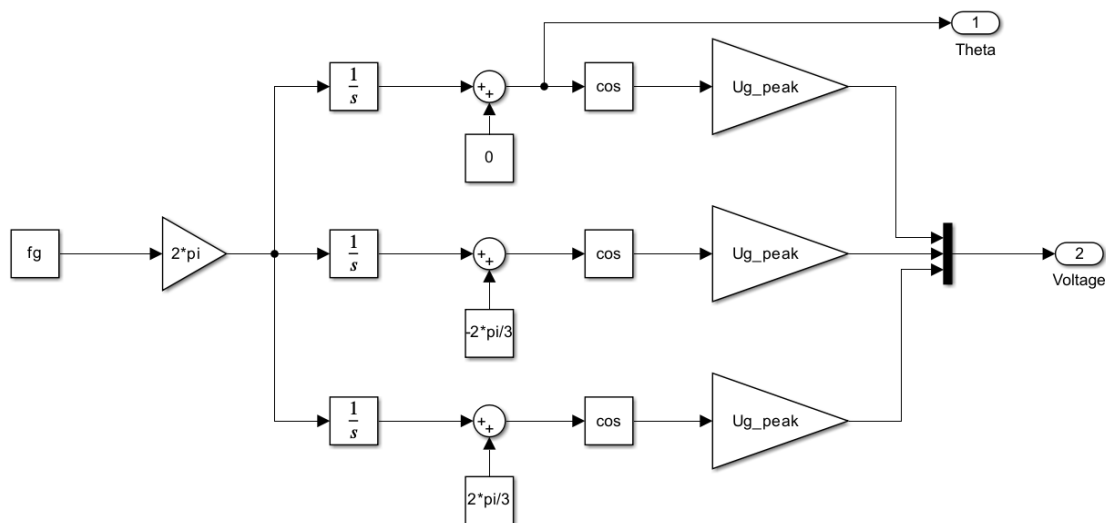
Figure 21 Three-phase voltage source in Simulink.

In the simulation, the grid frequency and the peak voltage are considered as known and predefined values in the MATLAB code. The frequency corresponds to the nominal frequency of 50 Hz. The peak voltage refers to the maximum value of the sinusoidal voltage in each phase, which will be 563.3826 V (Ug = 690 V).

From the voltage source unit, the theta angle is calculated and the grid voltage values in phases a, b and c are obtained. The theta angle is used to represent the phase difference between the phases of the electrical network and is set to 120 degrees.

Using these parameters, the sinusoidal voltage signals corresponding to each phase of the power grid can be generated, thus simulating the behavior of the three-phase voltage source.

It is important to note that the 120-degree delay between phases is fundamental to ensure the correct operation and synchronization of the system components, as well as to maintain the stability and quality of the energy supplied by the photovoltaic plant to the grid.

In order to verify the correct implementation of the above parameters and to check the proper alignment of the network phases, one can make use of Figure 22, which shows the theta angle and the phases of the electrical network.
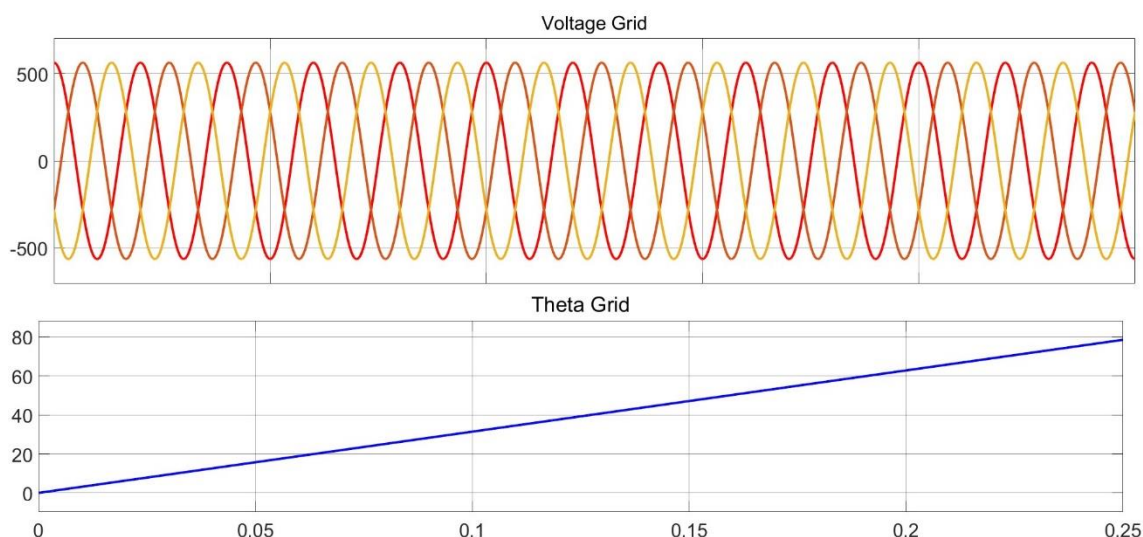
Figure 22 Grid voltages and angle.

4.2. VSC model

In this section, the model of the VSC (Voltage Source Converter) used in the integration of the photovoltaic plant to the grid is discussed. The VSC is responsible for converting the electrical energy generated by the solar panels into a form suitable for connection to the grid. The following are the subsections related to the VSC model.

4.2.1. Park Transformation

The Park transformation block is an essential component within the Phase-Locked Loop (PLL) in the VSC model. It is also used in the current control loop as the inverse Park

transformation. This block allows for a change of reference coordinate system from abc to qd0 and vice versa, facilitating the representation of voltages and currents in a stationary reference frame.

The Park transformation is responsible for rotating the reference frame by an angle theta, typically obtained from the PLL, and converting the grid voltages from the abc system to the qd0 system. By applying the rotation matrix to the grid voltages, the transformed voltages in the qd0 reference system can be obtained.

In the inverse Park transformation, the process is reversed. The transformed voltages in the qd0 reference system are multiplied by the inverse rotation matrix to obtain the voltages in the abc reference system. This is particularly useful in the current control loop, where the desired voltage values in the qd0 reference system are transformed back to the abc reference system for modulation and control purposes.

The Park transformation and its inverse are crucial for maintaining a constant voltage reference in the qd0 reference system, which simplifies the control algorithms and facilitates the regulation of voltages and currents in the VSC model.

In Figure 23, the input parameters required for the Park transformation block are the angle theta, typically obtained from the PLL, and the grid voltages in the abc reference system. For the inverse Park transformation, the input parameter is the voltage vector in the qd0 reference system.
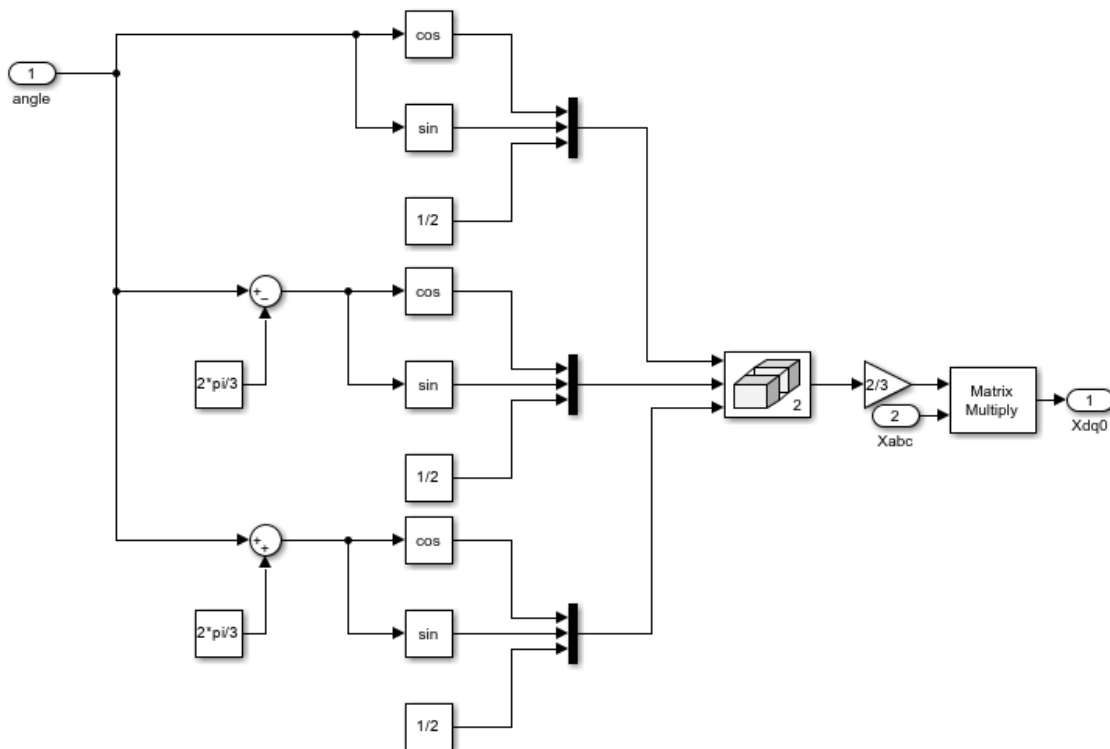
Figure 23 Park transformation in Simulink.

By utilizing the Park transformation and its inverse within the VSC model, the conversion between different reference systems becomes possible, enabling accurate voltage regulation and control in the system. To facilitate the implementation, the specific block called "Park Transformation" available in Simulink software will be used. This block provides dedicated functionality to perform the Park transformation accurately and efficiently. In Figure 24, the block can be seen in the system.
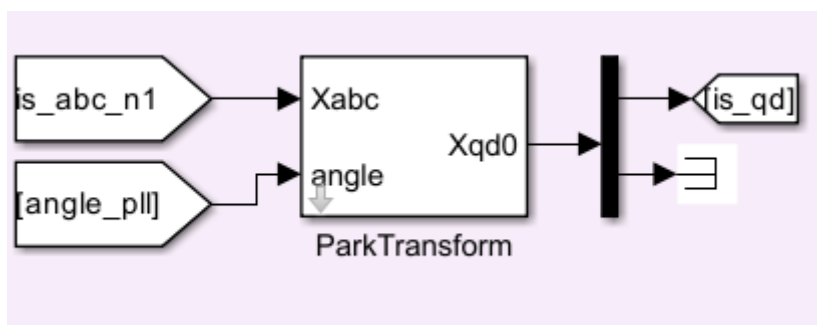
Figure 24 Park Transform predefined block.

To verify the correct operation of the system, it is important to ensure that the voltages in the reference system qd0 are correctly aligned. This check ensures that the voltage signals are in the proper position for processing and control.

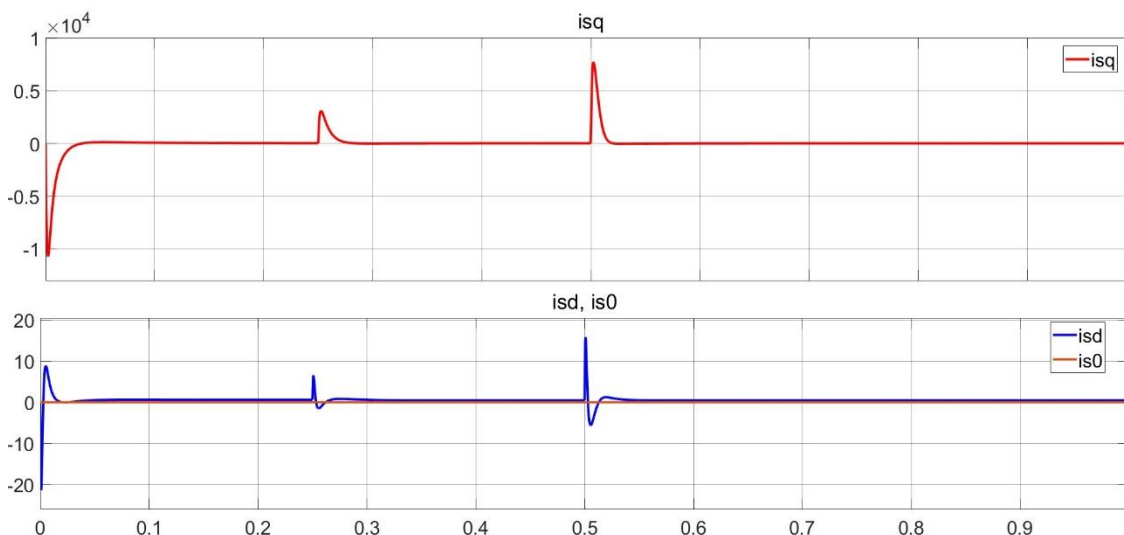A visual example of properly aligned qd0 voltages is shown in Figure 25.

Figure 25 Park transformation voltages.

By observing this graph, it is possible to verify if the stresses are in the expected position and if their behavior is consistent with the operating conditions. deseadas.

4.2.2. Phase-locked loop (PLL)

It is a closed-loop system that incorporates the Park transformation discussed earlier. The objective of the PLL is to synchronize the voltage and frequency of the inverter output with the grid. In the closed-loop PLL, one of the voltages from the qd0 reference system is regulated to have a value of zero, as shown in Figure 26. This process ensures that the inverter output voltage is aligned with the grid voltage.
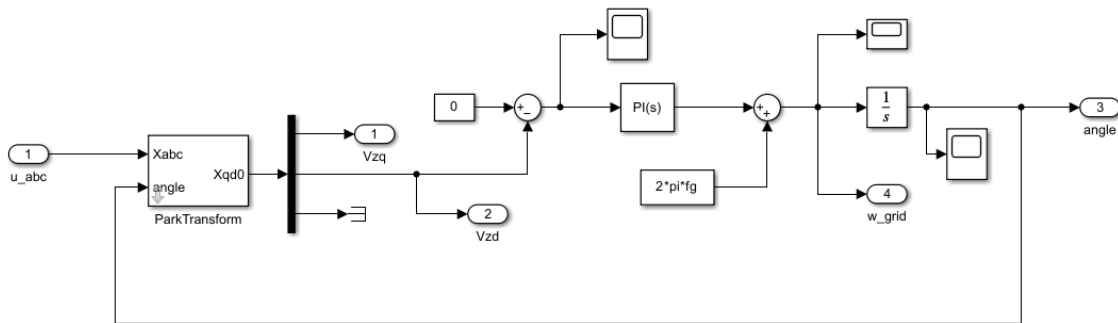

Figure 26 Phase-locked loop in Simulink.

Once the voltage is regulated to zero, the angle obtained in the control loop should match the angle of the grid voltage. This alignment can be verified by comparing the angles in Figure 27. If the angles match, it indicates that the PLL has achieved synchronization between the inverter and the grid.
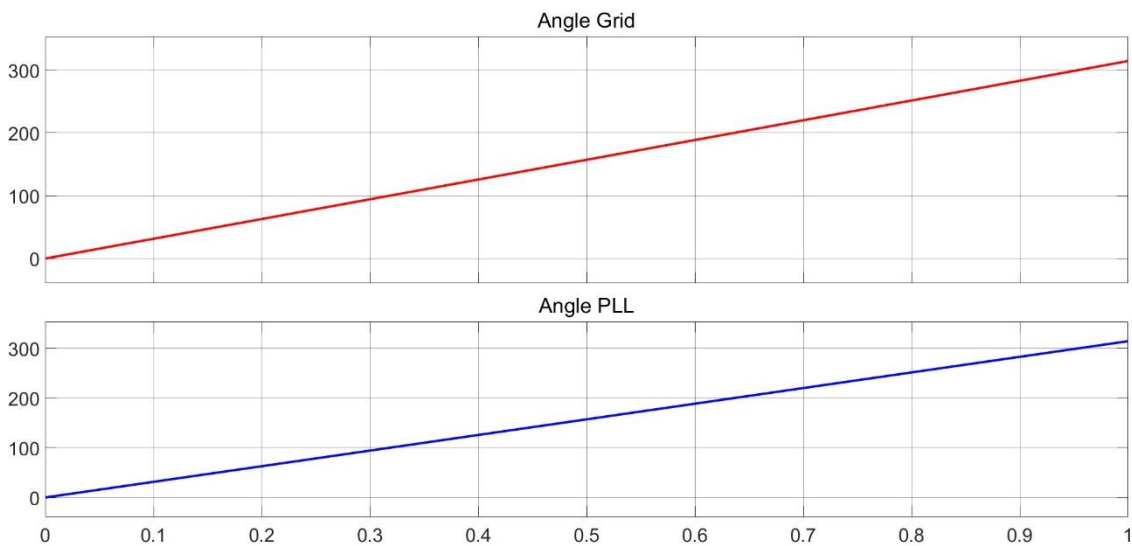

Figure 27 Angle Grid vs Angle PLL.

The PLL plays a crucial role in maintaining the stability and synchronization of the voltage source converter (VSC) with the grid. It allows the VSC to accurately track the grid voltage and frequency, enabling seamless integration of the PV plant into the grid.

4.2.3. Current control loop

The purpose of this subsystem is to calculate the voltage to be applied to the electrical network. To achieve this, Park's transformation is used to obtain the current values in the reference system qd0. Once these values are obtained, a control loop is used to calculate the voltage of the VSC (Voltage Source Converter). In addition, another important function is performed in this module, which is the decoupling of active and reactive power. This is crucial because it allows the active and reactive power to be regulated independently, i.e. without changing the value of the other power.

In this block, the desired current (reference current) is compared with the current qd0 calculated from the current value of the mains. In addition, the angle theta and the voltage qd0 are needed. The two current references are set as steps. In Figure 28, the main structure of the current control loop can be seen.
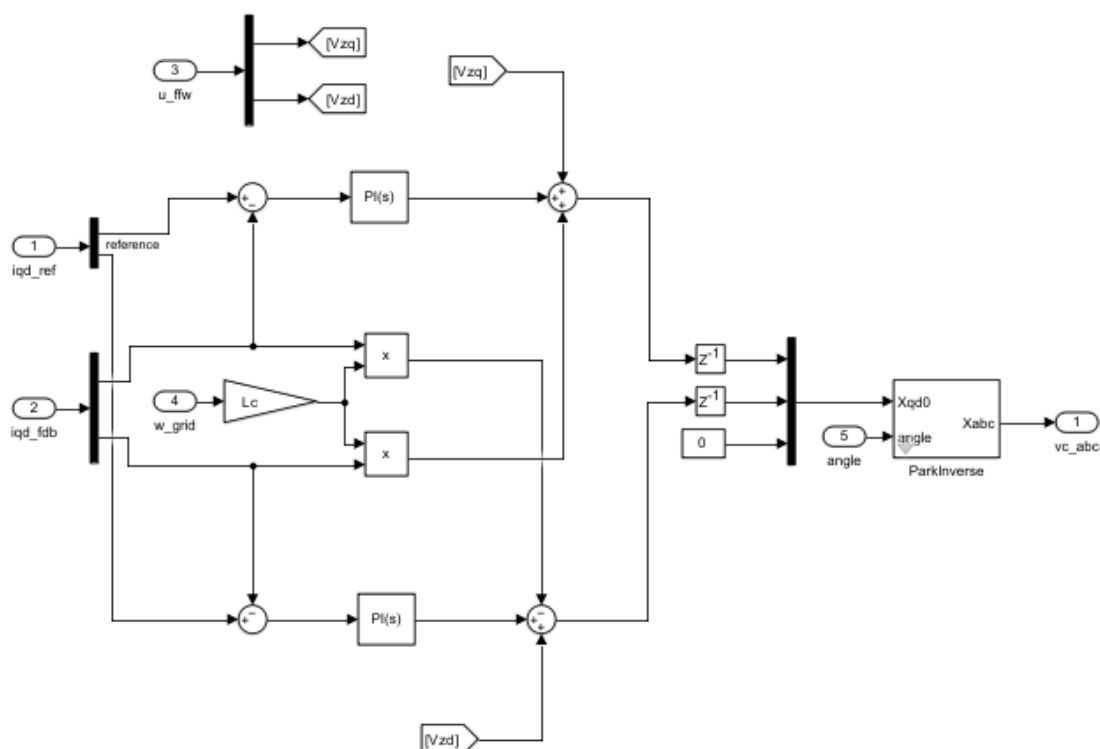

Figure 28 Current loop in Simulink.

4.2.4. Power control loop

Two different methods have been considered in order to implement the power control loop: the direct calculation of the current reference and the cascaded PI control. Both start from the reference power values to finally obtain the current, which is needed in the current control loop. Since the final control of our case study 1 will focus on the bus and reactive power, the results of this part will not be shown. However, in Annex 02, access to all simulations in .slxs format will be provided for further information. Two step blocks have been introduced in Simulink with the following base values.

4.2.4.1. Direct current reference calculation

It is a simple method to obtain the reference current without any additional controller. As its name indicates, it consists of the direct calculation of the current using the values of P and Q by means of the following equations:

Equation 41

$$i_q^* = \frac{2}{3} \frac{P^*}{v_{zq}}$$

Equation 42

$$i_d^* = \frac{2}{3} \frac{Q^*}{v_{zq}}$$

Based on the voltage measured at the PLL output and selecting the power reference values, the structure in Simulink is as shown in Figure 29.
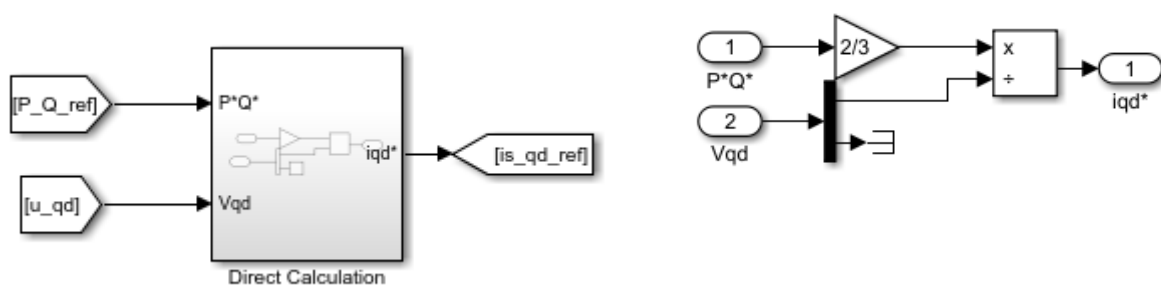

Figure 29 Direct current reference in Simulink.

4.2.4.2. Cascaded PI control

In this case, the current calculation is performed by a PI controller. In addition, the P and Q values of the mains are needed. For this purpose, the mains voltage and current as well as

Design and simulation of converter operating in a
renewable energy based smart grid
Pág. 61

the block "Power (3ph, instantaneous)" are required. The structure in Simulink is as shown in Figure 30.
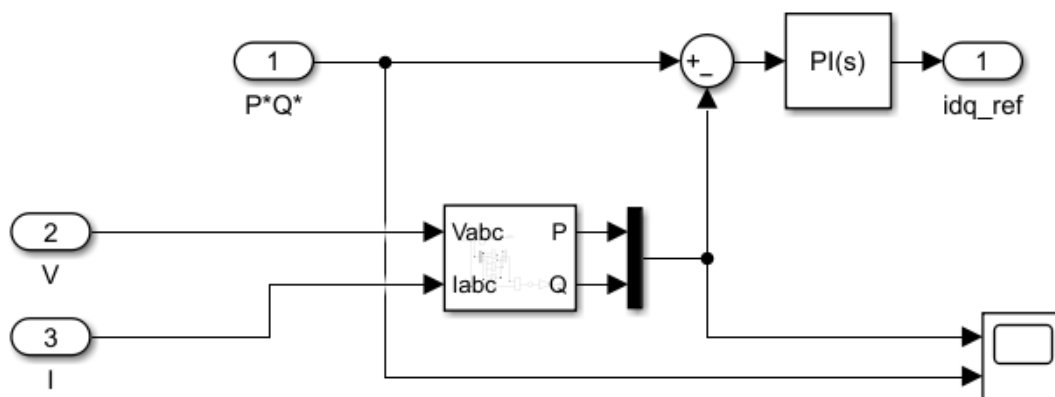

Figure 30 Cascade PI Control in Simulink 1.

A common power control loop has been used for P and Q, depending only on the proportional and integral values. As in the current control loop, a parameter τ_p has been set, whereby the proportional and integral values are regulated by the following equations:

Equation 43

$$k_{p\_p} = \frac{\tau_c}{\tau_p}$$

Equation 44

$$k_{i\_p} = \frac{1}{\tau_p}$$

4.3. PV Plant

In the first section, the modeling of the PV array will be addressed, which consists of developing a mathematical model that describes the behavior of the solar panels and their response to solar radiation and environmental conditions. Specific equations and parameters will be used to characterize the power generation of the PV array as a function of incident sunlight intensity, temperature and other relevant factors.

In the second section, Maximum Power Point Point Tracking (MPPT), which is a technique used to optimize the power generation efficiency of the PV array, will be discussed. MPPT

is responsible for tracking the optimal operating point of the PV array by continuously adjusting the input voltage or current to maximize the output power. Different MPPT algorithms will be explored and one of them will be implemented in Simulink to control the PV array and ensure its maximum power generation efficiency.

Both sections will be fundamental to understand and simulate the behavior of the PV plant and its interaction with the power grid in the context of renewable energy integration.

4.3.1. PV Array

The photovoltaic plant will be implemented in Simulink following the equations presented in section 3.7.1. The structure of the photovoltaic plant can be seen in Figure 31. The parameters and models described above will be used to simulate the behavior of the plant and evaluate its integration into the power grid. Through this implementation in Simulink, analysis and tests can be performed to verify the operation and performance of the PV plant under real operating conditions.
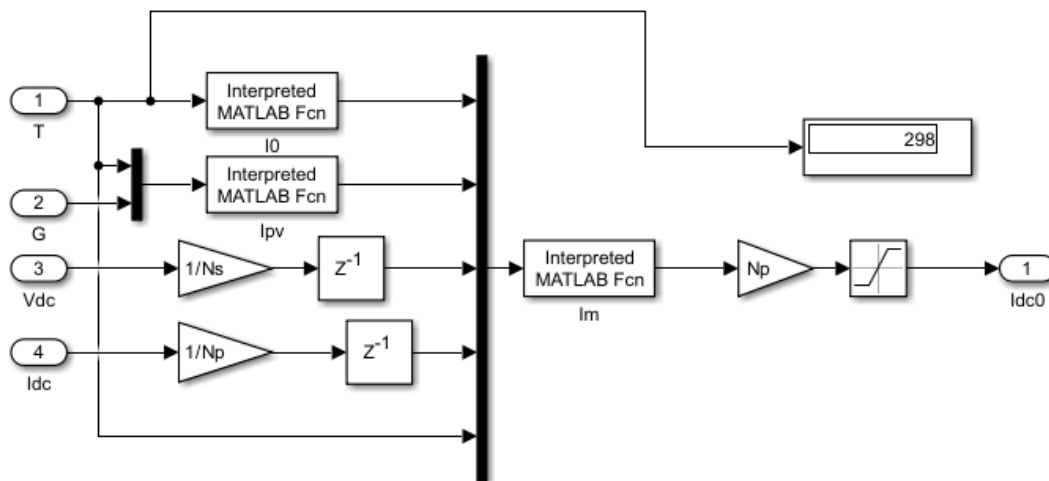

Figure 31 PV Array implementation in Simulink.

4.3.2. Control overview

In Figure 32, the control loop for the integration of the Case Study 1 can be observed. It consists of an outer control for the DC bus voltage and a control for reactive power. These control mechanisms ensure that the voltage of the DC bus is regulated within the desired reference, while also managing the reactive power flow to maintain stability and optimal operation of the system.
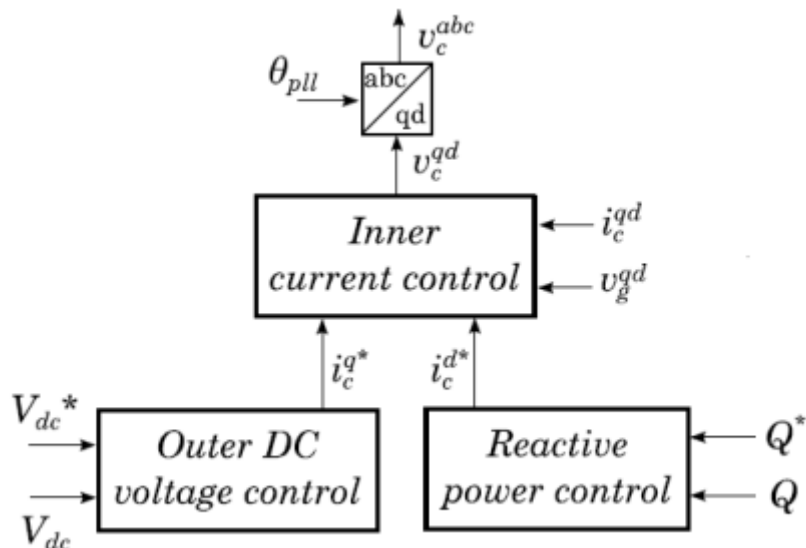
Figure 32 Case study 1 control overview.

- **DC Voltage Control Block**

In Figure 33, the implemented schematic of the DC control can be observed in Simulink. This control system is responsible for regulating the voltage of the DC bus in the VSC.
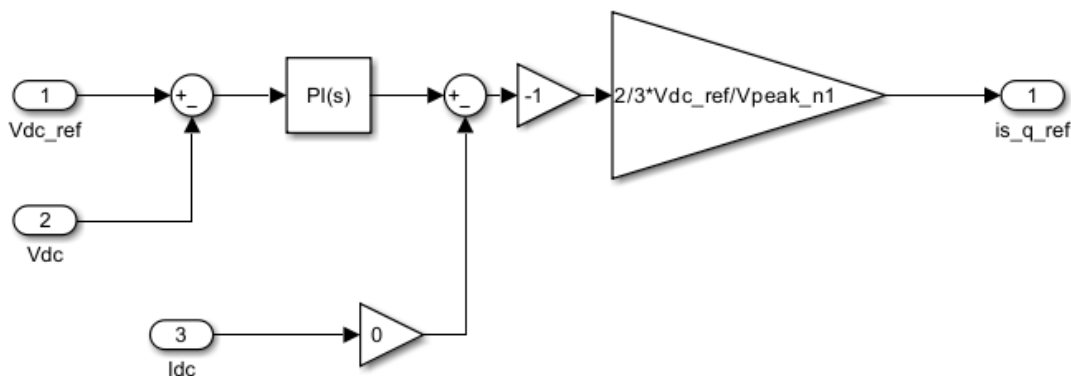

Figure 33 DC Voltage Control in Simulink.

- **Reactive Power Control**

In Figure 34, the implemented schematic of the reactive power control can be observed in Simulink. This control system is responsible for managing the reactive power flow in the photovoltaic system.
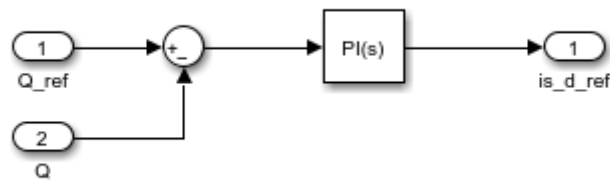
Figure 34 Reactive power control in Simulink.

4.3.3. Maximum Power Point Tracking (MPPT)

In the model of the previous task, an MPPT needs to be implemented. An MPPT is a mechanism that optimizes the PV array by ensuring that the panels operate at their maximum power point. In this task, the MPPT serves as a replacement for the reference voltage used in other exercises. The implementation of the MPPT in Simulink can be observed in Figure 34.
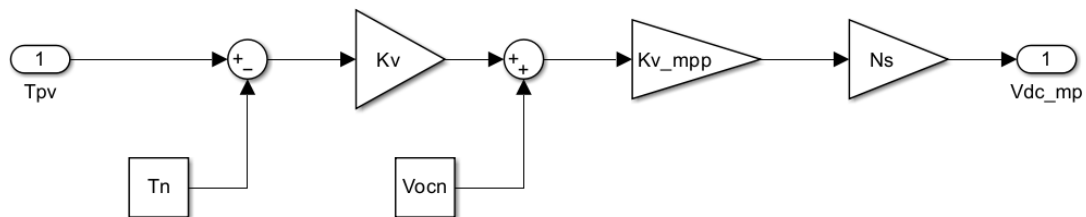

Figure 35 MPPT implementation in Simulink.

In addition, one more subsystem is created in order to simulate a switch. In Figure 36 is shown. Este interruptor se ha situado para evaluar los dos métodos de referencia del bus de DC. This switch has been placed to evaluate the two reference methods for the DC bus. In the first scenario, the reference will come from the MPPT control. Conversely, in the second case, the DC voltage reference will be set by the DC control loop.
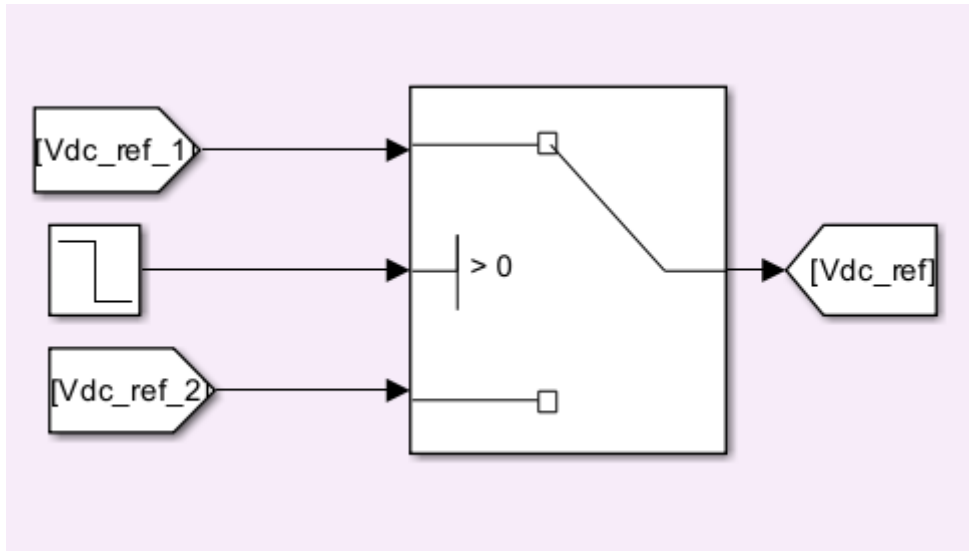
Design and simulation of converter operating in a
renewable energy based smart grid
Pág. 65

Figure 36 Vdc reference switch.

4.4. Case Study 1: Results

In Figure 37, the complete schematic implemented in Simulink can be seen.
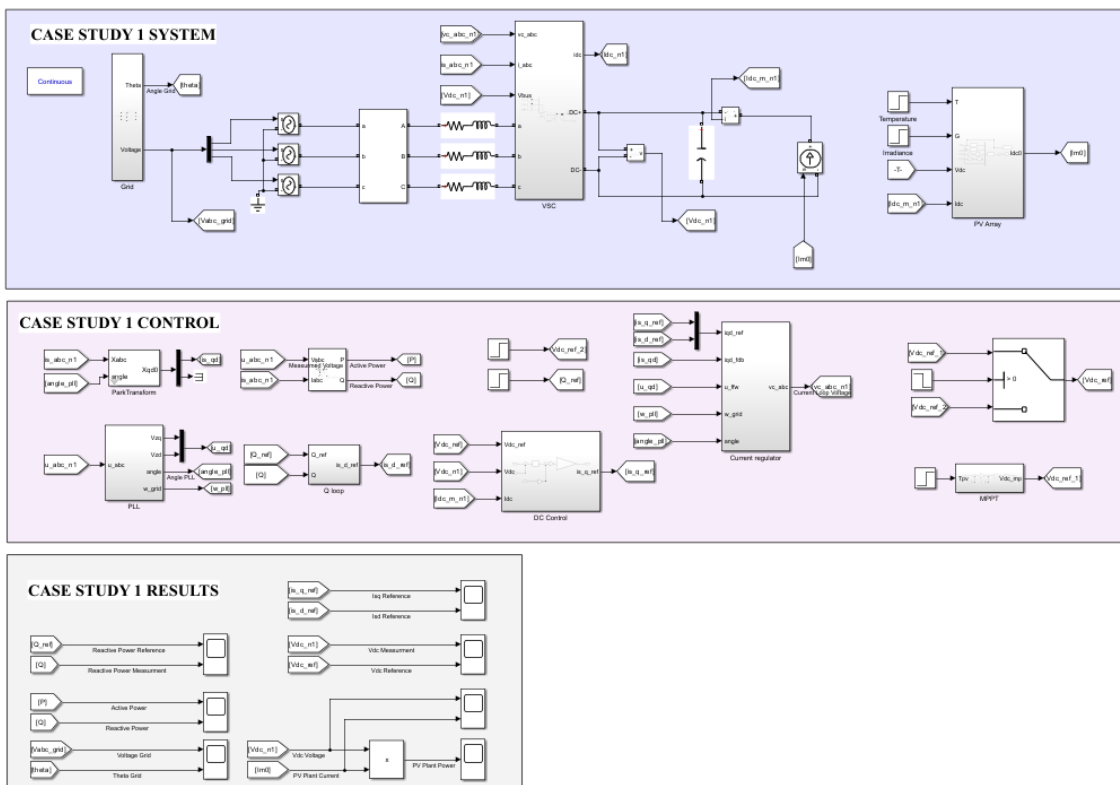

Figure 37 Case Study 1. Full Schematic.

In this way, the simulation of this first system has been conducted based on the following conditions:

- Simulation time: 5s
- Reactive power reference between 0-1s: 500 VA
- Reactive power reference between 4-5s: 400 VA
- Vdc reference between 0-4s: MPPT
- Vdc reference between 4-5s: DC Control Loop
- Temperature rises 17ºC in the second 2.5.

Therefore, the different simulation results can be observed under the presented conditions.

4.4.1.   Reactive Power Reference vs Reactive Power Measurement

In Figure 38, the results of the comparison between the reference reactive power and the measured reactive power can be seen. It can be observed that, despite the temperature rise and the change in reference, the system is fully capable of maintaining the injection according to the reference.

Figure 38 Reactive Power Reference vs Reactive Power Measurement.

4.4.2.   Active Power Measurement & Reactive Power Measurement

In Figure 39, the results of the comparison between the measured active and reactive power can be seen. It can be observed that, despite the temperature rise and the change in reference, the system is fully capable of maintaining the injection according to the reference.
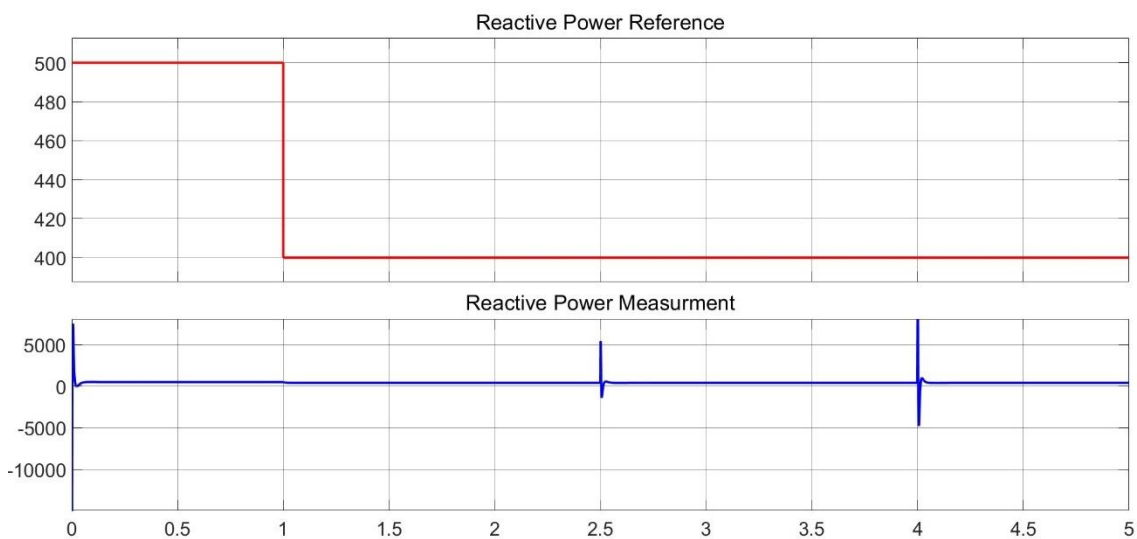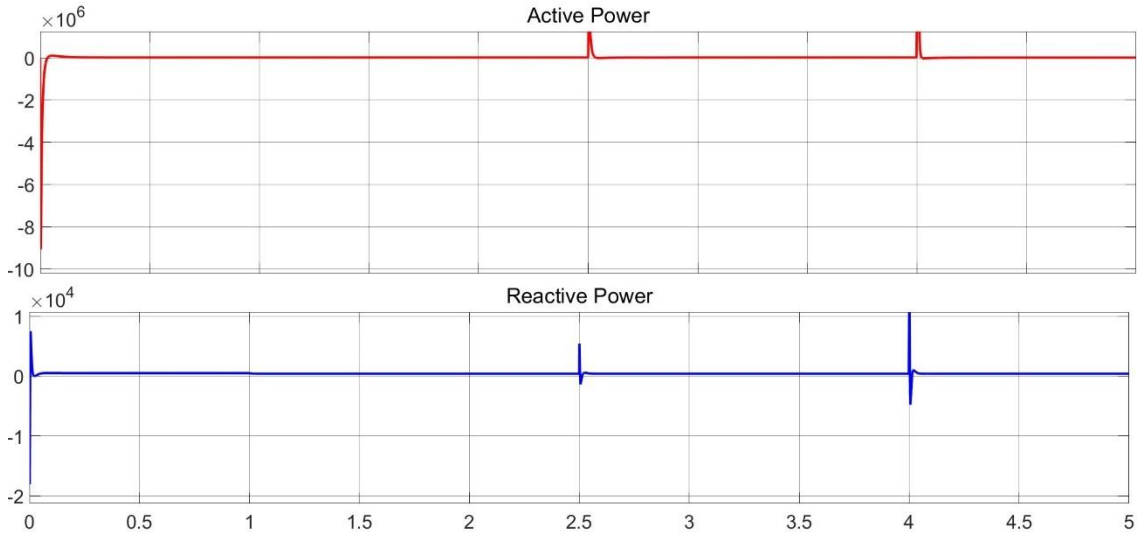
Figure 39 Active Power Measurement & Reactive Power Measurement.

4.4.3. Isq Reference & Isd Reference

In Figure 40, the results of the comparison between the reference currents isq and isd can be seen. It can be observed that, despite the temperature rise and the change in reference, the system is fully capable of stabilizing itself.

Figure 40 Isq Reference & Isd Reference.

4.4.4.   Vdc Reference vs Vdc Measurement

In Figure 41, the results of the comparison between the reference voltage Vdc and the measured voltage can be seen. It can be observed that, despite the temperature rise and the change in reference, the system is fully capable of stabilizing itself. In this section, we can distinguish three stages:
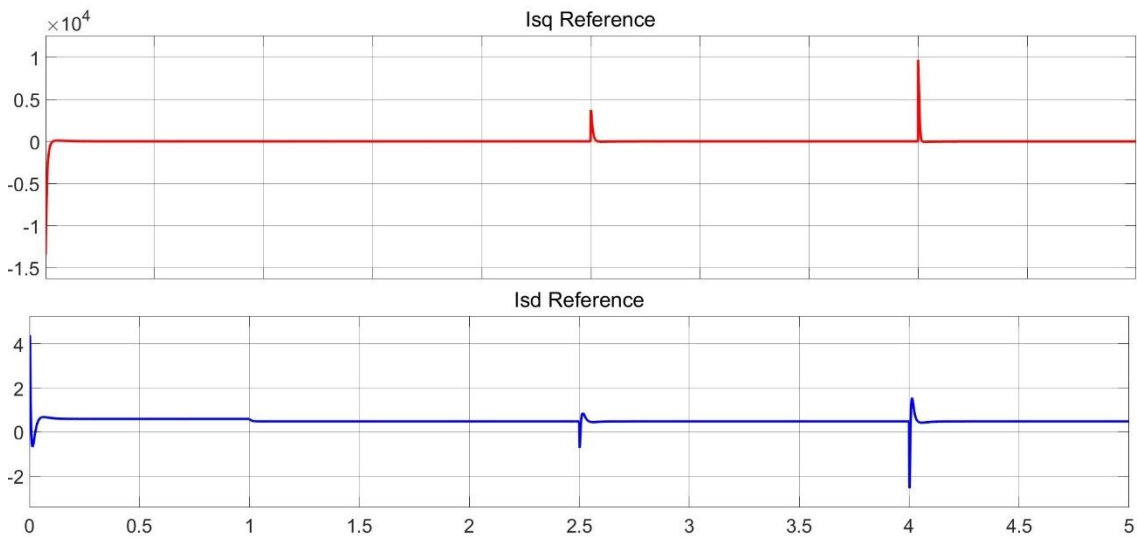
- 0-2.5s - Reference of approximately 800 V according to MPPT with an irradiation of 800 W/m2 and a temperature of 25ºC.
- 2.5-4s - Reference of approximately 700 V according to MPPT with an irradiation of 800 W/m2 and a temperature rise of 17ºC.
- 4-5s - Reference of 400 V according to DC Control with an irradiation of 800 W/m2 and a temperature rise of 17ºC.
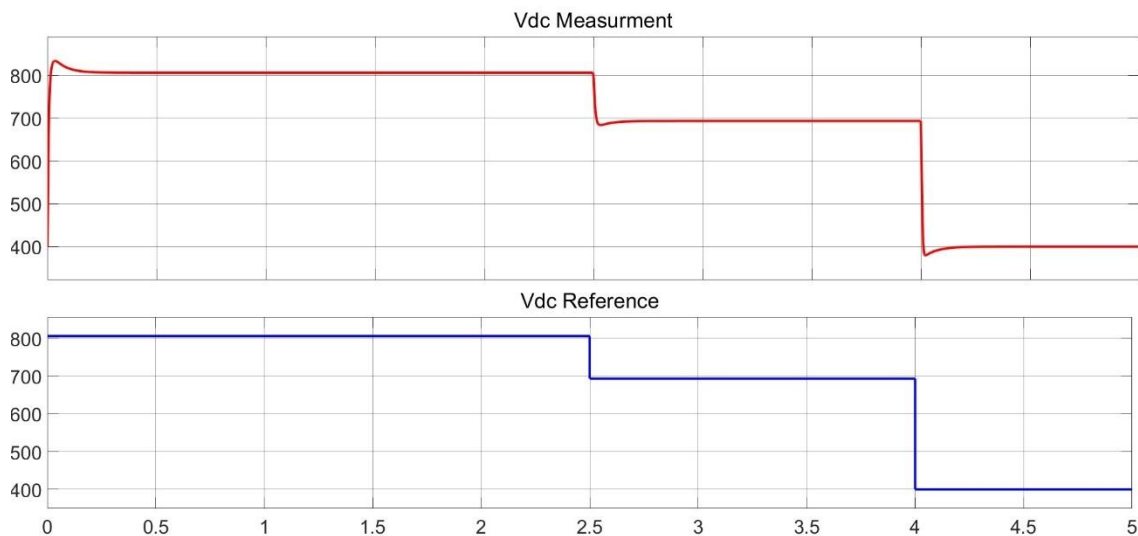

Figure 41 Vdc Reference vs Vdc Measurement.

4.4.5.   Voltage, Current & Power of the PV Plant

In Figures 42 and 43, the results of the comparison of voltage, current, and power generated by the photovoltaic plant can be seen. It can be observed that, despite the temperature rise and the change in reference, the system is fully capable of stabilizing itself. We can observe a decrease in power due to the temperature change. Therefore, it should be verified with the manufacturer and their respective datasheet if it corresponds to the V-I and PV curves. Additionally, in the last section, we can observe a greater drop in power due to limiting the

Design and simulation of converter operating in a
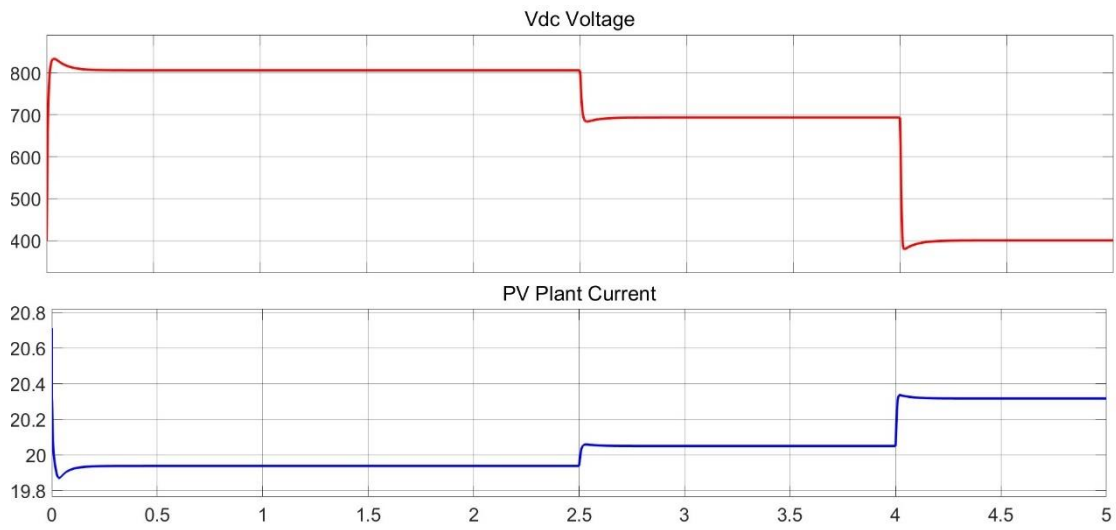renewable energy based smart grid
Pág. 69

bus to 400 V.

Figure 42 Voltage & Current of the PV Plant.

Figure 43 Power of the PV Plant.

5. Case Study 2: Smart Grid

5.1. PV Plant model

The implementation of the photovoltaic plant is simplified by the existence of a specific block in Simulink that simulates the operation of a group of photovoltaic panels. This block takes into account two variables: irradiance and temperature. However, in our case temperature will not be considered, since we treat this block as a robust discrete model and have internally set its value to 25°C.

Simulink also offers the option to choose a panel model that exists in the real market. In our project, we have selected the A10Green Technology A10J-S72-175 as the panel model.

In addition, it is important to enter the number of solar panels present in the installation. This will allow us to modify the output voltage and current of the plant in different scenarios.

The layout of the photovoltaic plant, as well as the V-I (voltage-current) and P-V (power-voltage) characteristics of the modules, are shown in Figures 44 and 45.
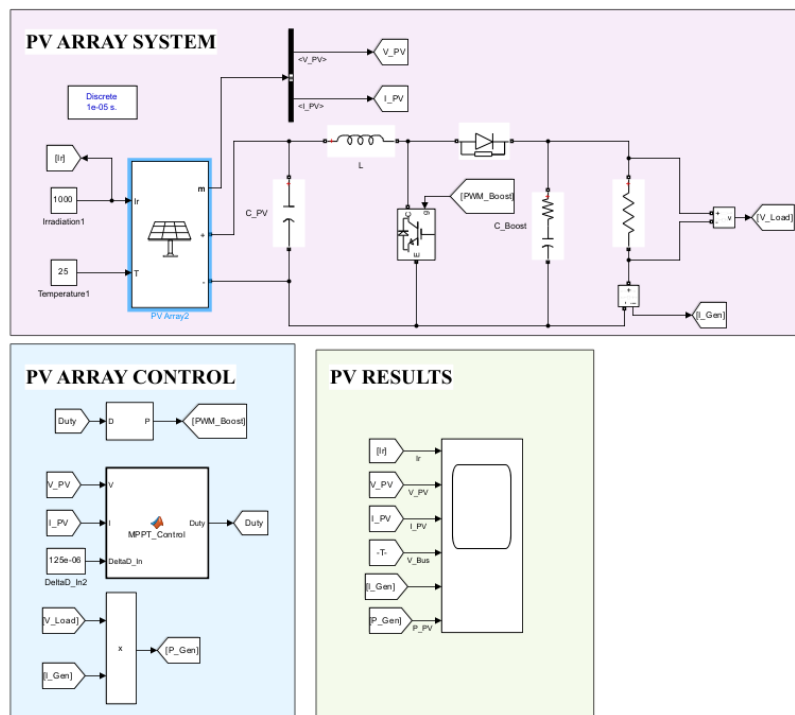

Figure 44 PV Array system in Simulink.
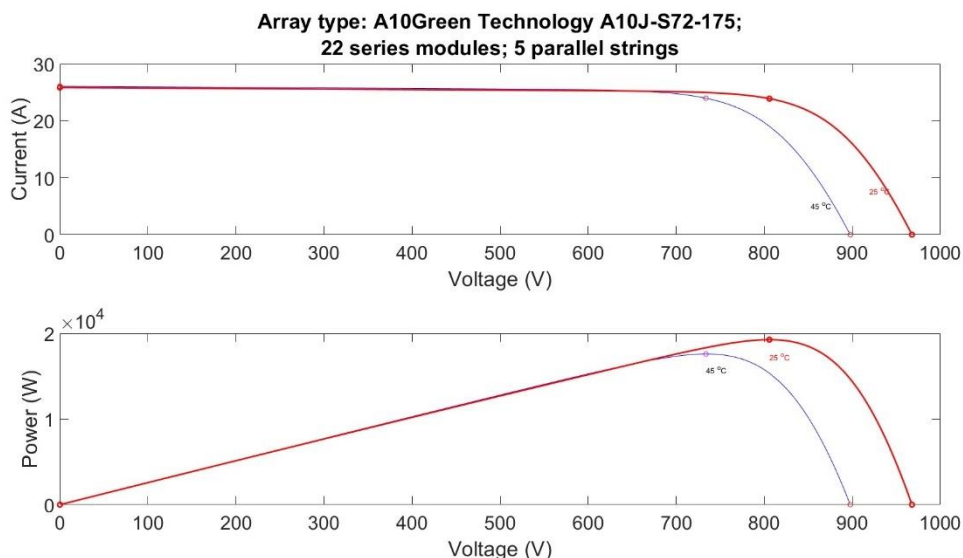
Figure 45 V-I (voltage-current) and P-V (power-voltage) characteristics of the modules.

The output of the PV plant will be regulated by a maximum power point tracking (MPPT) system. This system will adjust the output voltage and current of the PV panels to obtain the maximum power that the system can achieve. In Simulink, this system will be implemented using a MATLAB code that uses the perturbation and observation technique. This code will constantly change the voltage values to find the optimal duty cycle. This algorithm is commonly used to optimize the power output of a photovoltaic system by continuously adjusting the duty cycle of the power converter.

The program code is shown in Figure 46.

```matlab
function Duty = MPPT_Control(V, I, DeltaD_In)

Duty_Init = 0.05;
Duty_Min = 0;
Duty_Max = 0.75;

persistent Vold Pold Dutyold;

if isempty (Vold)
    Vold = 0;
    Pold = 0;
    Dutyold = Duty_Init;
end
P = V * I;
dV = V - Vold;
dP = P - Pold;
Duty = Dutyold;
DeltaD = DeltaD_In;

if dP ~= 0
    if dP < 0
        if dV < 0
            Duty = Dutyold - DeltaD;
        else
            Duty = Dutyold + DeltaD;
        end
    else
        if dV < 0
            Duty = Dutyold + DeltaD;
        else
            Duty = Dutyold - DeltaD;
        end
    end
end

if Duty >= Duty_Max
    Duty = Duty_Max;
elseif Duty < Duty_Min
    Duty = Duty_Min;
end

Dutyold = Duty;
Vold = V;
Pold = P;
```

Figure 46 MPPT MATLAB Code.

The code begins by initializing variables to store previous voltage, power, and duty cycle values. It then receives the current voltage (V) and current (I) values, along with a parameter for the incremental change in duty cycle (DeltaD_In).

Using these inputs, the code calculates the power (P) based on the current voltage and current values. It also computes the voltage difference (dV) and power difference (dP) between the current and previous samples.

Next, the duty cycle (Duty) is adjusted based on the signs of dP and dV. If dP is negative and dV is negative, the duty cycle is decreased. If dP is negative and dV is positive, the duty cycle is increased. If dP is positive and dV is negative, the duty cycle is increased. And if dP is positive and dV is positive, the duty cycle is decreased.

To ensure that the duty cycle stays within defined limits, the code checks if the adjusted duty cycle exceeds the maximum value (Duty_Max) or falls below the minimum value (Duty_Min). If necessary, the duty cycle is constrained accordingly.

Finally, the code updates the previous values (Vold, Pold, and Dutyold) with the current values for the next iteration.

This MPPT control algorithm continuously tracks the maximum power point of the photovoltaic system, maximizing the power output and optimizing the utilization of available solar energy.

To regulate the output of the PV plant, it is necessary to use a boost DC-DC converter. In this case, the pulse width control (PWM) is performed directly in the converter, using the duty cycle obtained with the MPPT program.

ETSEIB

5.2. Battery model

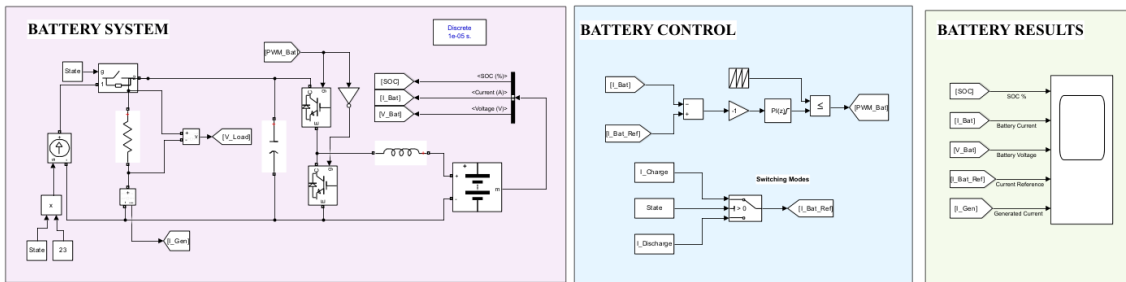In Figure 47, the implementation of the Battery Model can be observed in Simulink.

Figure 47 Battery system in Simulink.

The implementation of the battery in the system builds upon the knowledge and insights gained from the preceding chapters. It incorporates a DC-DC charger specifically designed for the battery, along with the control mechanism. The charger operates in two distinct modes: charging and discharging, each capable of delivering a current of 11.5 A.

The charging mode facilitates the replenishment of the battery's energy storage capacity, ensuring it is ready to provide power when needed. On the other hand, the discharging mode enables the battery to supply electricity to the grid during periods of high demand or when solar generation is insufficient, such as at night. This capability enhances the system's overall reliability and grid integration, as it enables the utilization of stored energy when renewable generation is limited.

To ensure seamless operation, the control system governing the battery and its charger orchestrates the switching between charging and discharging modes. It monitors the battery's state of charge, taking into account the energy needs of the system and grid conditions. This intelligent control mechanism optimizes the usage of the battery, maximizing its efficiency and lifespan.

ETSEIB

5.3. Pump or load model

In Figure 48, the implementation of the Battery Model can be observed in Simulink.
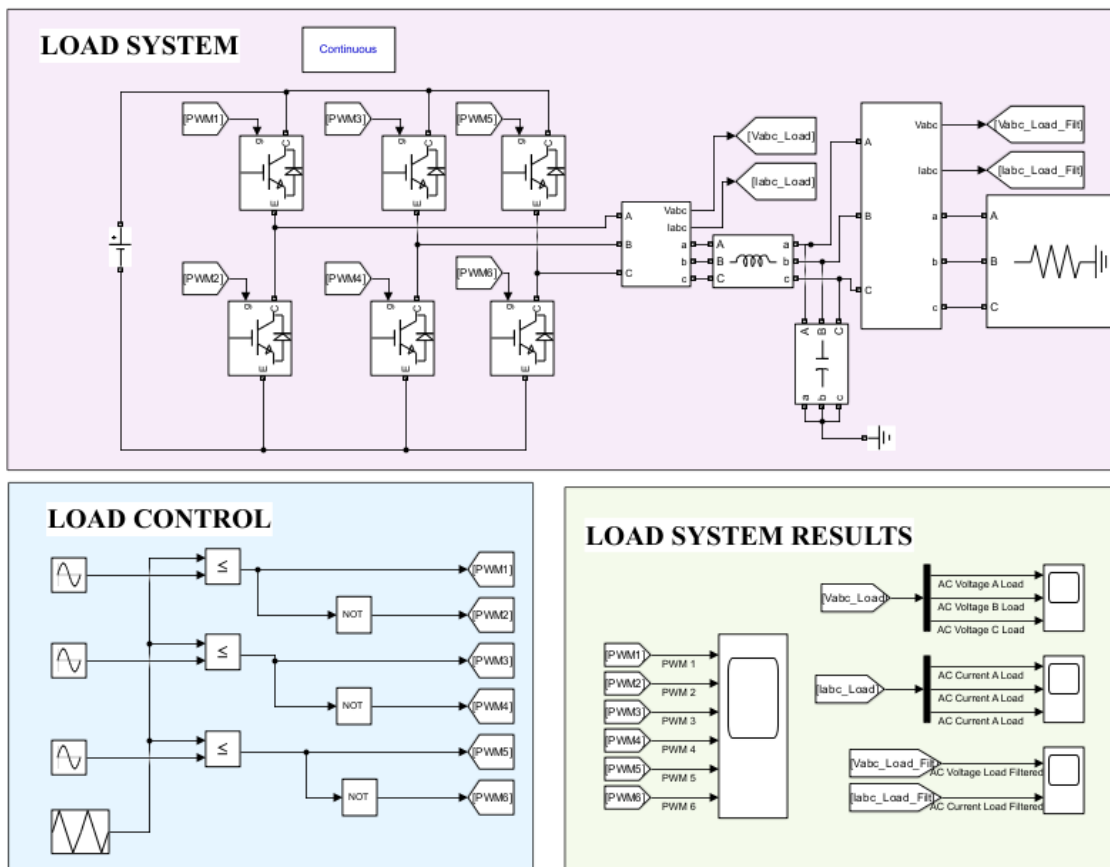

Figure 48 Load system in Simulink.

The implementation of an AC load with a three-phase DC-AC inverter, connected to both the battery and the photovoltaic array, builds upon the concepts and methodologies discussed in the preceding chapters. This configuration simulates the supply of power to a pump through the 400V bus.

To ensure the smooth operation of the AC load and to mitigate potential harmonics and disturbances, a filter has been incorporated into the system. This filter effectively cleans the three-phase signal, removing any unwanted noise or interference. By integrating this filtering mechanism, the system guarantees a clean and stable power supply to the pump, minimizing the risk of operational issues and optimizing overall system performance.

Overall, this implementation of an AC load, supported by a three-phase DC-AC inverter connected to the battery and the photovoltaic array, exemplifies the system's versatility and capability to deliver power to various applications. The integration of the filter further enhances the quality and reliability of the power supply, ensuring optimal performance of

the pump and contributing to the overall efficiency and effectiveness of the system.

5.4. Case Study 1: Results

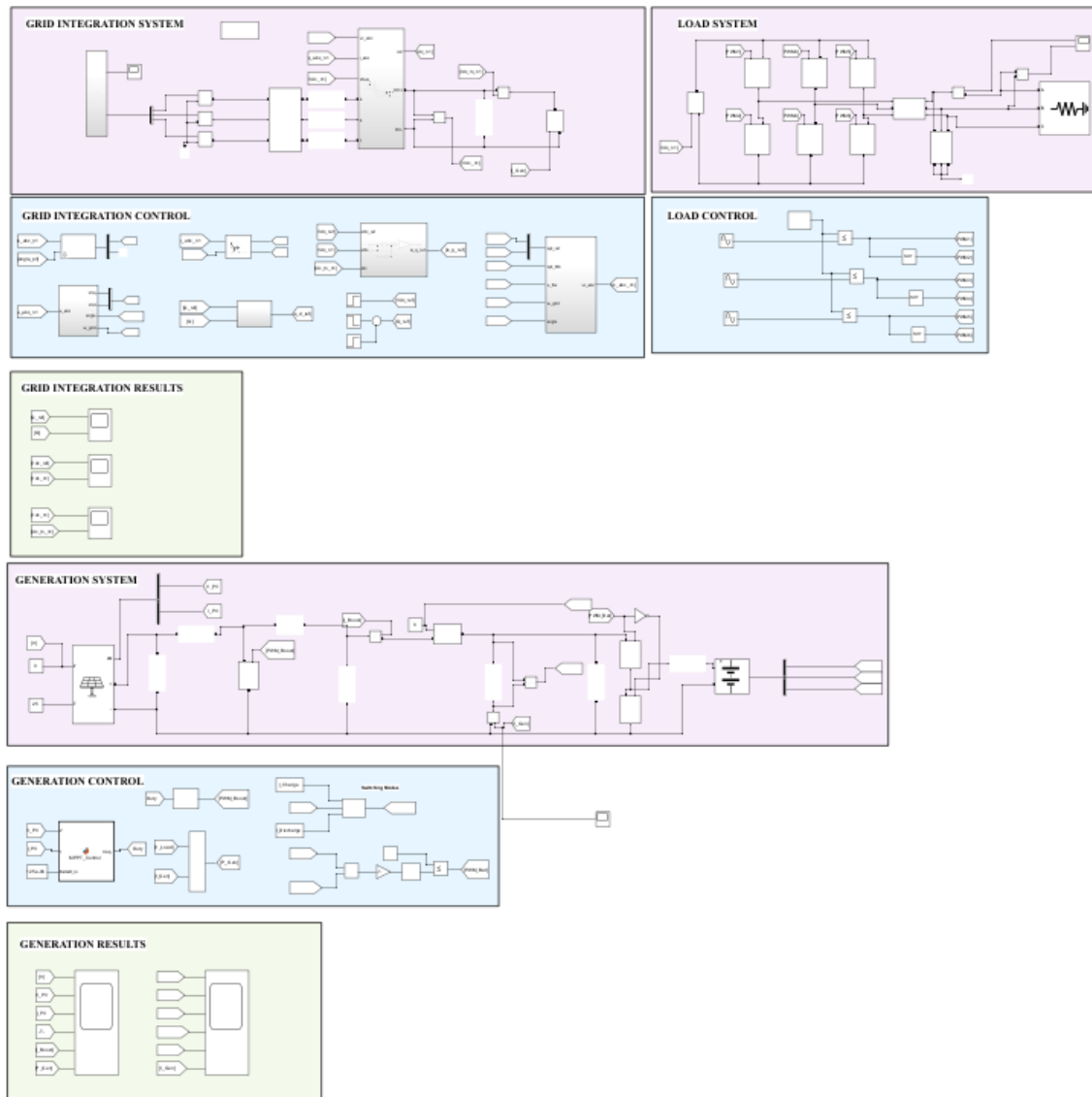In Figure 49, the complete schematic implemented in Simulink can be seen.

Figure 49 Case Study 2. Full Schematic.

Table 3 summarizes the characteristics of all system components.

PV Array		VSC	
I_{mp}	4,78 A	$S_{c,n}$	5 MVA
V_{mp}	36,63 V	$U_{c,n}$	690 V
$P_{max,m}$	175,0914 W	$V_{dc,n}$	400 V
I_{sc}	7,61 A	L_c	30,31 μH
V_{oc}	43,99 V	R_c	30,31 $m\Omega$
K_V	$-0,3616\ V/K$	C_{dc}	278 mF
K_I	0,041509 A/K	**AC Grid**	
a	1,3	U_g	690 V
R_p	249,6758 Ω	f_g	50 Hz
R_s	0,38412 Ω	**Battery**	
N_{series}	22	V_N	400 V
$N_{parallel}$	5	C_X	150 Ah
Pump Load			
P_N		1,5 kW	

Table 3 System parameters.

5.4.1. PV Array Results

Figure 50 shows the results obtained for an Irradiance of 800 W/m2. Thus, the plant will be giving the maximum current by MPPT control. Se puede observar que la planta suministrará casi 15kW para un voltaje de casi 700 V. It can be seen that the plant will supply almost 15kW for a voltage of almost 700V. This is an ideal scenario, since, we will be working on a 400 V bus and feeding the battery during the day. The real result can be seen in section 5.4.4.
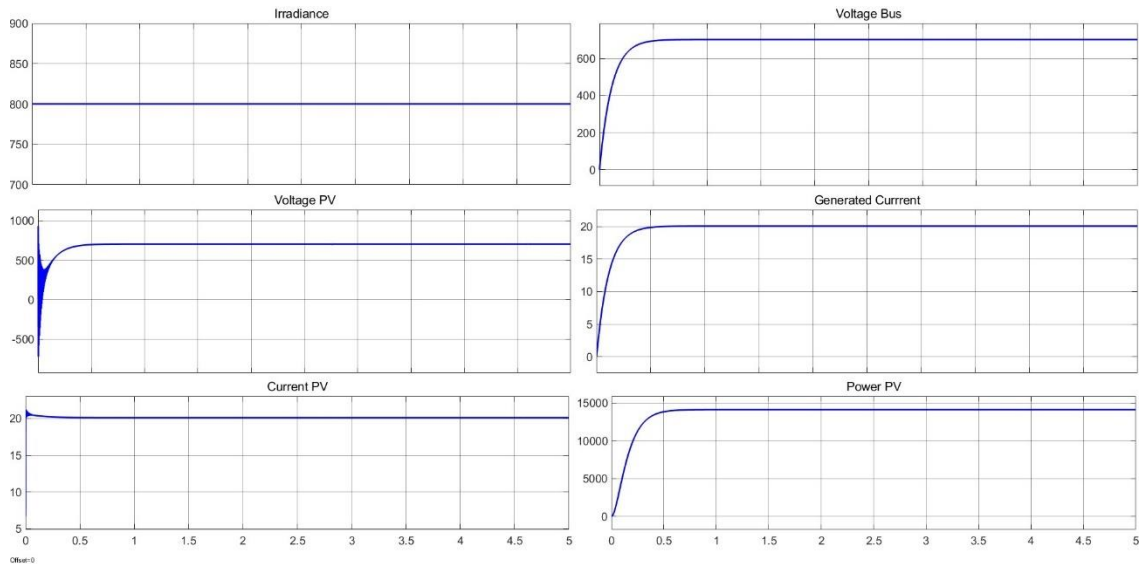
Figure 50 PV Array simulation for Irradiance of 800 W/m2.

Figure 51 shows the results obtained for an irradiation of 0 W/m2. In this way, the plant will be off, since it will be the battery that will oversee supplying the system. This scenario will be seen in the results for the system.
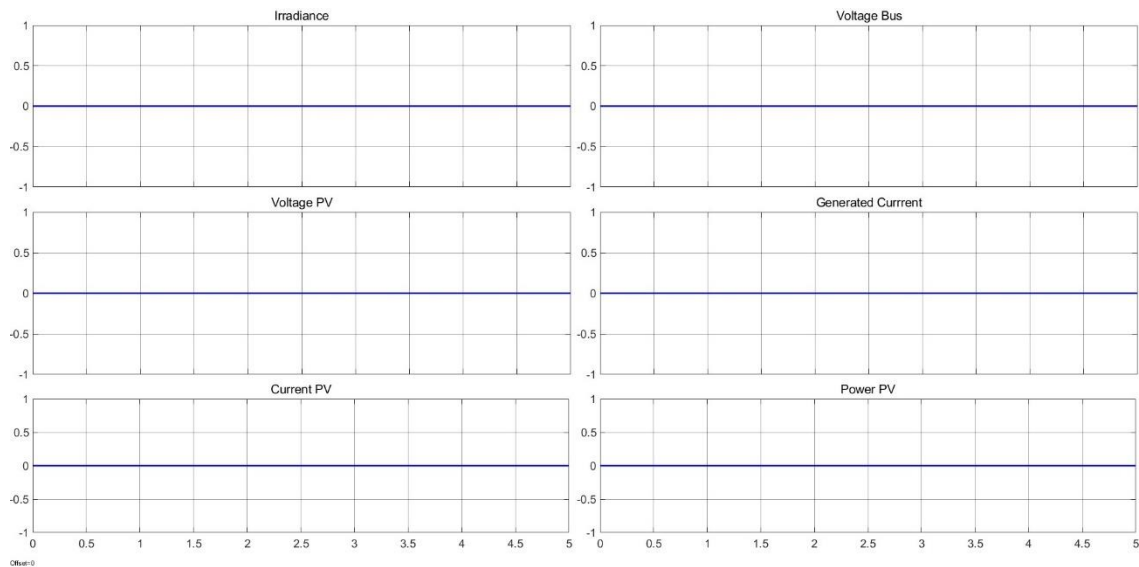

Figure 51 PV Array simulation for Irradiance of 0 W/m2.

Design and simulation of converter operating in a
renewable energy based smart grid
Pág. 79

5.4.2. Battery Results

In Figure 52, the simulation results of the battery charging process are presented. The figure illustrates the behavior of various parameters during the charging phase.

The graph shows the battery's state of charge (SoC) over time, indicating how the battery's capacity is being replenished during the charging process. The SoC typically starts at a lower value and gradually increases as the battery absorbs energy from the charging source. This trend demonstrates the successful charging operation of the battery.

Additionally, the graph may display the charging current, which represents the flow of electric current into the battery during the charging process. The charging current initially starts at a higher value, gradually decreasing as the battery reaches a higher SoC. This behavior is expected as the battery's internal resistance increases as it charges.

Moreover, other relevant parameters such as voltage is shown in the graph. The voltage typically increases as the battery charges. It cannot be fully appreciated as it is a brief simulation.
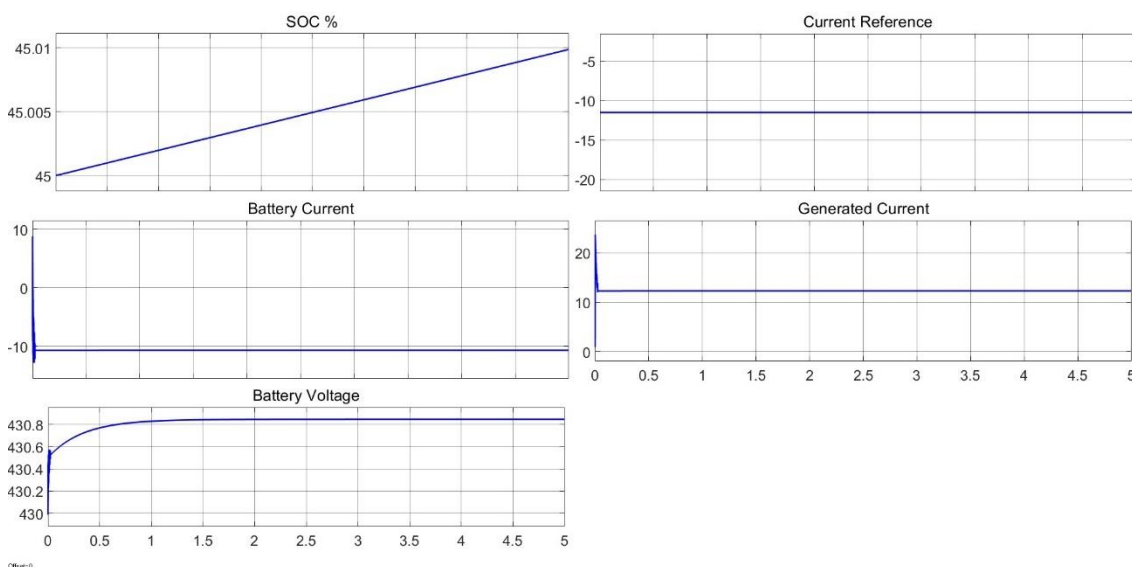
Figure 52 Battery charge mode.

In Figure 53, the obtained results for an irradiation of 0 W/m2 are depicted. In this particular scenario, where there is no solar irradiation available, the PV plant remains inactive, and the system relies solely on the battery as the power source. This can be observed in the results of the system, where the PV plant's contribution is absent, and the battery takes over the responsibility of supplying the required power.
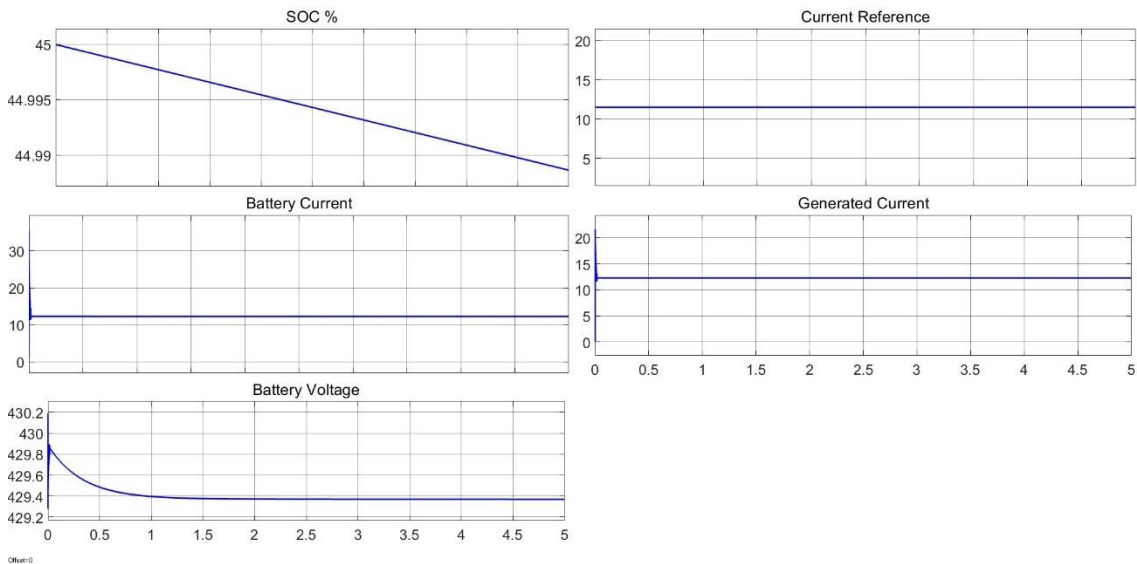
Figure 53 Battery discharge mode.

5.4.3. Load Results

In the Figure 54, it is evident that the unfiltered three-phase voltage waveform bears a resemblance to a square wave. This characteristic is primarily due to the switching nature of the inverter, which generates abrupt transitions between voltage levels. As a result, the waveform exhibits sharp edges and steep slopes, resulting in a square-like appearance.

The square wave nature of the unfiltered waveform signifies the presence of higher harmonics and rapid voltage transitions, which can have detrimental effects on the connected load and overall system performance. These harmonics and rapid transitions can lead to increased electromagnetic interference, reduced power quality, and potential stress on the load components.
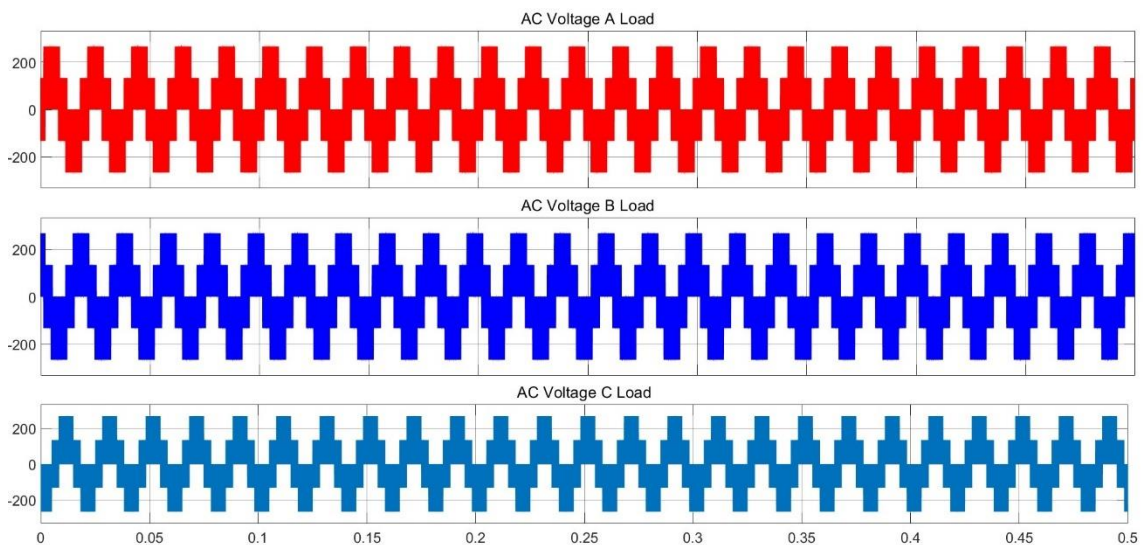
Figure 54 Three-phase voltages without filter.

However, as can be seen in Figures 55 and 56, through the implementation of the filtering process, as demonstrated in the filtered waveform, these undesirable characteristics are significantly mitigated. The filtering action smooths out the transitions, suppresses the high-frequency components, and promotes a more sinusoidal waveform. This transformed waveform is crucial in providing a stable and reliable power supply to the connected load, ensuring efficient operation, and reducing the risk of electrical disturbances.
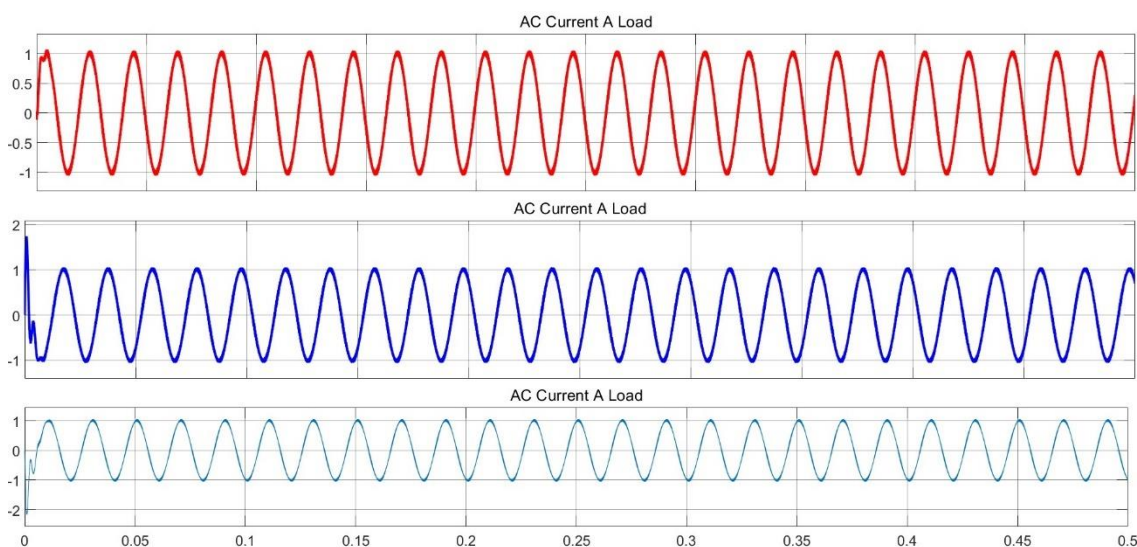
Figure 55 Three-phase currents with filter.

Therefore, the comparison between the unfiltered and filtered waveforms not only highlights the square wave nature of the unfiltered waveform but also emphasizes the effectiveness of the filtering process in improving power quality and mitigating potential issues associated with the unfiltered waveform. By achieving a cleaner and more sinusoidal waveform through filtering, the system can operate more efficiently, minimize harmonic distortions, and provide a stable power supply to the connected load.
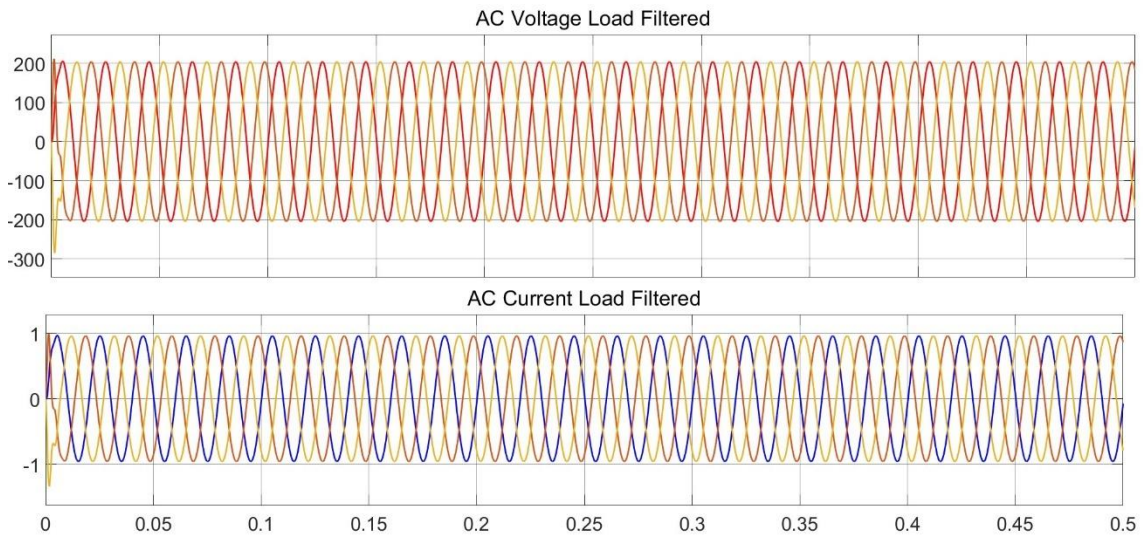
Figure 56 Three-phase voltage with filter.

5.4.4.   Case Study 2: Overall Results

5.4.4.1. Scenario 1: Irradiance of 0 W/m2

Figures 57 and 58 shows the results obtained for an irradiation of 0 W/m2. In this way, the PV plant will be off, since it will be the battery that will oversee supplying the system. The generated power and current is supplied by the battery.
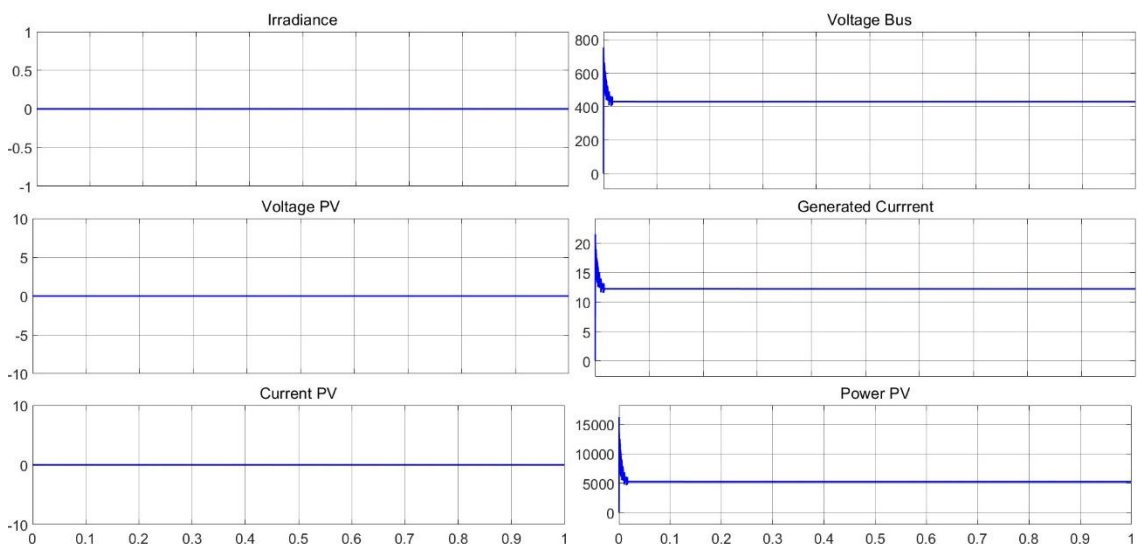
Figure 57 Scenario 1: PV Array results.
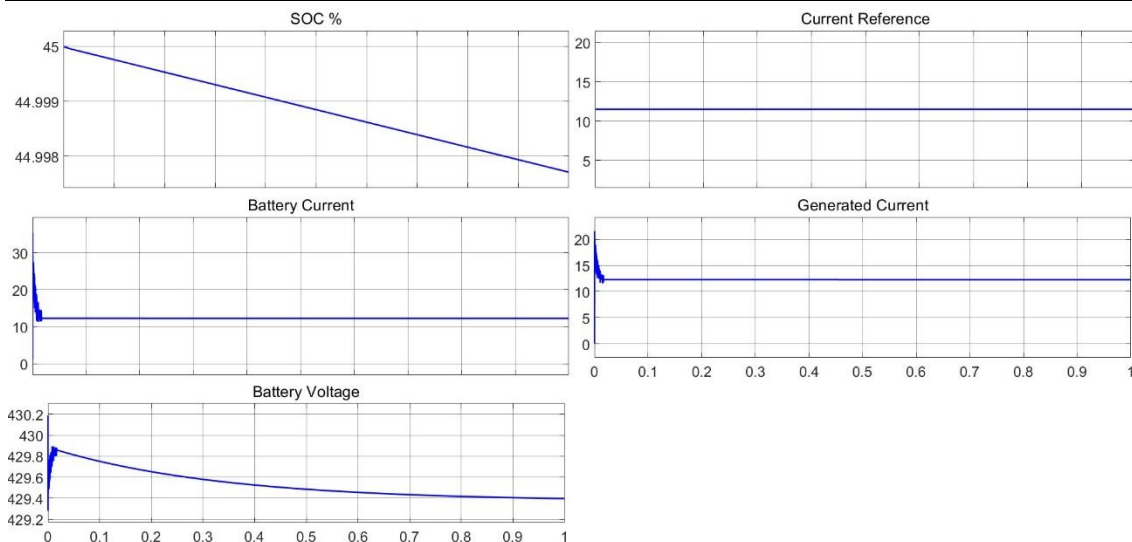
Figure 58 Scenario 1: Battery system results.

Figure 59 shows how the system is able to follow the reactive power reference using only the energy storage system.

Figure 59 Scenario 1: Reactive Power Reference vs Reactive Power Measurement.

In Figure 60, it can be seen how the system is able to maintain the VSC bus following the 400 V reference by means of the energy storage system alone.

Figure 60 Scenario 1: Vdc Reference vs Vdc Measurement

Figure 61 shows the power injection by the generation system. The power supplied is approximately 5 kW.
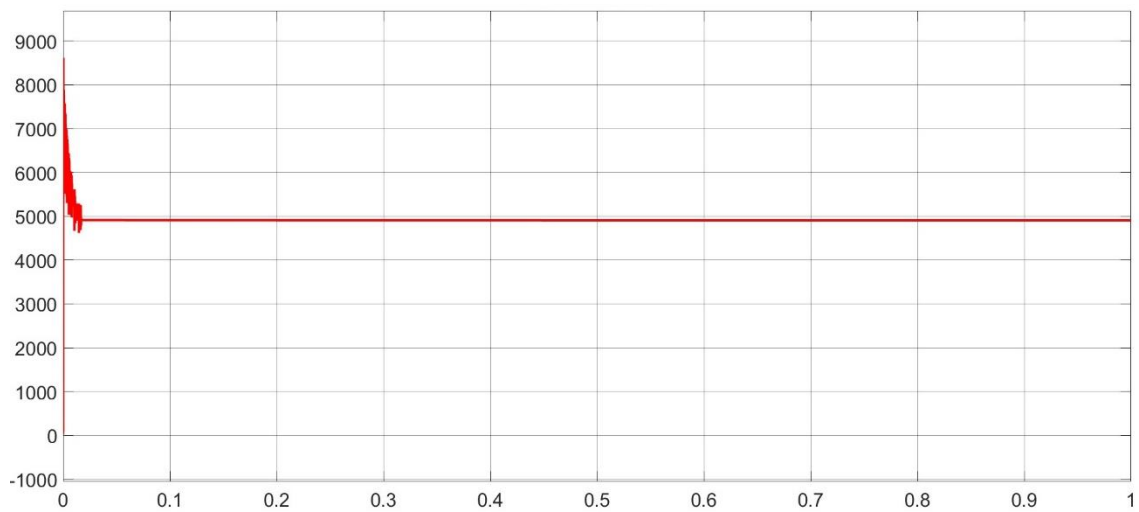
Figure 61 Scenario 1: Power of the Generation System.

5.4.4.2. Scenario 2: Irradiance of 800 W/m2

Figures 62 and 63 shows the results obtained for an irradiation of 800 W/m2. Therefore, the SoC of the battery can be seen increasing while the PV plant provides enough power to the system to maintain the DC bus of the VSC at 400V.
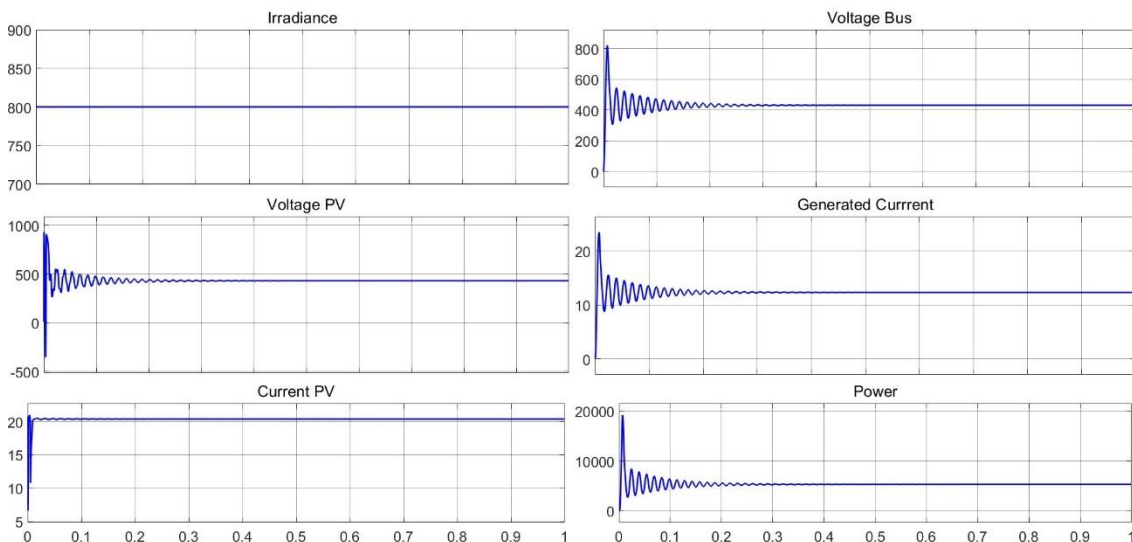
Figure 62 Scenario 2: PV Array results.
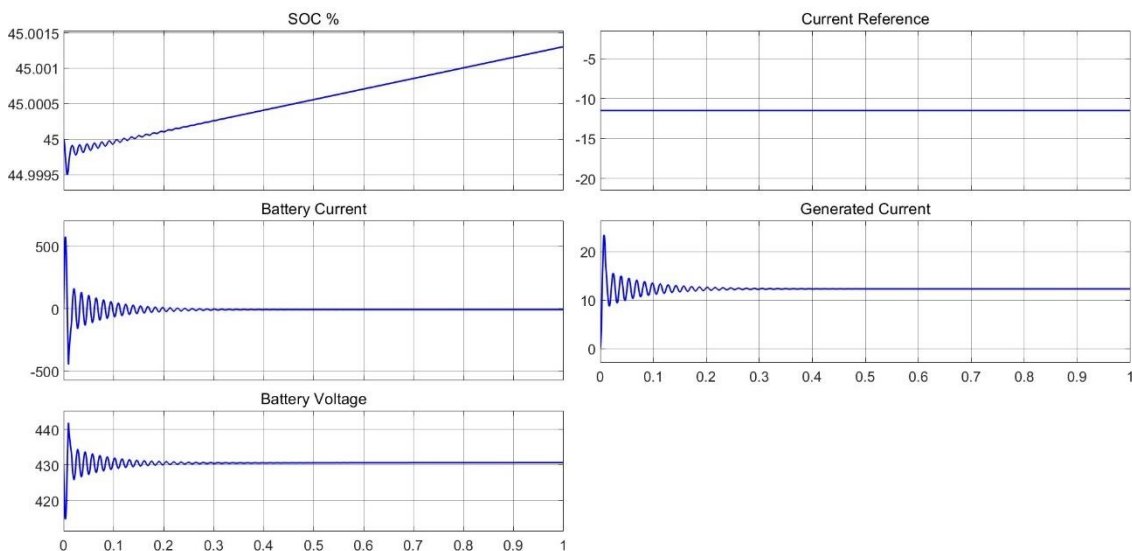
Figure 63 Scenario 2: Battery system results.

In Figure 64, it can be seen how the system is able to follow the reactive power reference

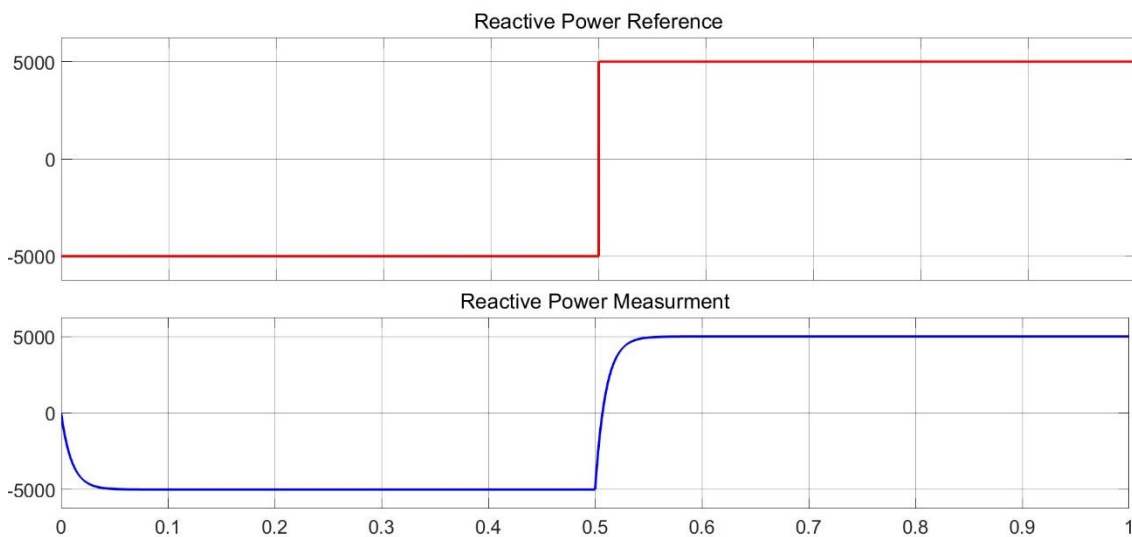even though the generation plant is feeding and charging the battery.
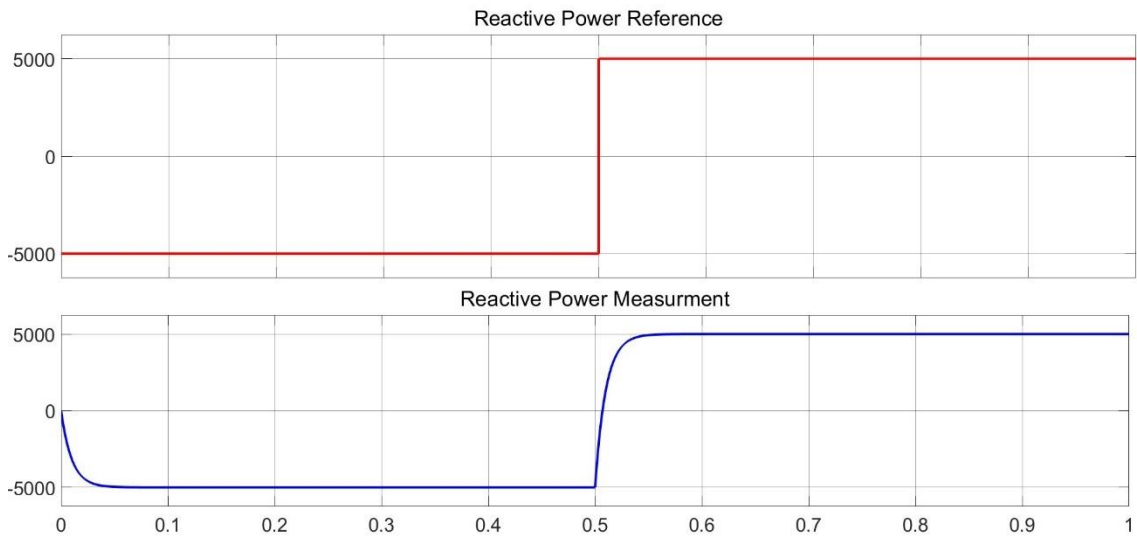
Figure 64 Scenario 2: Reactive Power Reference vs Reactive Power Measurement.

In Figure 65, it can be seen how the system is able to maintain the VSC bus following the 400 V reference despite the fact that the generation plant is feeding and charging the battery. In this second scenario, the disturbance is higher as all systems are operating.
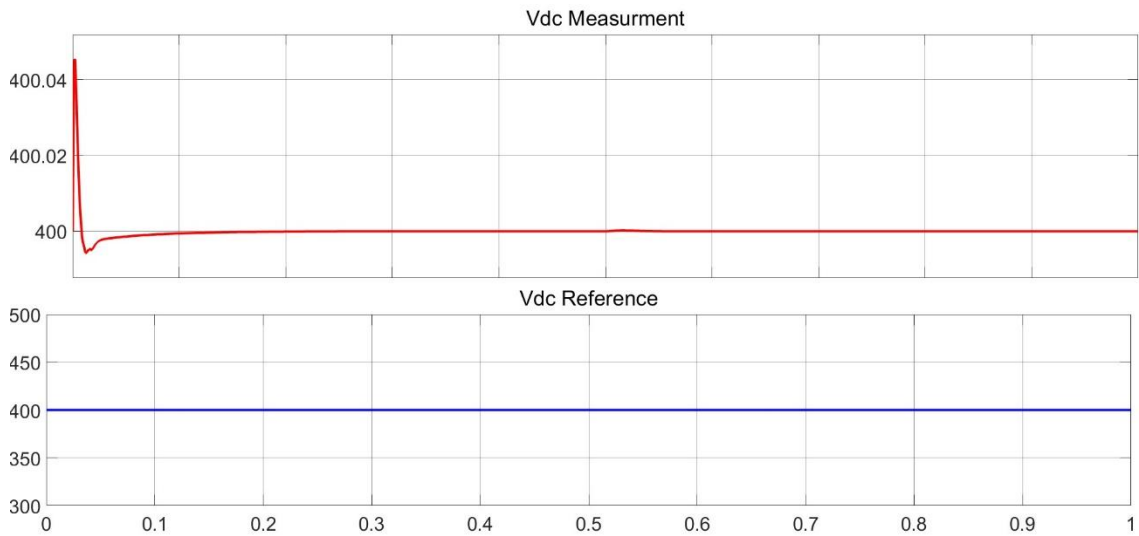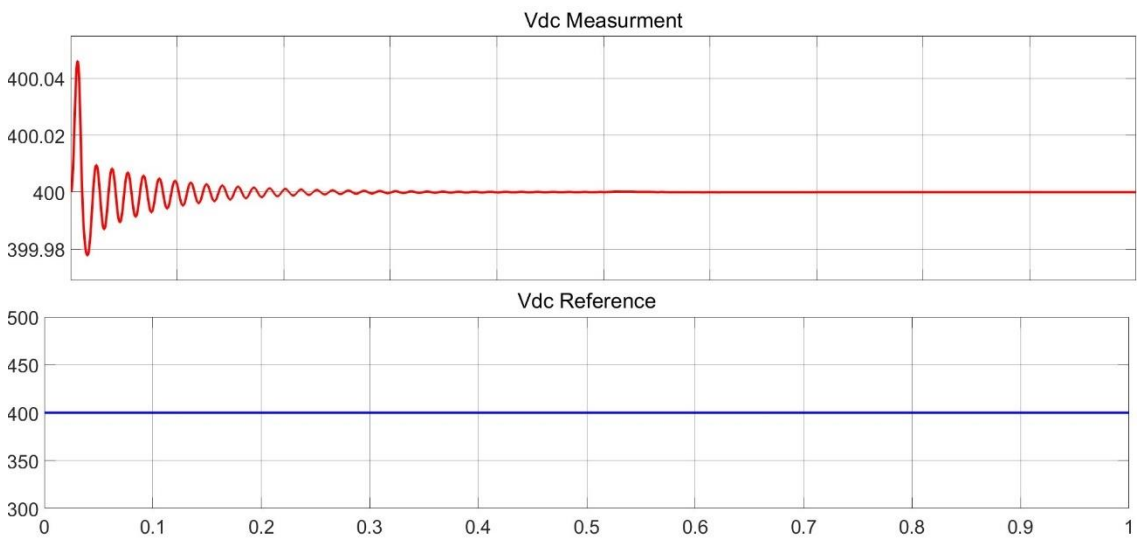

Figure 65 Scenario 2: Vdc Reference vs Vdc Measurement.

Figure 66 shows the power injection by the generation system. The power supplied is approximately 5.5kW.
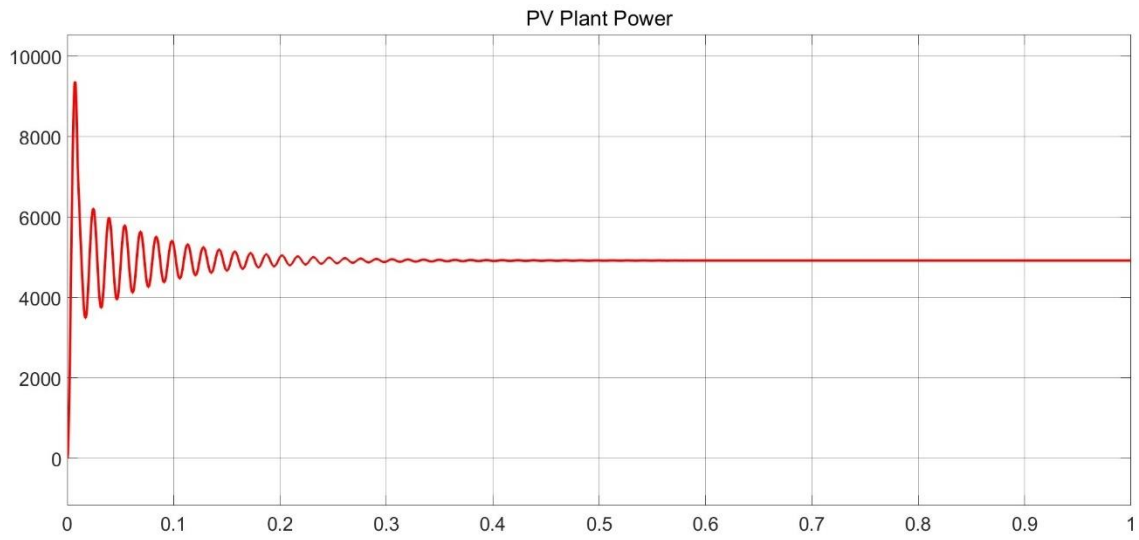
Figure 66 Scenario 2: Power of the Generation System.

6. Planning (Gantt chart)

Time scheduling is essential to efficiently organize and coordinate tasks, allocate resources appropriately and meet established deadlines. To clearly and concisely visualize this planning, a Gantt chart illustrating the scheduled activities and their distribution over time is presented below (Figure 62).

TASKS	MARCH				APRIL				MAY				JUNE				JULY			
Preliminary documentation	■	■	■	■																
Theoretical study					■	■														
Systems approach						■	■													
Design Case Study 1								■	■											
Simulation Case Study 1									■	■										
Design Case Study 2											■	■								
Simulation Case Study 2													■	■						
Report preparation	■	■	■	■				■	■				■	■	■					
Presentation of the report																	■			

Estimated date for submission of the report: July 03, 2023

Figure 67 Gantt chart of project planning.

This diagram will allow us to have an overview of the project, identify the dependencies between tasks and track their progress.

ETSEIB

7. Economic assessment

the budget corresponding to the project development is presented. Typically, the budget is divided into three phases: Material Execution Budget (MEB), Contract Price (CP), and finally the Total Budget (TB). In our project, it doesn't make sense to separate the three phases as the main difference will be the 13% for General Expenses, 6% for Industrial Profit, and the Value Added Tax (VAT) for the worker, who will be the student. Therefore, in the last section of this budget, we will include the VAT in the materials for the MEB and finally add the VAT for labor, along with General Expenses and Industrial Profit, in a final table, obtaining the CP and TB. We will have two items to divide the budget, which will be developed in the following sections:

- Software and computer equipment budget.
- Engineering cost budget.

Finally, the sum of the three phases results in a total cost of 23,892.65 €.

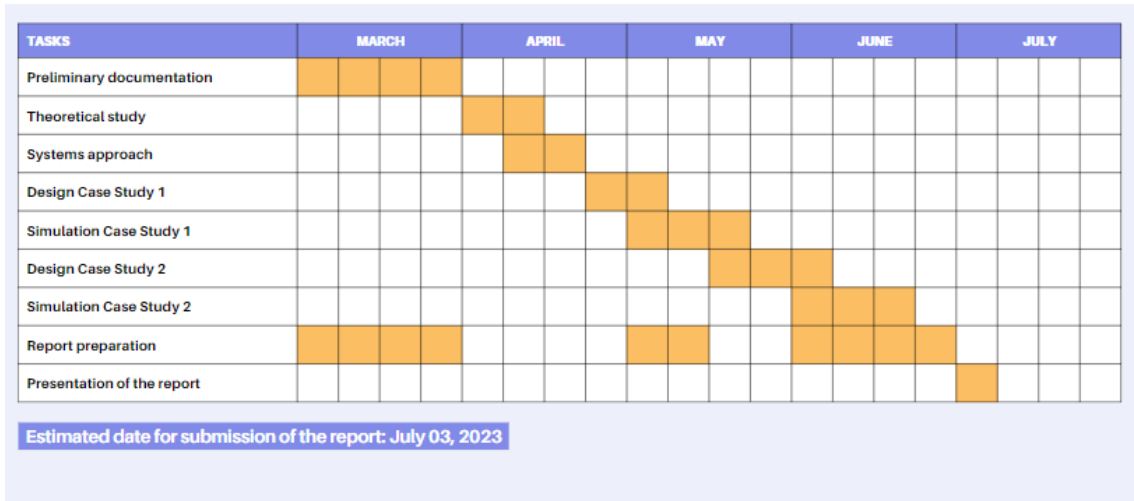| SOFTWARE AND COMPUTER EQUIPMENT			
ITEM	UNITARY COST	QUANTITY	SUBTOTAL
Windows 10 Professional	259 €	1 unit	259 €
Microsoft Office 365	10,5 €/month	5 months	52,50 €
MATLAB & SIMULINK	860 €/year	5 months	358,33 €
Dell Precision 5570 Workstation	1.923,44 €	1 unity	1.923,44 €
SUBTOTAL SOFTWARE AND COMPUTER EQUIPMENT			2.593,27 €
ENGINEERING			
TASK	UNITARY COST	QUANTITY	SUBTOTAL
Study and theoretical development of the subject.	75 hours	20 €/hour	1.500 €
Development of SIMULINK simulations	175 hours	40 €/hour	7.000 €
Analysis of results	50 hours	30 €/hour	1.500 €
Development of documentation	200 hours	20 €/hour	4.000 €
SUBTOTAL ENGINEERING			14.000 €
MATERIAL EXECUTION BUDGET (MEB)			16.593,27 €
GENERAL EXPENSES (13%)			2.157,13 €
INDUSTRIAL PROFIT (6%)			995,60 €
CONTRACT PRICE (CP)			19.746 €
VALUE ADDED TAX (VAT 21%)			4.146,66 €
TOTAL PROJECT BUDGET (TB)			23.892,65 €

Table 4 Overall project budget.

8. Environmental study

The environmental assessment is a fundamental aspect of any project, as it evaluates the potential impact on the natural environment and helps to identify ways to mitigate adverse effects. This phase involves collecting data on the project site, conducting environmental assessments, and analyzing the implications for air quality, water resources, biodiversity, and other relevant factors. The study aims to ensure that the project complies with environmental regulations and sustainable practices. It provides valuable information for decision making and allows the implementation of measures to minimize environmental damage and promote ecological balance.

However, for this type of project, a comprehensive environmental study is not considered necessary. The main benefit of this project lies in the implementation of renewable energies in the power grid. By focusing on the study of converter control and simulations, it seeks to improve the integration and efficient management of clean energy sources. This will help reduce dependence on fossil fuels, reduce greenhouse gas emissions and promote a more sustainable and environmentally friendly energy system. Therefore, the environmental focus is on the benefits of the transition to renewable energy sources and does not require an additional environmental study for the development of the project.

ETSEIB

9. Social and gender equality assessment

In this section, we will conduct a social and gender equality study to assess the potential impact of the project on different gender groups and promote inclusion. It is critical to critically analyze whether the work being carried out is influenced by or has the potential to create discriminatory differentiations based on gender or social status. We will address the following points to examine these issues:

1. Gender balance within the project team.
2. Consideration of gender-specific outcomes and impacts
3. Inclusive language and images
4. Avoidance of discrimination based on race, culture, and economic status.
5. Participation of social organizations
6. Monitoring mechanisms and indicators related to gender.
7. Gender representation in authorship
8. Impact on vulnerable groups
9. Alignment with the Sustainable Development Goals (SDGs).

In this social and gender equality study, we are pleased to state that no non-compliance has been identified in any of the eight points mentioned above. We have conducted a thorough analysis of the project and have taken the necessary steps to ensure gender equality and inclusion at all stages. From access to technology to gender representation on the team and consideration of gender-specific outcomes and impacts, we have worked diligently to avoid any form of discrimination and promote equity. In addition, we have used inclusive language and avoided gender stereotypes in our communications. We have also been aware of socioeconomic and cultural differences, avoiding the promotion of differentiating ideas among certain groups. With these measures, we ensure that our work complies with gender equality standards and promotes an inclusive approach for all groups, especially the most vulnerable.

In conducting this social and gender equality study, we seek to ensure that our project is inclusive, non-discriminatory and promotes gender equity throughout its development and implementation. It is important to note that if this project were to be carried out in real life, it would have to consider the existing gender inequality in the field of works and construction. Although we have worked to ensure gender equality at all stages of the project, it is crucial to recognize that there may be additional challenges related to gender discrimination in this specific field. Therefore, special attention and additional measures would be required to address and overcome any gender inequalities that may arise during project implementation. This involves promoting inclusive policies and practices, encouraging gender diversity in work teams, and providing equal opportunities for men and women in the construction industry.

ETSEIB

10. Conclusions

In this chapter, the general conclusions obtained from the development and study carried out in this work will be presented. We will evaluate the fulfillment of the initial objectives, discuss the performance of the case studies and propose possible extensions to the project.

First of all, it can be stated that the objectives set at the beginning of this work have been satisfactorily met. The study of smart grids, energy storage, solar photovoltaic energy and integration of converter control has been satisfactorily carried out. A thorough knowledge of these topics has been acquired and a solid understanding of the principles and techniques involved has been demonstrated.

In terms of case studies, two investigations have been carried out with positive results. In the first case, different control methods were applied for the integration of the energy generated by a photovoltaic plant into the grid. The results obtained have shown that these solutions are effective and efficient, allowing a successful integration of solar energy into the grid. In the second case study, a DC bus control and a reactive power control were implemented in the integration of a battery, a photovoltaic plant and a three-phase load into a smart grid. The results obtained have also been satisfactory, demonstrating the ability to optimally control and manage these complex systems.

It is important to highlight that both case studies have been contrasted by means of MATLAB/SIMULINK simulations. These simulations have allowed visualizing and quantifying the performance of the systems, validating the effectiveness of the proposed solutions and providing a solid basis for future implementations.

As possible extensions of the project, the evaluation and implementation of more scenarios in the second case study is suggested. This would allow exploring and analyzing the behavior of the systems under different conditions and workloads, thereby improving the understanding of their performance and enabling the optimization of their design and operation. In addition, after verifying the successful operation of the systems in the simulations, a feasibility and construction study is proposed. This study would involve a detailed analysis of the costs, resources required and the practical aspects of implementing the systems in a real environment.

The feasibility and construction study would assess the economic, technical and logistical feasibility of the project. Aspects such as infrastructure requirements, resource availability and applicable regulations would be considered. These analyses would provide a more accurate guide for the effective implementation of the systems in the real world.

ETSEIB

11. Acknowledgments

I would first like to thank my family for their unconditional support and for always believing in my abilities. To my friends and couple, your words of encouragement and your presence in difficult moments have given me strength and motivation to move forward in every step of my academic and personal journey. Thank you for believing in me and for being by my side throughout this process.

Secondly, I would like to express my gratitude to the Universitat Politècnica de Catalunya for giving me the opportunity to do this master's degree and to all the professors I have had during my time at the university. I am grateful for their dedication and knowledge shared in the lectures and seminars. In the same way, I sincerely thank my classmates from the master's program and from previous studies for their collaboration and friendship.

I would also like to thank my professors at the Escuela Politécnica de Ingeniería de Gijón, as well as my fellow students there. Their teaching and guidance laid the basis of my academic training and have left a permanent trace on my path.

ETSEIB

12. Bibliography

[1] Red Eléctrica de España. Generación. Retrieved from https://www.ree.es/es/datos/generacion

[2] Red Eléctrica de España. Estructura de la generación española. Retrieved from https://www.ree.es/es/datos/generacion/estructura-generacion

[3] EPE (El Periódico de la Energía). (2022, marzo 10). España compra gas a diferentes países. Recuperado de https://www.epe.es/es/economia/20220310/importa-gas-espana-13354317

[4] Red Eléctrica de España. Intercambios - Frontera físicos. Retrieved from https://www.ree.es/es/datos/intercambios/frontera-fisicos

[5] Red Eléctrica de España. (2021, diciembre). Sistema eléctrico español ingresa 110 millones por asignación de capacidad de intercambio con países vecinos [Nota de prensa]. Recuperado de https://www.ree.es/es/sala-de-prensa/actualidad/nota-de-prensa/2021/12/sistema-electrico-espanol-ingresa-110-millones-asignacion-capacidad-intercambio-paises-vecinos

[6] I. Diahovchenko, M. Kolcun, Z. Čonka, V. Savkiv, and R. Mykhailyshyn, "Progress and Challenges in Smart Grids: Distributed Generation, Smart Metering, Energy Storage and Smart Loads," Iran. J. Sci. Technol. - Trans. Electr. Eng., vol. 44, no. 4, pp. 1319–1333, 2020.

[7] N. Dkhili, J. Eynard, S. Thil, and S. Grieu, "A survey of modelling and smart management tools for power grids with prolific distributed generation," Sustain. Energy, Grids Networks, vol. 21, p. 100284, 2020.

[8] D. Markovic, I. Branovic, and R. Popovic, "Smart Grid and nanotechnologies: a solution for clean and sustainable energy," Energy Emiss. Control Technol., p. 1, 2015.

[9] P. H. A. Barra, D. V. Coury, and R. A. S. Fernandes, "A survey on adaptive protection of microgrids and distribution systems with distributed generators," Renew. Sustain. Energy Rev., vol. 118, no. November 2019, p. 109524, 2020.

[10] B. J. Brearley and R. R. Prabu, "A review on issues and approaches for microgrid protection," Renew. Sustain. Energy Rev., vol. 67, pp. 988–997, 2017.

[11] M. Beaudin, H. Zareipour, A. Schellenberglabe y W. Rosehart, «Energy storage for mitigating the variability of renewable electricity sources: An updated review,» de Energy Sustain. Develop., vol. 14, Dec. 2010, pp. 302-314.

ETSEIB

[12] M. Reuss, M. Beck y J. P. Muller, «Design of a seasonal thermal energy storage in the ground,» de Solar Energy, vol. 59, Apr.-Jun. 1997, pp. 247-257.

[13] S. M. Schoenung, «Characteristics and technologies for long- vs short-term energy storage: A study by the DOE energy storage systems program,» U.S. Dept. Energy, Mar. 2001.

[14] K. C. D. a. J. Ostergaard, «Battery energy storage technology for power,» de Electr. Power Syst. Res., vol. 79, Apr. 2009, pp. 511-520.

[15] «EPRI-DOE handbook of energy storage for transmission and distribution applications,» Washington, DC, USA, Electric Power Research Institute (EPRI), 2003.

[16] H. S. Chen y otros, «Progress in electrical energy storage system: A critical review,» de Progr. Natural Sci. vol. 19, mAR. 10, 2009, pp. 291-312.

[17] «U.S. Energy Storage Project Activities Demonstrations & commercial installations,» Washington, DC, USA, Electric Power Research Institute (EPRI), 2012.

[18] X. Luo y otros, «Overview of current development in electrical energy storage technologies and the application potential in power system operation. Applied Energy,» 2015. 137, pp. 511-536. [11]

[19] H. Chen y otros, «Progress in electrical energy storage system: A critical review. Progress in Natural Science,» 2009. 19(3):, pp. 291-312.

[20] T. Ma y otros, «Technical feasibility study on a standalone hybrid solar-wind system with pumped hydro storage for a remote island in Hong Kong. Renewable Energy,» 2014. 69:, pp. 7-15.

[21] S.L.A.-H.a. M.A.Rehman, «Pumped hydro energy storage system: A technological review. Renewable and Sustainable Energy Reviews,» 2015. 44:, pp. 586-598.

[22] Institute for Energy and Transport, «Pumped-hydro energy storage: potential for transformation from single dams. JRC IET scientific and technical report.EUR 25239 EN.,» Published on 24th February 2012..

[23] D. Connolly y otros, «The technical and economic implications of integrating fluctuating renewable energy using energy storage. Renewable Energy,» 2012. 43:, pp. 47-60.

[24] AMDC ENERGY LIMITED, [Online]. Available: http://www.amdcenergy.com/battery-energy-storage-system.html. [Last access: 1 June 2023].

[25] ReserarchGate, [Online]. Available: https://www.researchgate.net/figure/Schematic-

ETSEIB

diagram-of-pumped-hydro-storage-plant-Source-Pavlos-Nikolaidis-2017_fig7_343754956. [Last access: 1 June 2023].

[26] V. D. Biasi, «110 MW McIntosh CAES plant over 90% availability and 95% reliability,,» de Gas Turbine World, vol. 28, 1998, pp. 26-8.

[27] E. Swensen y B. Potashnik, «Evaluation of Benefits and Identification of sites for a CAES plant in New York State,» de EPRI, TR-104268, final report, August 1994.

[28] K. R. F.Crotogino, «Huntorf CAES: More Than 20 Years of Successful Operation,» Florida, USA, in Solution Mining Research Institute Meeting Orlando, 2001.

[29] Adunti,21 enero 2019. [Online]. Available: https://adunti.net/2019/01/21/almacenamiento-de-energia-magnetica-por-superconductividad/. [Last access: 10 June 2023]

[30] P.Tixador, «Superconducting magnetic energy storage: Status and perspective,» de IEEE/CSC&ESAS European superconductivity new forum No. 3, 2008.

[31] F. E. S. Inc., 1.5 kW Electromechanical battery system flywheel energy systems Inc. CETC-0100-01 Rev. 2., Nepean, Ontario, Canadá, Enero 2000.

[32] AIRBUS,[Online].Available: https://www.airbus.com/newsroom/news/en/2020/10/hydrogen-fuel-cell-cross-industry-collaboration-potential-for-aviation.html.[Last access: 25 June 2023].

[33] Foster, R. (2013). Photovoltaic Materials and Devices. In Solar Energy: Renewable Energy and the Environment. CRC Press.

[34] Hadjsaid, N., & Sabonnadiere, J. (2012). Modeling and Control of Sustainable Power Systems Towards Smarter and Greener Electric Grids (1st ed.). Green Energy and Technology. ISBN: 3-642-22904-2.

[35] MathWorks. (s.f.). mcb_clarkeabc.png [Captura de pantalla]. Retrieved from https://www.mathworks.com/help/mcb/ref/mcb_clarkeabc.png

[36] MathWorks. (s.f.). parktransform. Retrieved from https://es.mathworks.com/help/sps/ref/parktransform.html

[37] Egea-Alvarez, A., Junyent-Ferre, A., & Gomis-Bellmun, O. (2012). Active and reactive power control of grid-connected distributed generation systems.

[38] Wikipedia, [Online]. Available: https://es.wikipedia.org/wiki/Convertidor_reductor. [Last acces: 8 July 2021]

[39] Arabul, F. K., Arabul, A. Y., Senol, I., & Boynuegri, A. R. (2015, January). Providing
Energy Management of a Fuel Cell-Battery Hybrid Electric Vehicle. Zenodo.

[40] Montero Moreno, C. Control Predictivo con Horizonte Variable para Convertidores de
Potencia [CAPÍTULO2. MODELO DEL SISTEMA].

ANNEX 1: MATLAB CODE

ANNEX 2: SIMULINK FILES

- Annex 2.1: Case Study 1. Simulink file.
- Annex 2.2.1: Case Study 2. Overall Simulink file.
- Annex 2.2.2: Case Study 2. PV Array Model Simulink file.
- Annex 2.2.3: Case Study 2. Battery Model Simulink file.
- Annex 2.2.4: Case Study 2. Load Model Simulink file.

ETSEIB